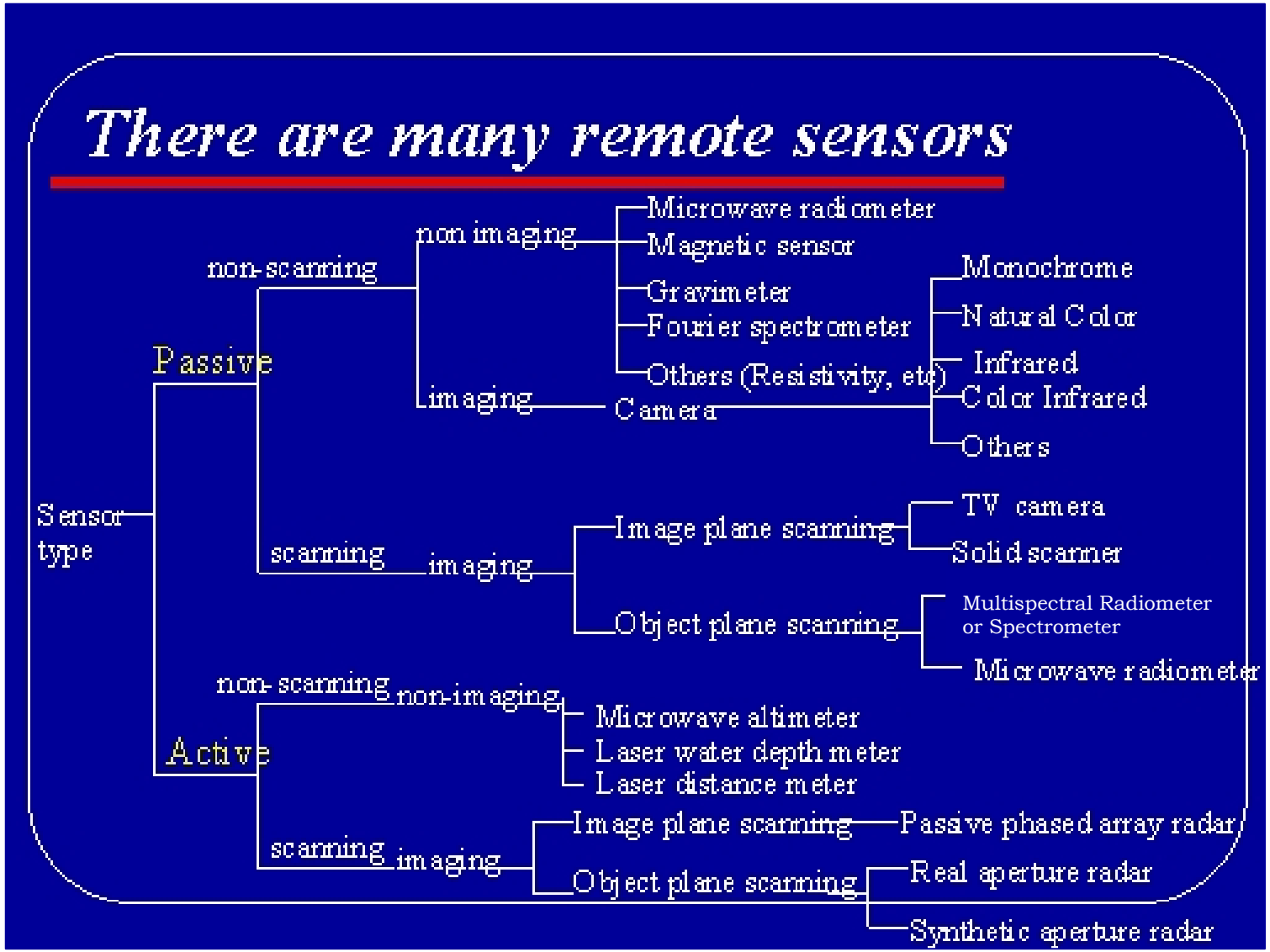
There are many remote sensors
Sensor type
Passive
non-scanning
non imaging
Microwave radiometer
Magnetic sensor
Gravimeter
Fourier spectrometer
Others (Resistivity, etc)
imaging
Camera
Monochrome
Natural Color
Infrared
Color Infrared
Others
scanning
imaging
Image plane scanning
TV camera
Solid scanner
Object plane scanning
Multispectral Radiometer or Spectrometer
Microwave radiometer
Active
non-scanning
non-imaging
Microwave altimeter
Laser water depth meter
Laser distance meter
scanning
imaging
Image plane scanning
Passive phased array radar
Object plane scanning
Real aperture radar
Synthetic aperture radar

Detection of EM radiation reflected (scattered) or emitted by the earth's surface

Reflection of solar radiation	Emission of thermal radiation
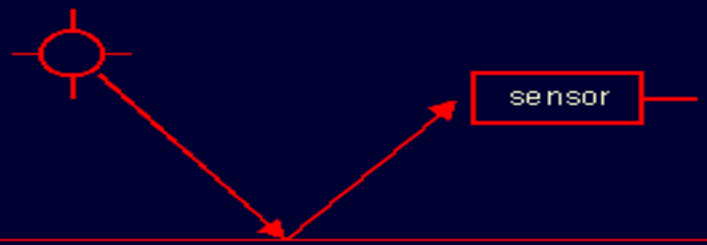 REFLECTION (MULTISPECTRAL)	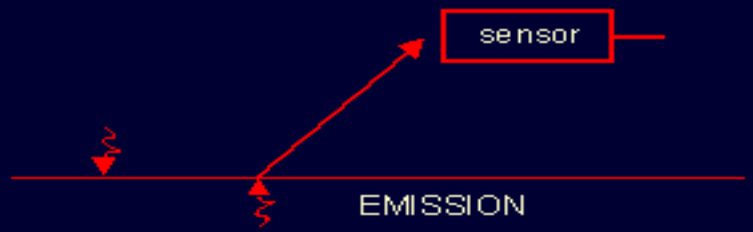 EMISSION
0.3 - 0.4 µm: UTRAVIOLET 0.4 - 0.7 µm: VISIBLE LIGHT 0.7 - 2.5 µm: REFLECTIVE INFRARED	3 - 5 µm 8 - 14 µm } : THERMAL INFRARED 1 - 30 GHz : PASSIVE MICROWAVES
OBSERVATION BY DAY IN THE ABSENCE OF CLOUD COVER	OBSERVATION BY DAY AND NIGHT THERMAL INFRARED : IN THE ABSENCE OF CLOUD COVER PASSIVE MICROWAVES: NO INTERFERENCE WITH CLOUD COVER
MULTISPECTRAL SCANNING (MSS) AERIAL PHOTOGRAPHY (AP) MULTISPECTRAL PHOTOGRAPHY (MSP) SYSTEMATIC RECONNAISSANCE (SRF)	THERMAL INFRARED SCANNING (TIRS) PASSIVE MICROWAVE DETECTION (MICRO-WAVE RADIOMETRY)
"Passive" Remote Sensing (sensor without its own source of radiation)	"Passive" Remote Sensing (sensor without its own source of radiation)

Figure Continued

Reflection of transmitted optical radiation  OPTICAL BACKSCATTER (MONOSPECTRAL REFLECTION)	Reflection of transmitted microwave radiation  RADAR BACKSCATTER
0.25 - 0.35 µm : UTRAVIOLET 0.4 - 11 µm: VISIBLE AND INFRARED	X-BAND RADAR : 9.4 GHz (3.2 cm) C-BAND RADAR : 5.3 GHz (5.7 cm) L-BAND RADAR : 1.3 GHz (23.0 cm) P-BAND RADAR : 0.44 GHz (68.0 cm)
OBSERVATION BY DAY AND NIGHT LIMITED BY ATMOSPHERIC ATTENUATION OPERATING IN PROFILES	OBSERVATION BY DAY AND NIGHT AND NO INTERFERENCE WITH CLOUD COVER
LIDAR SYSTEMS : AIRBORNE / SPACEBORNE : GROUND BASED	SIDEWAYS LOOKING AIRBORNE RADAR (SLAR) SYNTHETIC APERTURE RADAR (SAR)
"Active" Remote Sensing (sensor with its own source of radiation)	"Active" Remote Sensing (sensor with its own source of radiation)

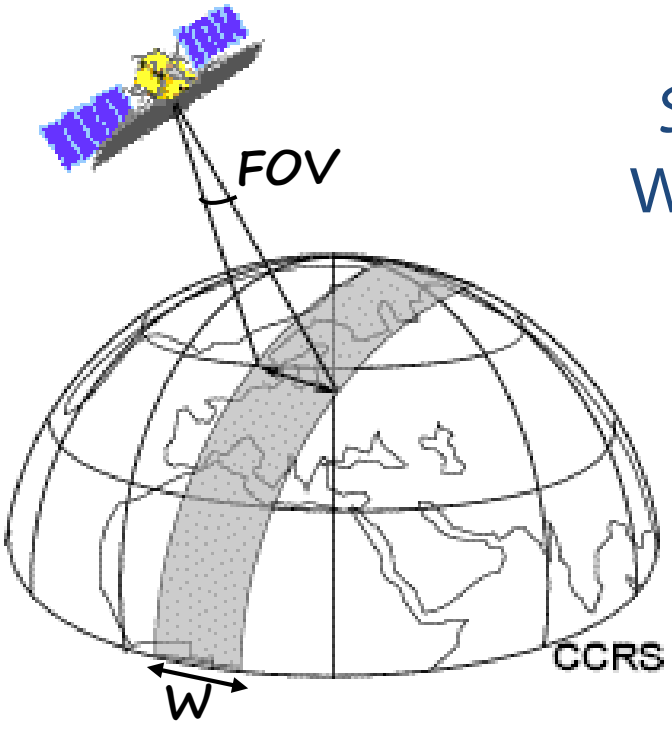

Swath Width

$W = 2 \cdot h \cdot tg(FOV/2)$

FOV = Field of View

It is the <u>total</u> angle through which the remote sensing measurements are performed

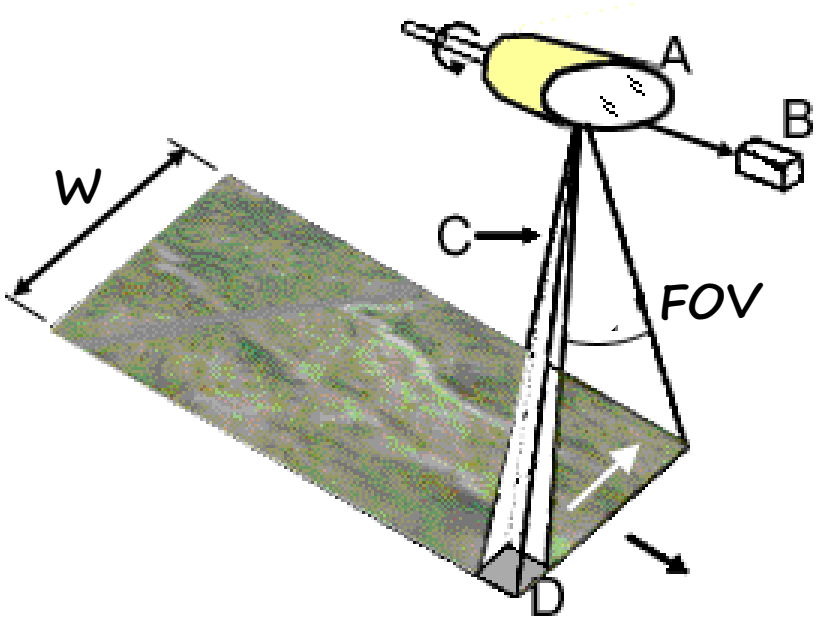

Scanning Instruments sense at variable angles –measure radiation point by point

cross-track scanners (whiskbroom)

- mirror that is rotated by electrical motor
- horizontal axis of rotation is aligned parallel to flight direction
- mirror sweeps across terrain in parallel scan lines oriented perpendicular to the flight direction

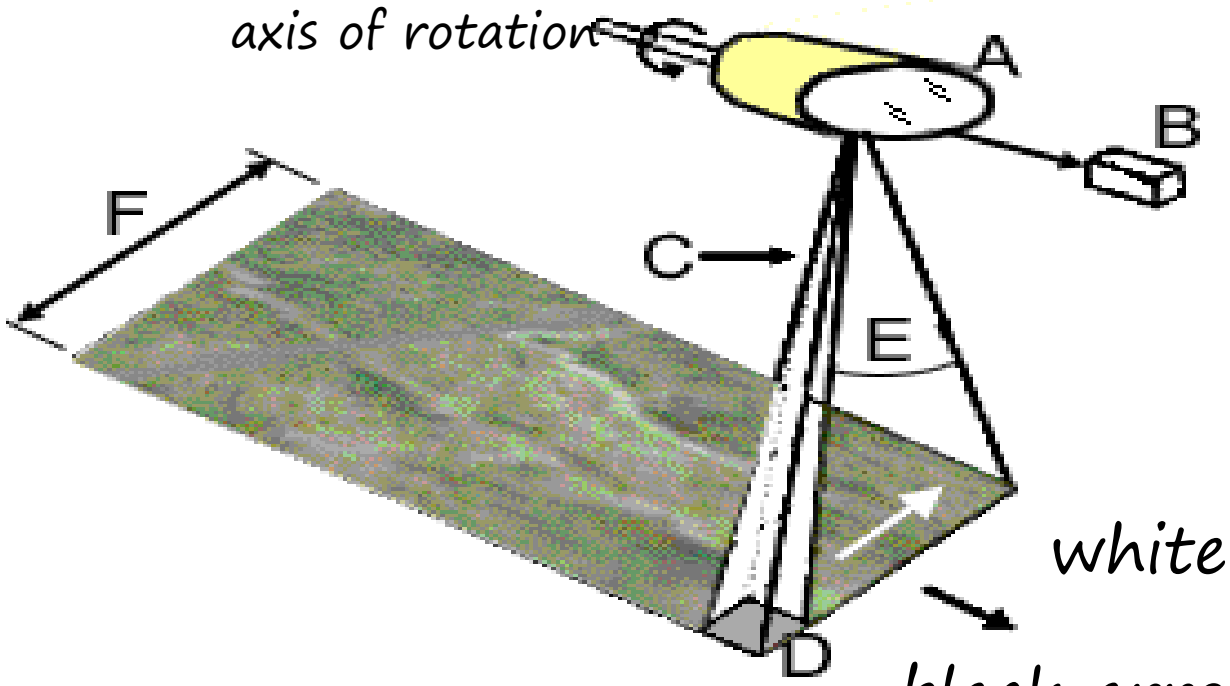

A: rotating mirror
B: detector
C: IFOV of sensor
D: ground resolution cell
E: angular field of view (**FOV**) (sweep of mirror)
F: swath

white arrow is scan direction

black arrow is flight direction

Non-scanning (framing) instruments measure radiation at a specific direction

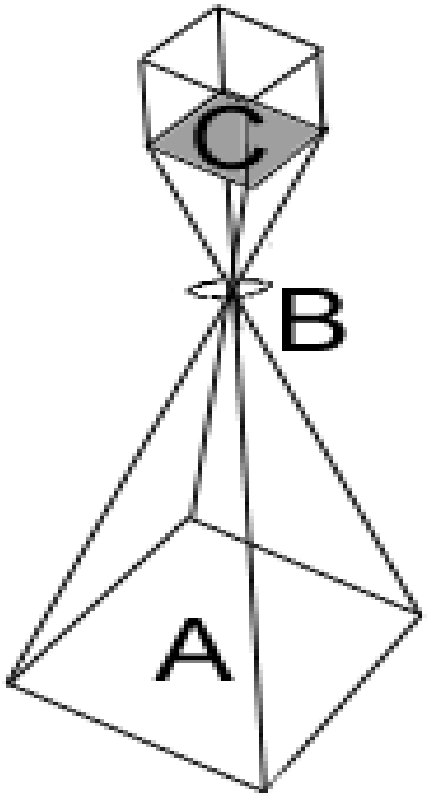

Instantaneously acquire a single measurement, for example:

Camera acquires a picture of an area (aerial photographs)

vidicon: television camera and photosensitive electronically charged surface

A: ground coverage
B: lens system
C: focal plane with detector (film)

EM Spectrum Regions Used in Remote Sensing

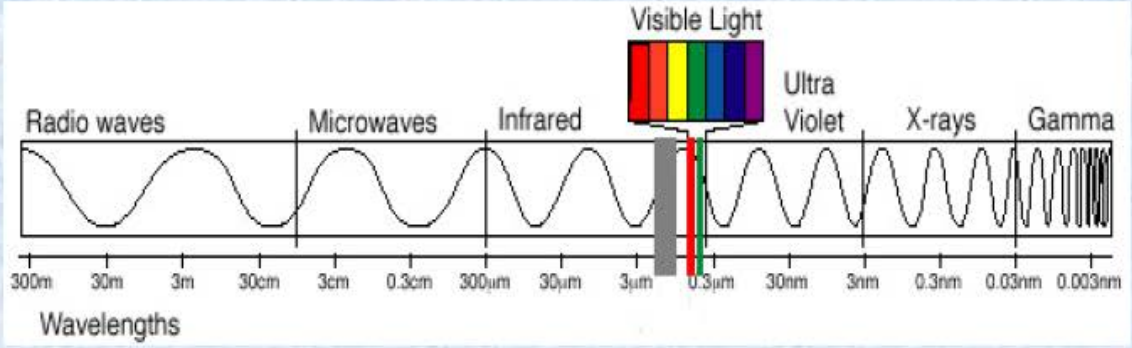

λ = EM radiation wavelength

1. Ultraviolet ($\lambda < 0.4\ \mu m$)
2. Visible ($0.4\ \mu m < \lambda < 0.7\ \mu m$)
3. Reflected IR ($0.7\ \mu m < \lambda < 2.8\ \mu m$)
4. Emitted (thermal) IR ($2.4\ \mu m < \lambda < 20\ \mu m$)
5. Microwave ($1\ cm < \lambda < 1\ m$)

Optical wavelengths

Visible Light Region of the Electromagnetic Spectrum

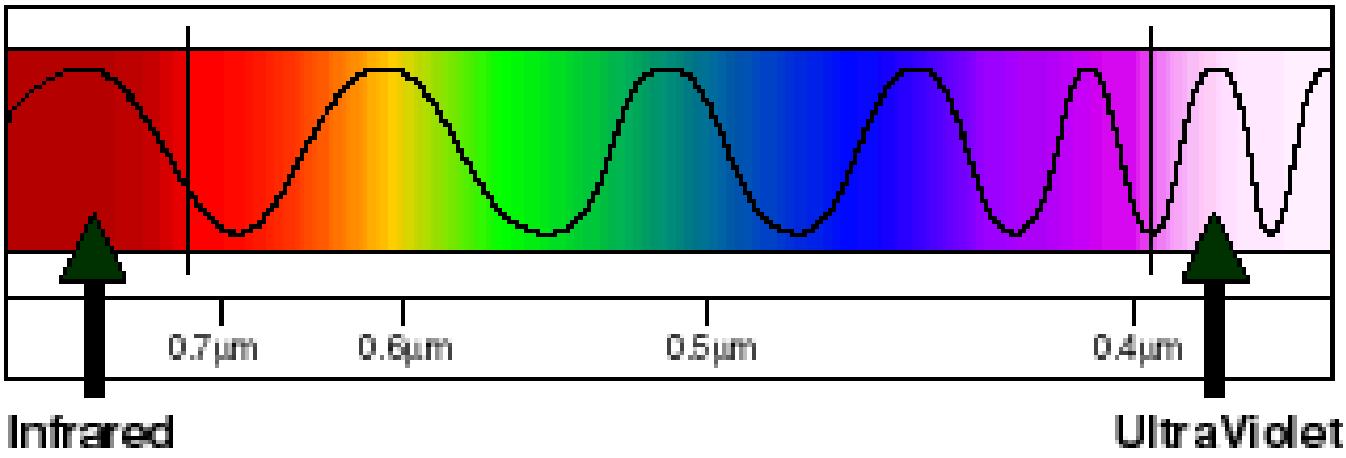

Infrared Region of the Electromagnetic Spectrum

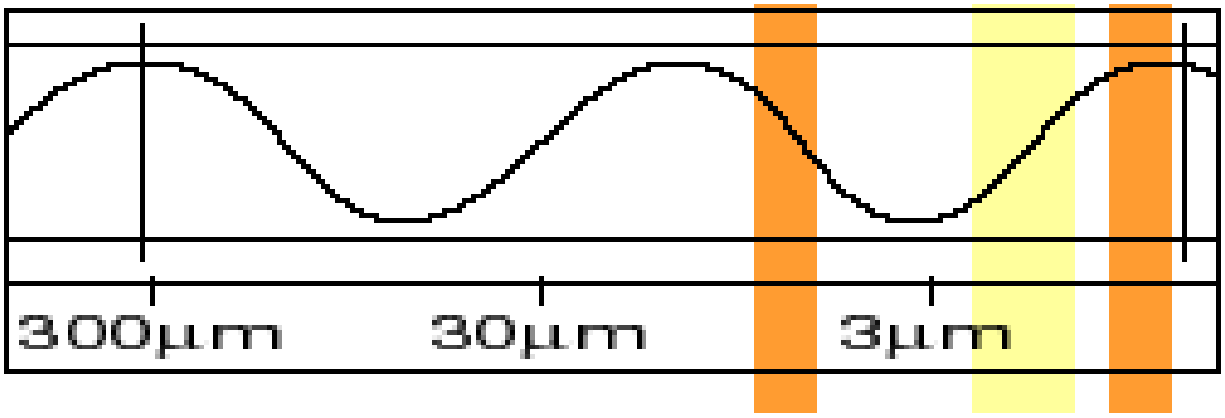

Far Mid ShortWave NIR
>5µ [3- 5µ] [1.4-3µ] [0.7-1.4]

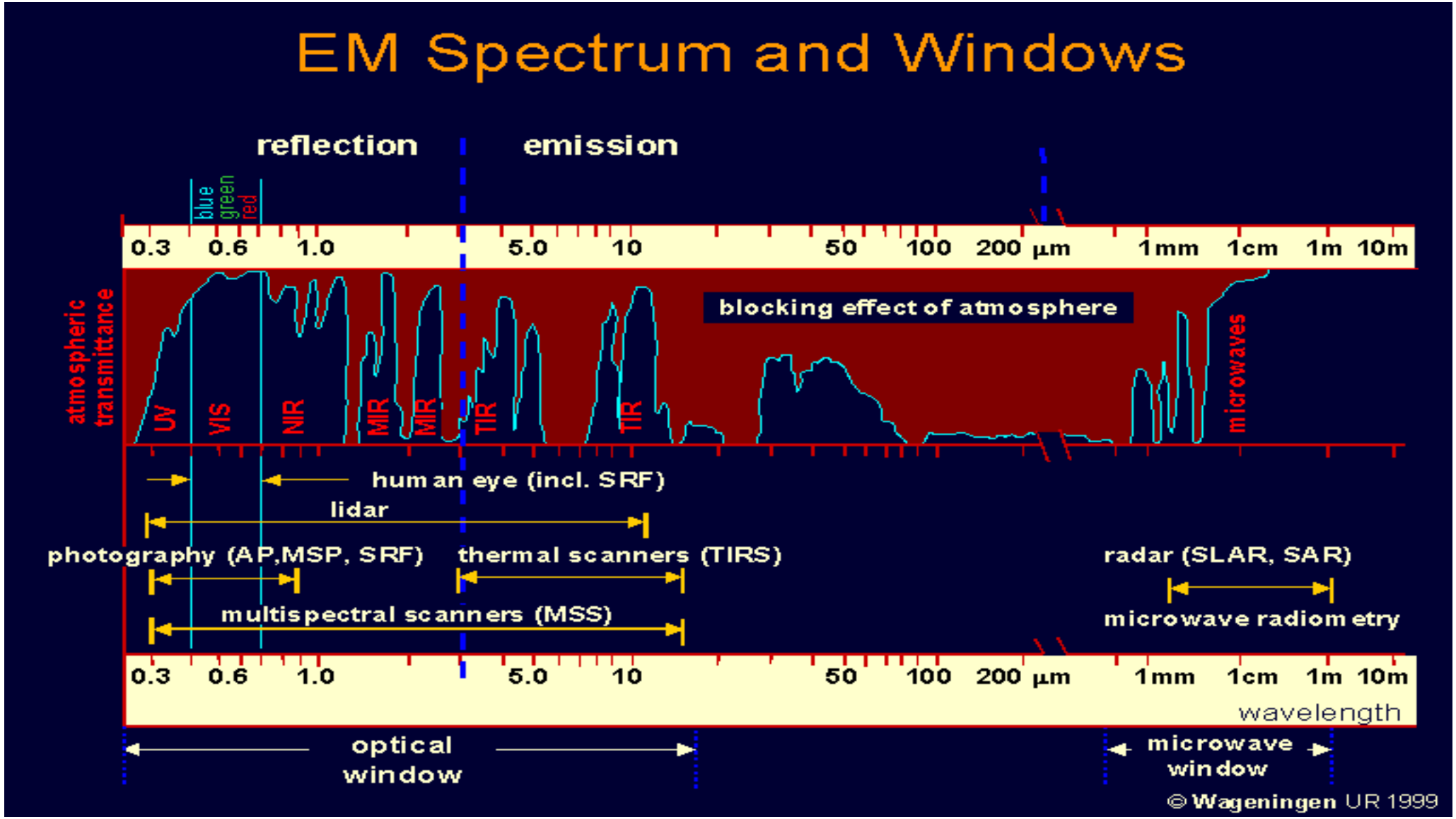
EM Spectrum and Windows
reflection
emission
blue
green
red
0.3
0.6
1.0
5.0
10
50
100
200 µm
1mm
1cm
1m
10m
atmospheric transmittance
blocking effect of atmosphere
UV
VIS
NIR
MIR
MIR
TIR
TIR
microwaves
human eye (incl. SRF)
lidar
photography (AP,MSP, SRF)
thermal scanners (TIRS)
radar (SLAR, SAR)
multispectral scanners (MSS)
microwave radiometry
wavelength
optical window
microwave window
© Wageningen UR 1999

Radiometric Units and Terms

- In Remote Sensing, we care about *energy*!
- *Energy* is in units of => [kg m^2/ s^2] = Joule, J
- For EMR, the form of energy is *Radiant Energy*: **Q**
- *Power* is simply the rate at which *energy* changes in time
- *Power* is what produces a response in a satellite sensor
- In remote sensing lingo, *power* is called ***Radiant Flux***, $\Phi = dQ/dt$
- Φ has units of *energy/ time* [J/s] = Watt, W

- ***Flux Density*** is simply the *radiant flux*, or *power*, per unit area **[W/m^2]**
- It is important because in remote sensing we are concerned with *radiant flux* over surfaces like a sensor lens or antenna

The Two Faces of *Flux Density*

- Incoming *flux density*, incident upon a surface is called ***irradiance***:

$$E = \frac{d\Phi}{dA}$$

- Outgoing *flux density*, emitted from a surface, is called ***emittance*** (or ***exitance***):

$$M = \frac{d\Phi}{dA}$$

Irradiance - E

Irradiance is the amount of incident radiant flux per unit area of a plane surface in Watts / square meter (W m^{-2})

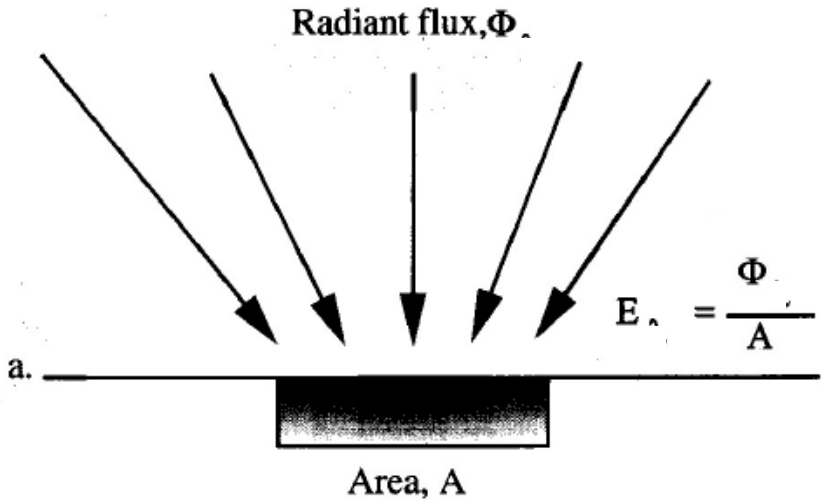

Exitance - M

- Exitance is the amount of radiant flux per unit area leaving a plane surface in Watts per square meter (W m^{-2})

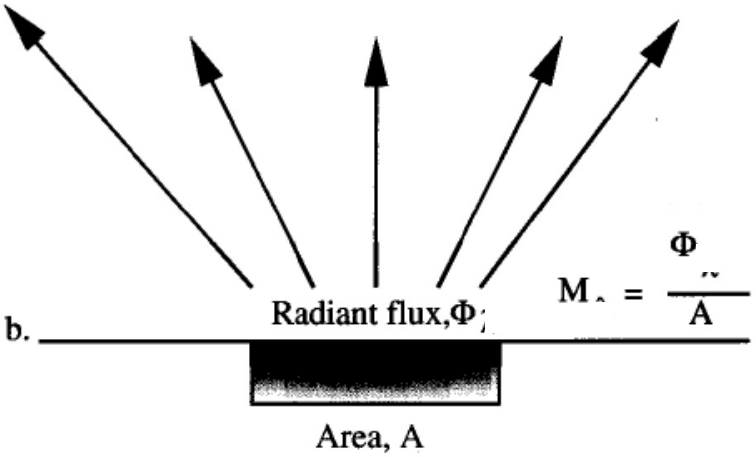

Detection of flux by a remote sensing system

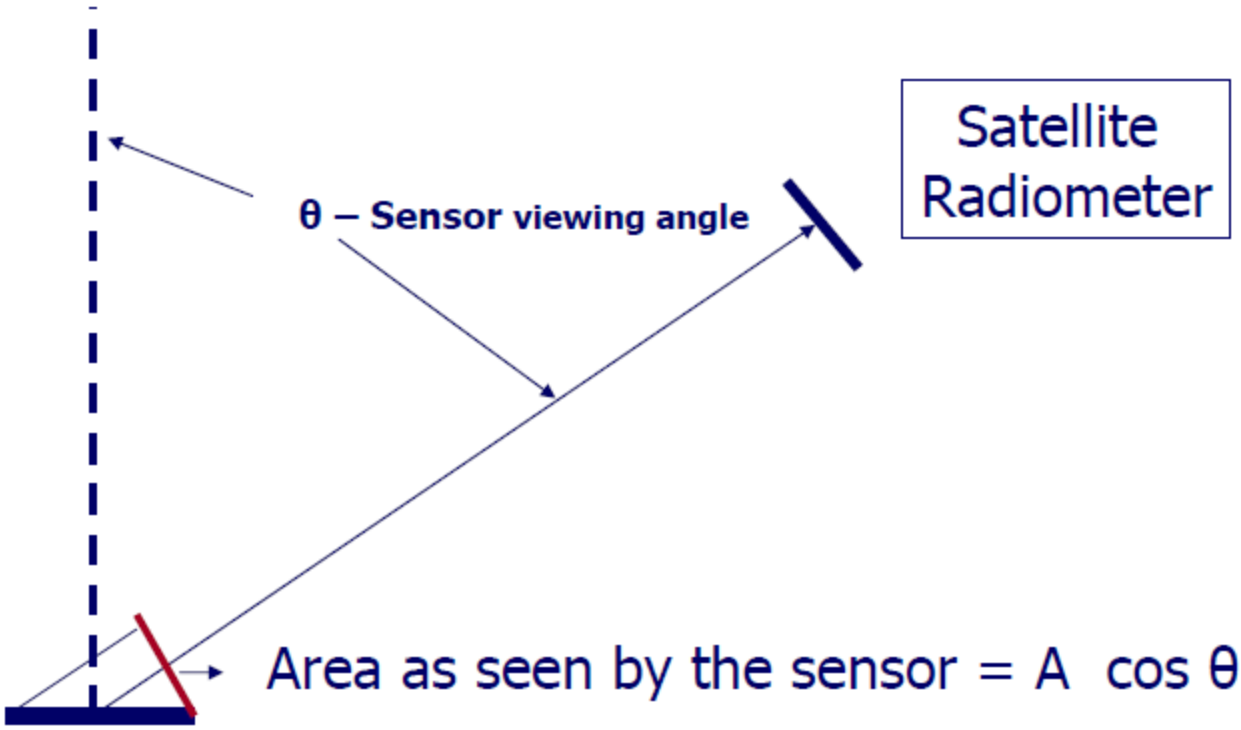

Radiance - L

- Radiance – the radiant flux per unit solid angle leaving an extended source in a given direction per unit of projected source area in that direction

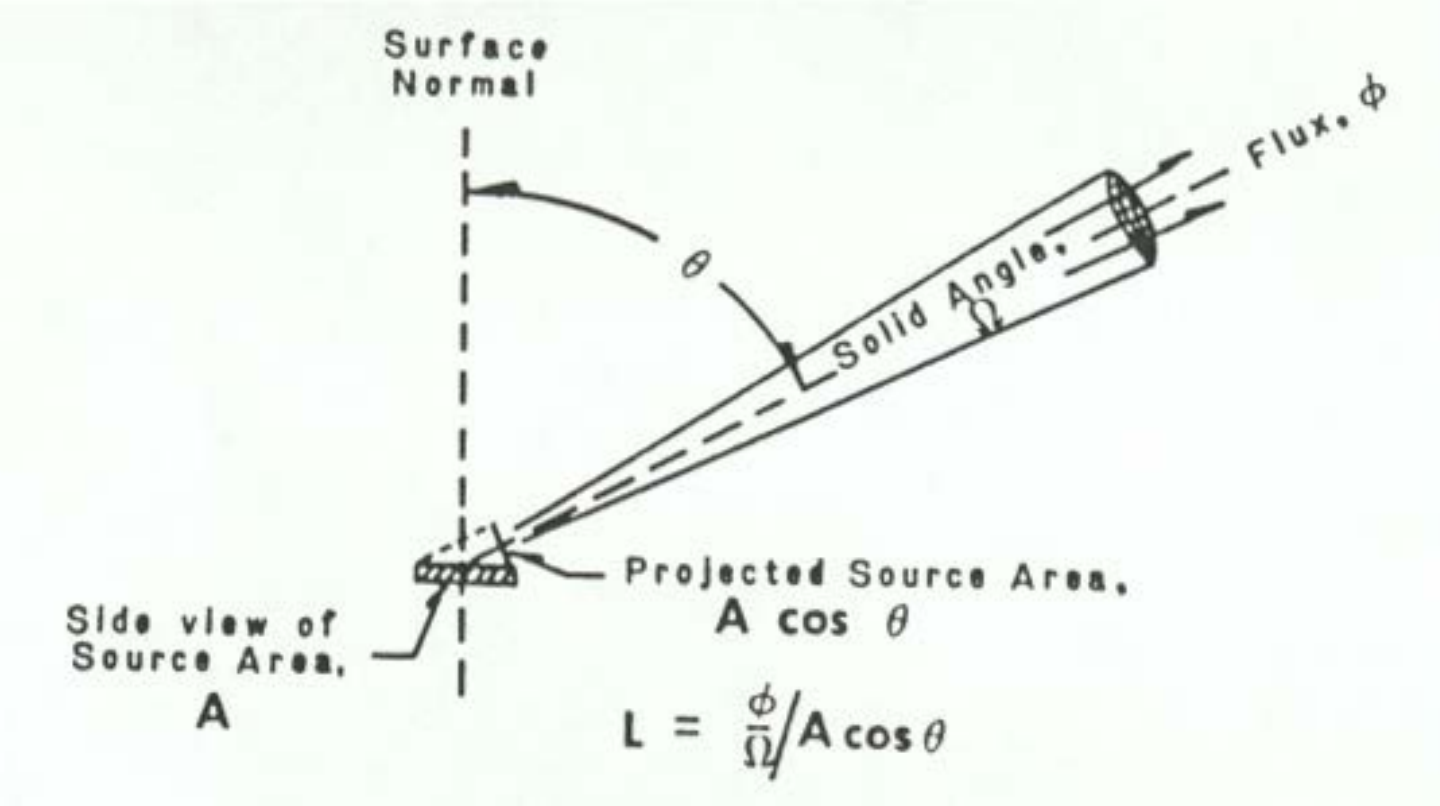

Radiance is what sensors detect.
It is measured in
Watts per squared meter per steradian

$[Wm^{-2}\ sr^{-1}]$

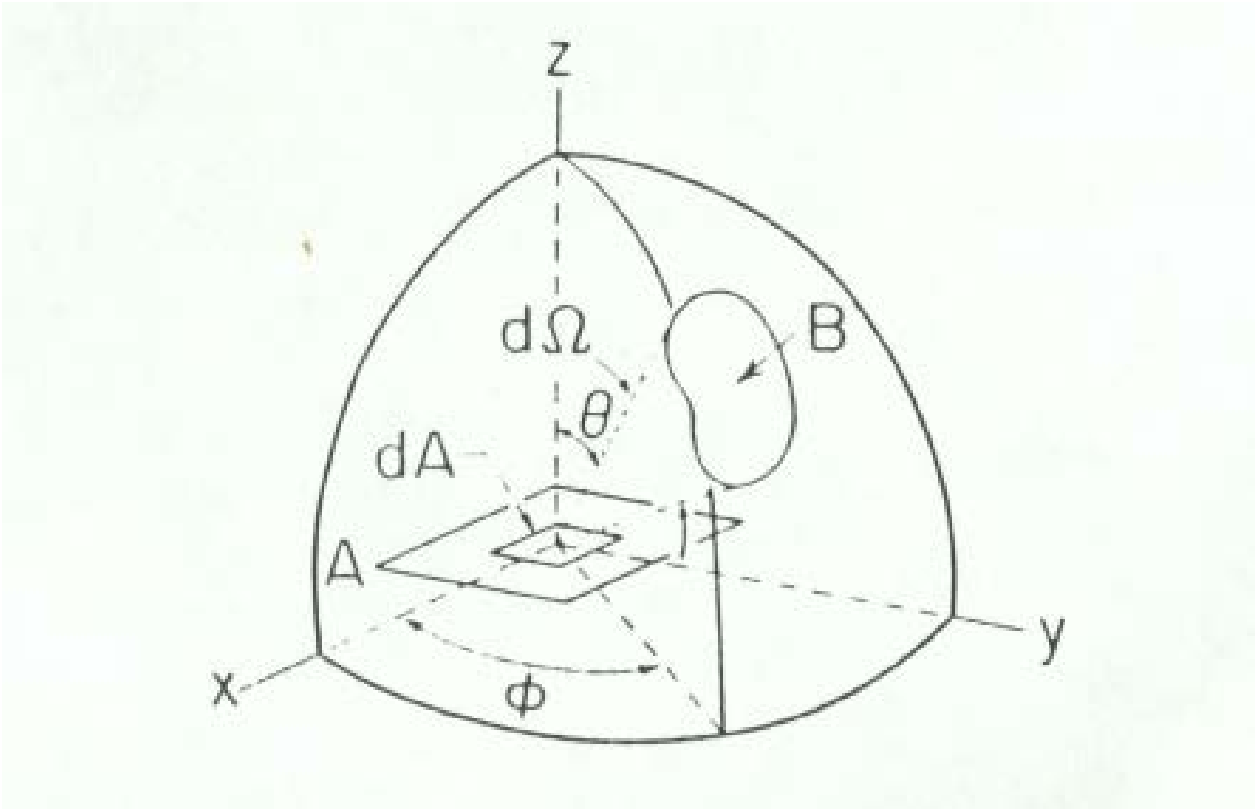

In terms of "infinitesimal" quantities suitable for integrating:

Incident or exiting radiant flux

$$L = \frac{d^2\Phi}{d\Omega dA\cos\theta}$$

Solid angle

Area projected in the incident or exiting direction

The Radiance invariance

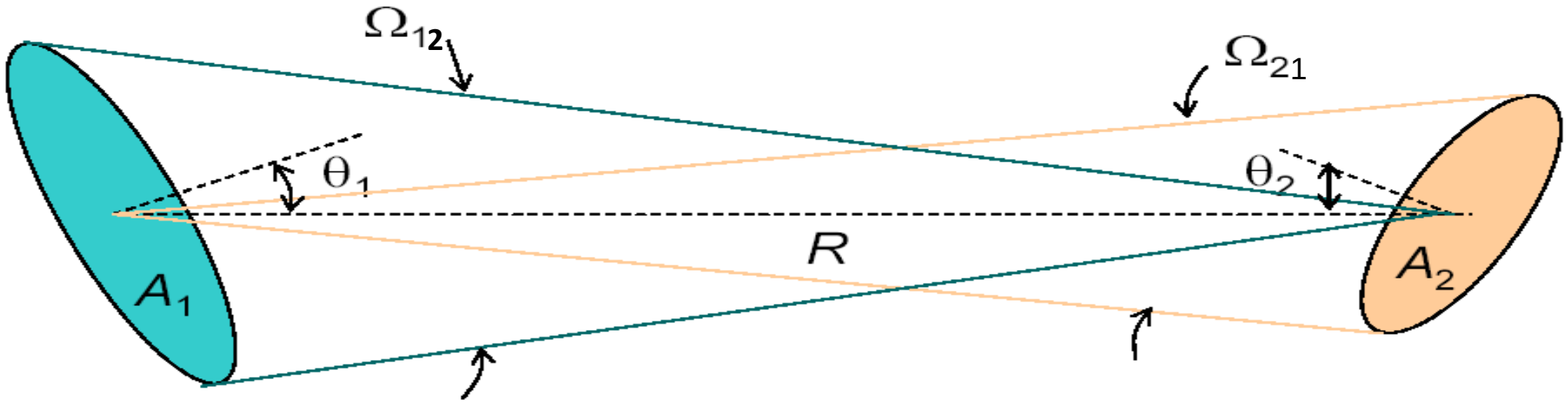

- How is the radiance at surface 1 (L_1) related to the radiance at surface 2 (L_2)?

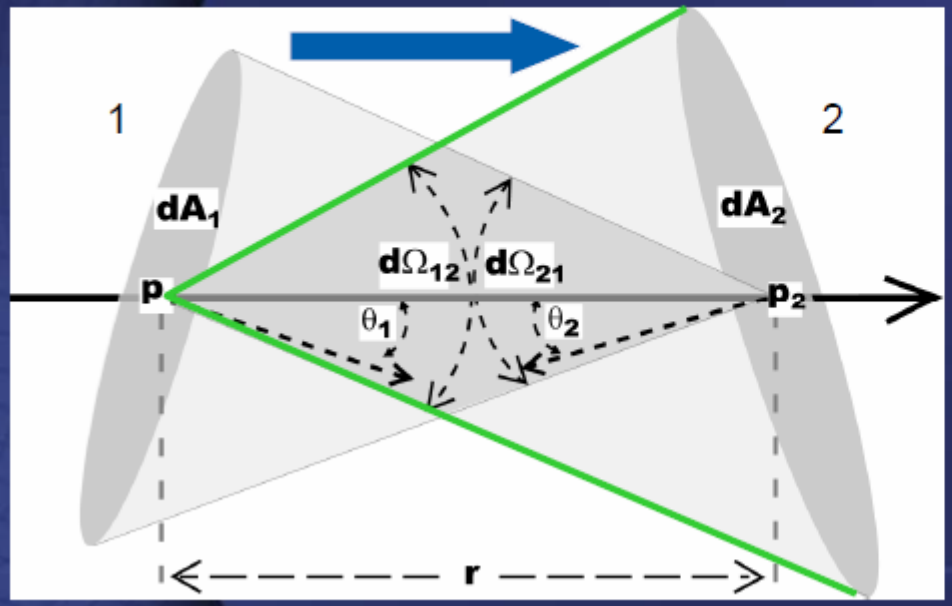

$$L_1 = \frac{d^2\Phi_1}{dA_1 \cos\theta_1 d\Omega_{12}}$$

- Radiance from the Earth, p_1

- How is the radiance at surface 1 (L_1) related to the radiance at surface 2 (L_2)?

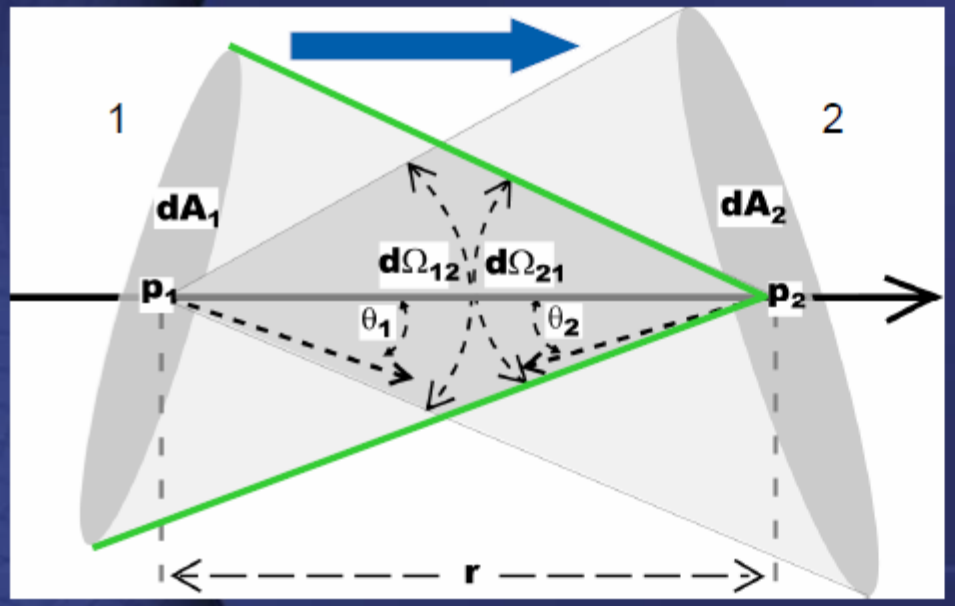

- Radiance at the sensor, p_2

$$L_2 = \frac{d^2\Phi_2}{dA_2 \cos\theta_2 d\Omega_{21}}$$

Throughput is Invariant in an Optical System

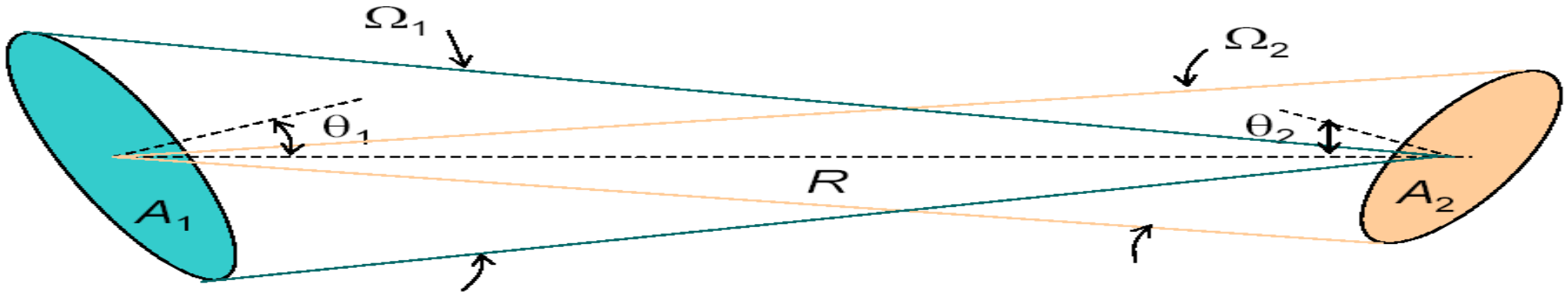

$$\tau_1 = d\Omega_1 dA_2 \cos\theta_2 = \frac{dA_1 \cos\theta_1 dA_2 \cos\theta_2}{R^2}$$

$$\tau_2 = d\Omega_2 dA_1 \cos\theta_1 = \frac{dA_2 \cos\theta_2 dA_1 \cos\theta_1}{R^2}$$

$$L_1 = \frac{d^2\Phi_1}{\tau_1}, \quad L_2 = \frac{d^2\Phi_2}{\tau_2}$$

But: $\tau_1 = \tau_2$ and $d\Phi_1 = d\Phi_2$, so that $L_1 = L_2$

This tells us that radiance along a ray is costant over distance in a lossless medium

Now, Spectral Quantities

In remote sensing, radiance is observed over narrow wavelength, or frequency, bands. So, *spectral* versions of the previous terms must be defined per unit wavelength (dividing by the bandwidth):

$$L_\lambda = \frac{dL}{d\lambda},\ L_f = \frac{dL}{df}$$

$$E_\lambda = \frac{dE}{d\lambda},\ M_\lambda = \frac{dM}{d\lambda}$$

In summary:

$$L_\lambda = \frac{dL}{d\lambda} = \frac{d^3\Phi}{d\Omega d\lambda dA\cos\theta} = \frac{d^4Q}{dtd\Omega d\lambda dA\cos\theta}$$

Planck's law

$$B_\lambda(T) = \frac{2hc^2}{\lambda^5\left(e^{\left(\frac{hc}{\lambda kT}\right)} - 1\right)}$$

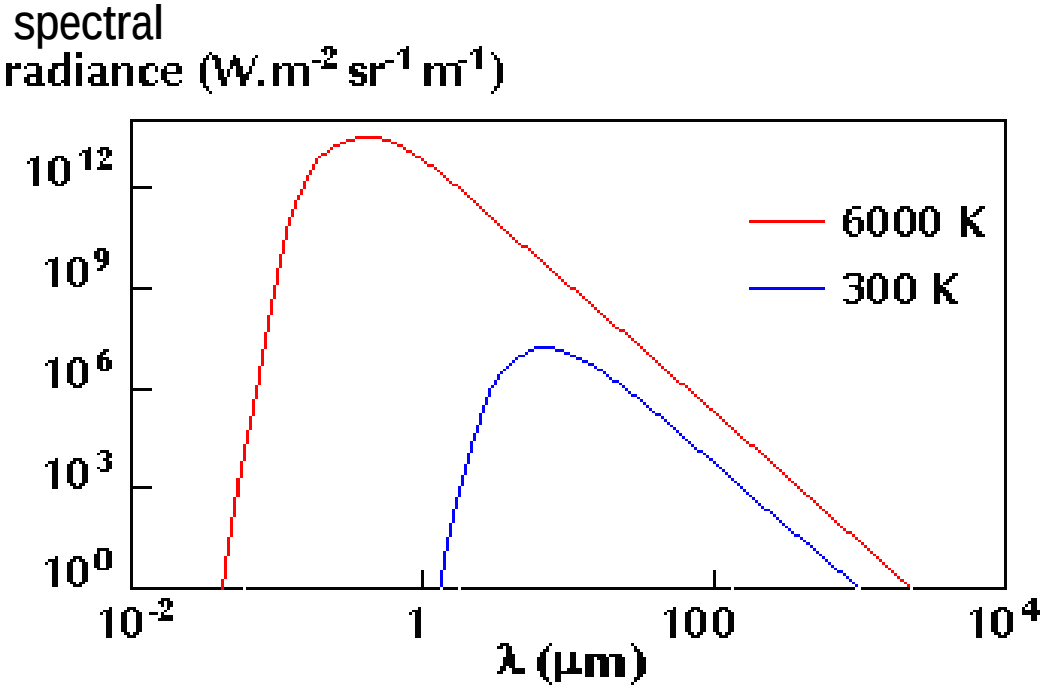

$$B_f(T)df = B_\lambda(T)d\lambda$$

$$B_f(T) = B_\lambda(T)\frac{d\lambda}{df} = \frac{\lambda^2}{c}B_\lambda(T)$$

Rayleigh Jeans approximation

If $hf << 1$,

$$e^{\frac{hf}{KT}} - 1 = \frac{hf}{KT}$$

$$B_f(T) = 2\frac{f^2}{c^2}KT = 2\frac{KT}{\lambda^2}$$

Solar-Terrestrial Comparison

Plots here show the energy from the sun at the sun and at the top of the earth's atmosphere

Also show the emitted energy from the earth

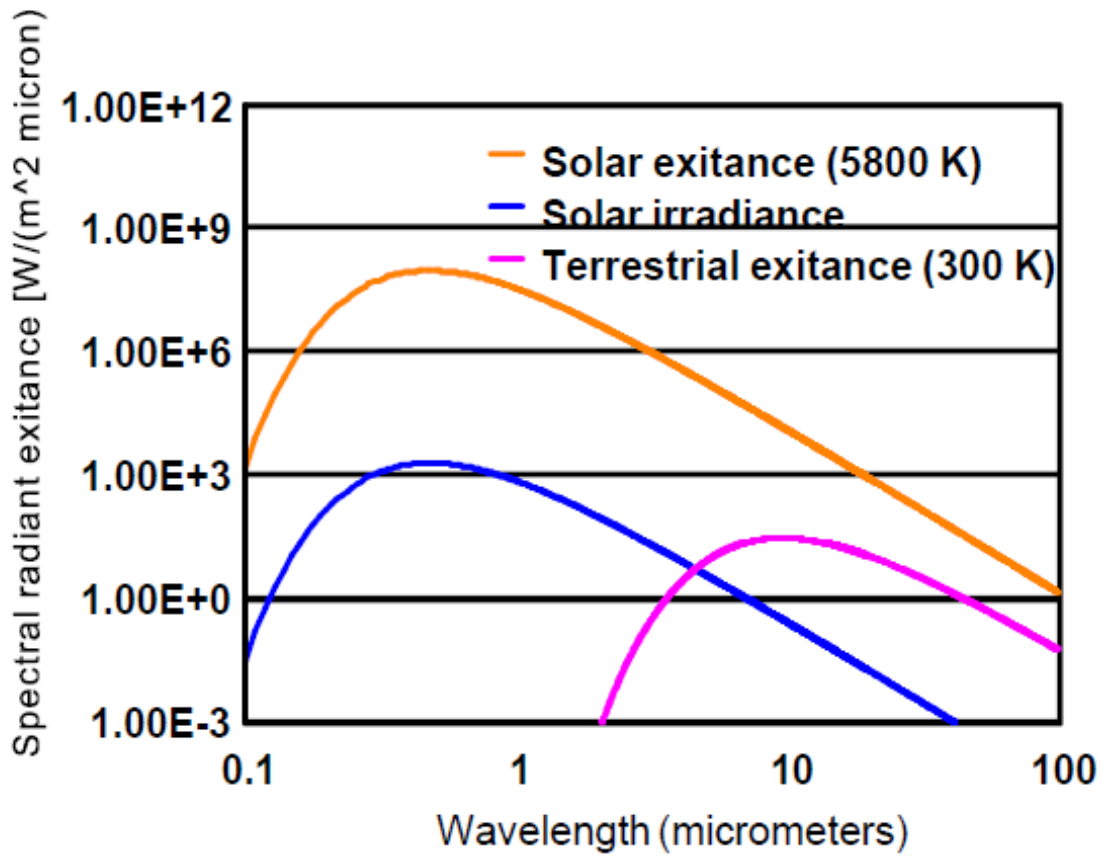

Spatial (or geometric) resolution defines the minimum distance that can be distinguished by a sensor.

It is measured in [m].

In passive sensors (radiometers), spatial resolution depends on the satellite altitude $\boldsymbol{h}$ and on $\boldsymbol{IFOV}$, through the ground resolution cell $\boldsymbol{\Delta x}$.

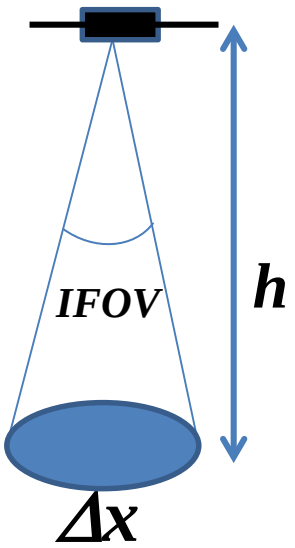

$$\boldsymbol{\Delta x = h \cdot IFOV}$$

IFOV is the <u>istantaneous</u> field of view of the sensor, through which the measurement is performed.
Conventionally, spatial resolution is quantified by means of $\boldsymbol{\Delta x}$.

The remote sensing measurements are arranged in a matrix format that can be displayed as an image.
An image is composed by pixels whose gray level corresponds to the measured radiance that is coded in Digital Numbers

DN			
50	150	250	250
0	100	200	200
0	50	150	200
50	100	100	150

numerical values

Gray levels

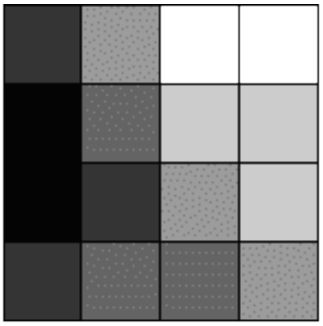

corresponding pixel display

An image with n-bit resolution has 2^n gray levels

0=black

2^n-1=white

16 Gray levels

32 Gray levels

128 Gray levels

In images at full resolution,
the pixel represents the istantaneous measurement performed within the ***IFOV***,
and its dimensions coincide with the ground resolution cell.
(In full resolution images, a pixel corresponds to an area Δx^2.)

The pixel dimension may be different from Δx^2, but the spatial resolution of the sensor remains the same.

Spatial Resolution

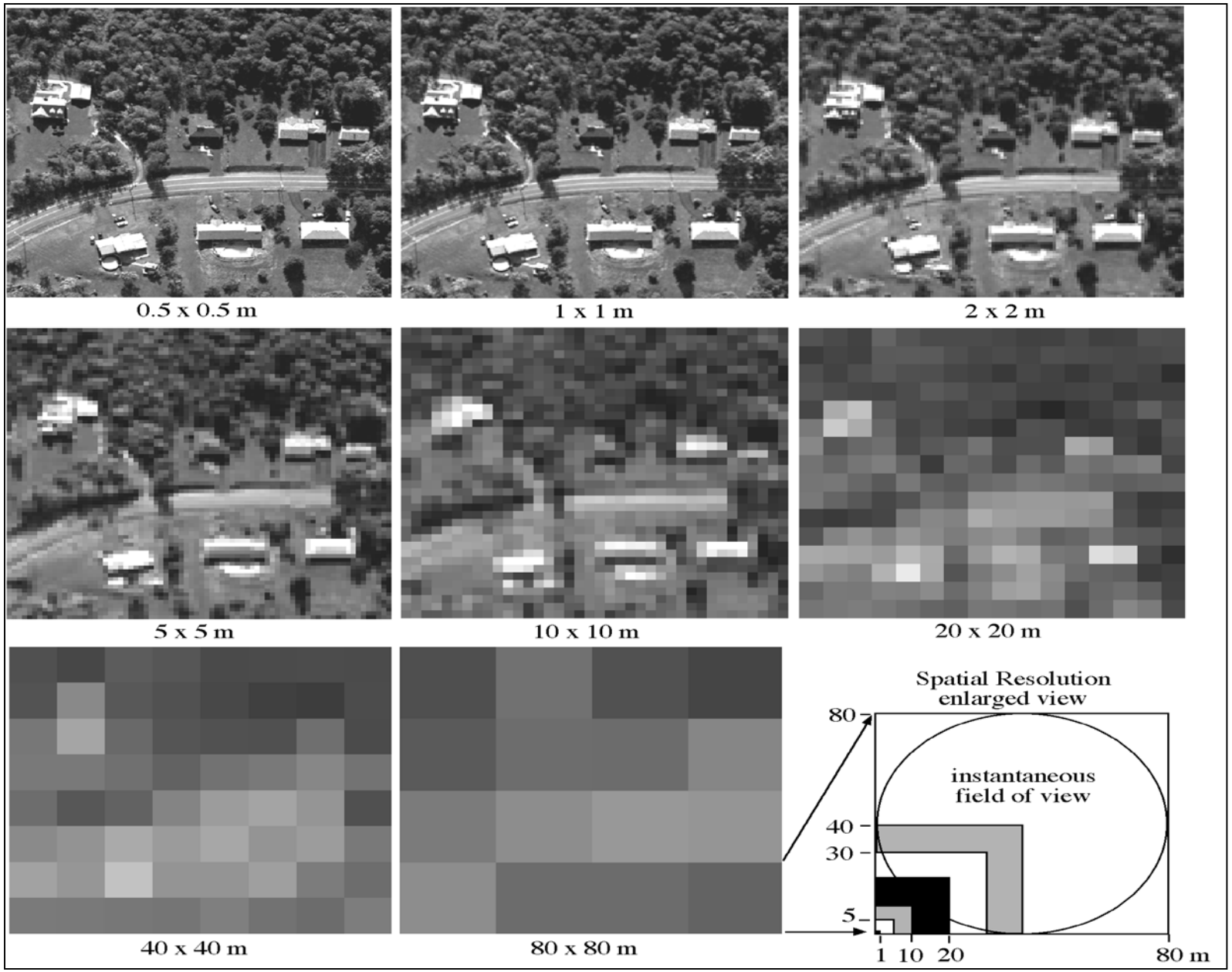

Jensen, 2000

You may find that spatial resolution is defined as the smallest object that can be identified by the instrument. But, this is not always the case:

LandSat TM ($\Delta x=30m$)

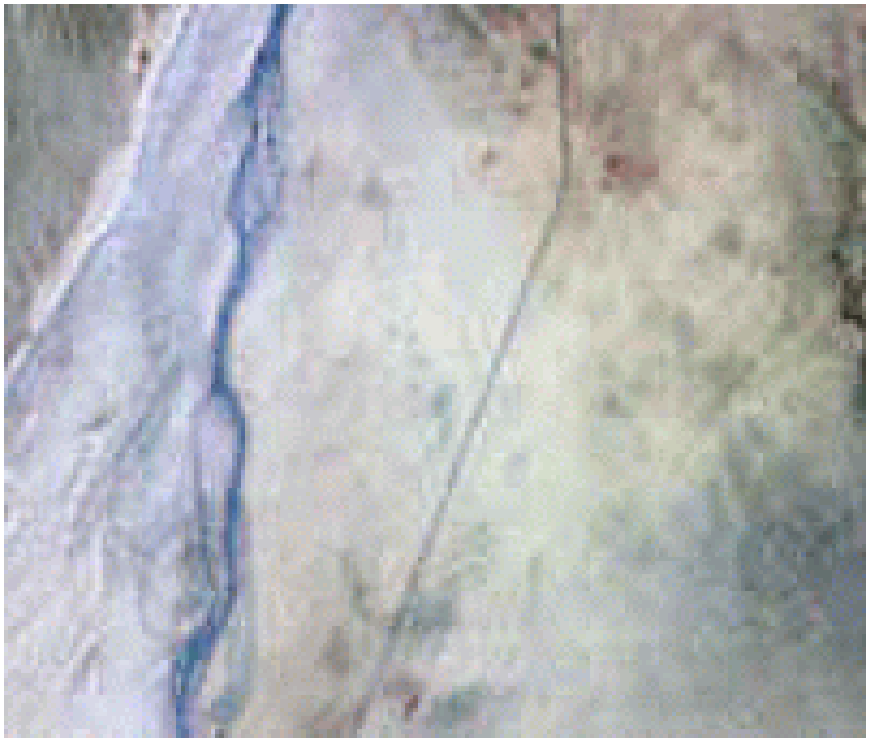

Tunisia

Under certain conditions, objects smaller than Δx can be identified

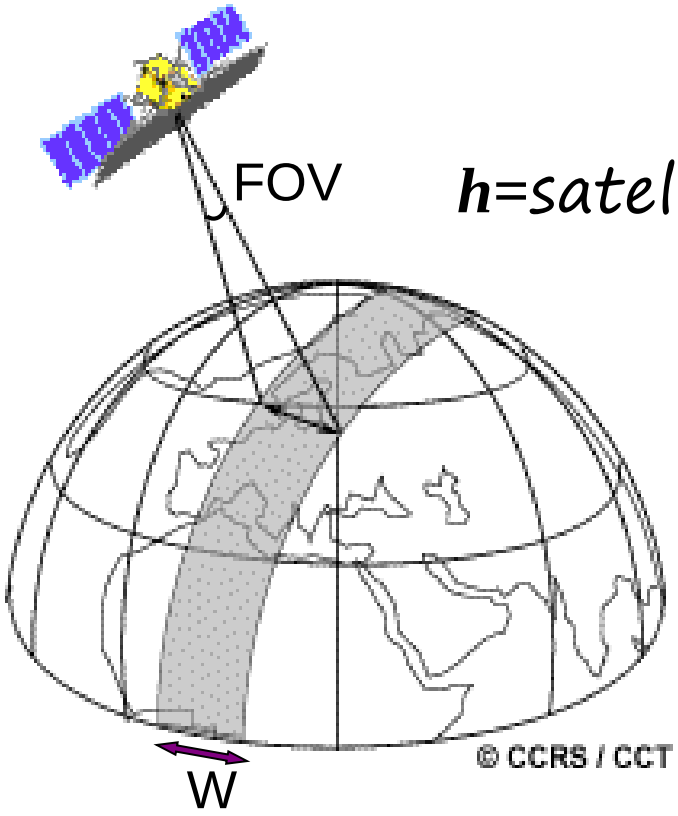

$$W = 2 \cdot h \cdot tg(FOV/2)$$

FOV=Field of View
is the total angle under which the measurements are performed.

If the spatial resolution is high (small Δx), the swath does not cover a wide region (small **W**).
If resolution is low, it is possible to cover large areas

Canberra (Australia)

LandSat MSS
W=185 km, Δx=80 m

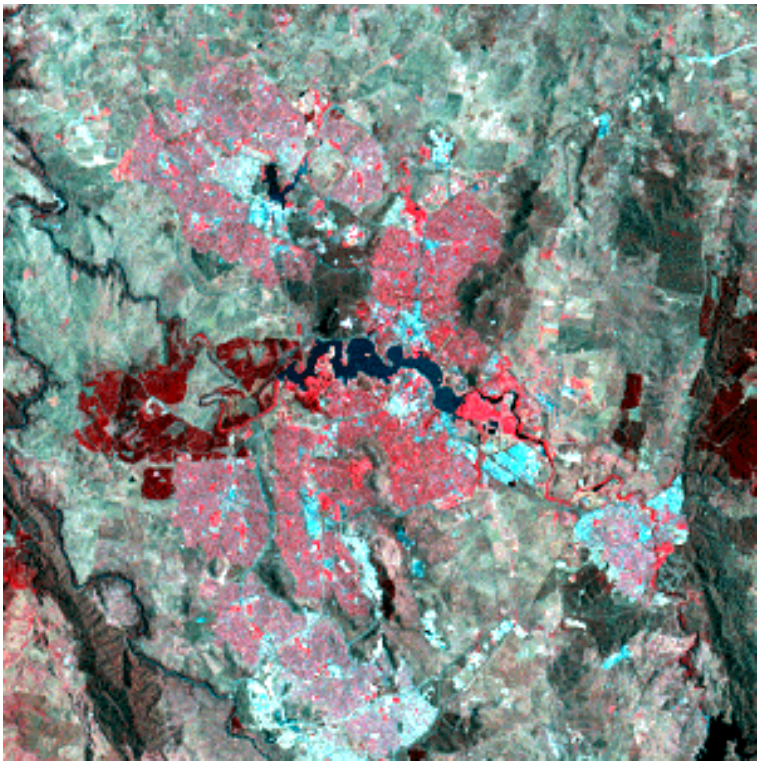

SPOT XS
W=60 km, Δx=20 m

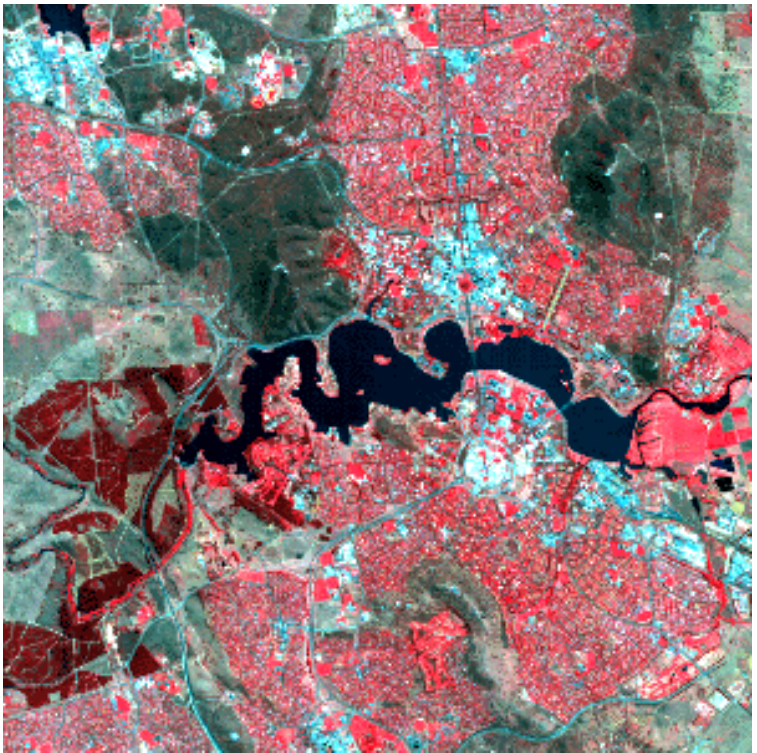

The spatial resolution of passive systems is given by the geometric relationship:

$$\Delta x = h \cdot IFOV$$

The istantaneous field of view of a diffraction-limited sensor is:

$$IFOV = \frac{\lambda}{D}$$

D is the linear dimension of the aperture of the observation system.

In order to get spatial resolutions of the order of tens of meters from satellite altitudes, you would need instruments with $\boldsymbol{IFOV=10^{-4} \div 10^{-5}}$ rad

At microwave frequencies, high resolutions are forgone in favor of **D** with a maximum value of 10 m

At optical wavelengths, very small apertures would be required to get high resolutions (***D~1***mm). However, such small sensors are not used. To understand why, let's calculate the radiant flux arriving at the sensor:

$$\Phi = \int L \cdot dA_a \cdot \cos\vartheta \cdot d\Omega = L \cdot D^2 \int_0^{2\pi} \int_0^{IFOV/2} \cos\vartheta \cdot \sin\vartheta d\vartheta d\phi =$$

$$= \pi L \cdot D^2 \sin^2 \frac{IFOV}{2}$$

with $\boldsymbol{L}$ = radiance (supposed uniform within ***IFOV***) of the surface observed within ***IFOV***

The power measured by the sensor gets higher as the aperture area gets higher, and as ***IFOV*** gets higher.

At optical wavelengths, the radiant flux of diffraction-limited sensors is very low. For this reason, sensors that do not depend on the diffraction limit are used instead.

In optical sensor, the aperture is made up by a lens with dimensions **D**, that collects the electromagnetic radiation and focuses it on a photodetector of length D_f, positioned at the focus of the lens (at distance **f**).
The photodetector transforms the electromagnetic energy in another form (heat, current) that is then measured.

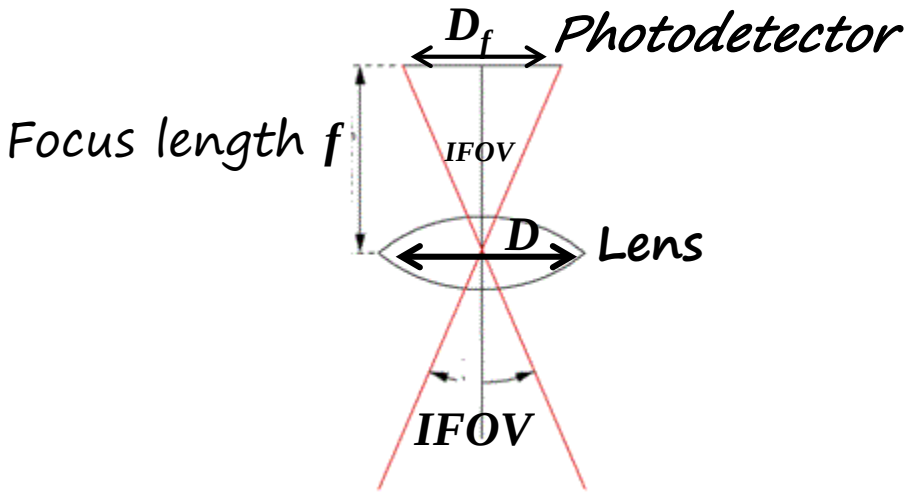

Therefore, you have:

$$IFOV = \frac{D_f}{f}$$

that depends on the optical parameters of the sensor only (it does not depend on λ, **h** and **D**)

The aperture dimensions **D** are selected on the basis of the power that must be measured.
Usually:

$$f \cong D \approx 50cm$$

RADAR Principles

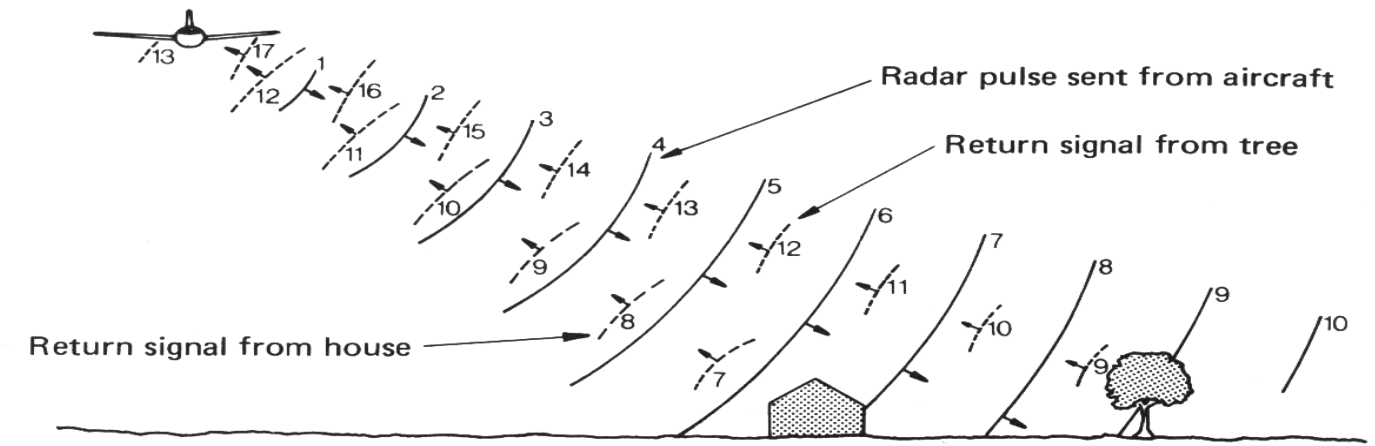

(a) Propagation of one radar pulse (indicating the wavefront location at time intervals 1–17)

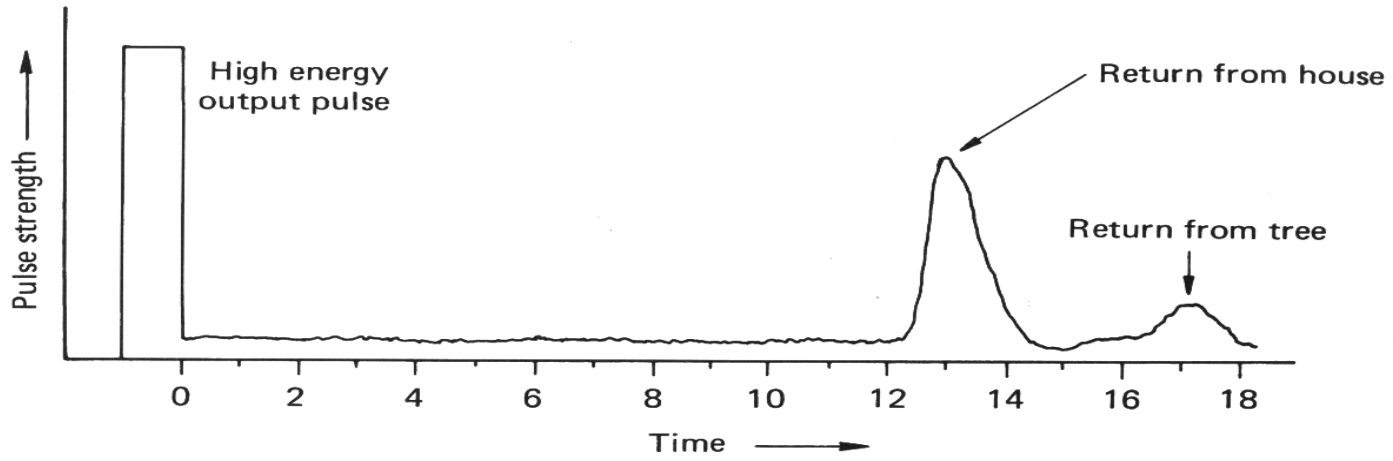

(b) Resulting antenna return

Slant range (SR) is distance between transmitter and object

$$SR = ct/2$$

c = speed of light
t = time between transmission and echo reception.
"2" is there because the pulse has to go to and from the object

By calculating **SR**, we can then transform the return signal into an image!

...radar terms

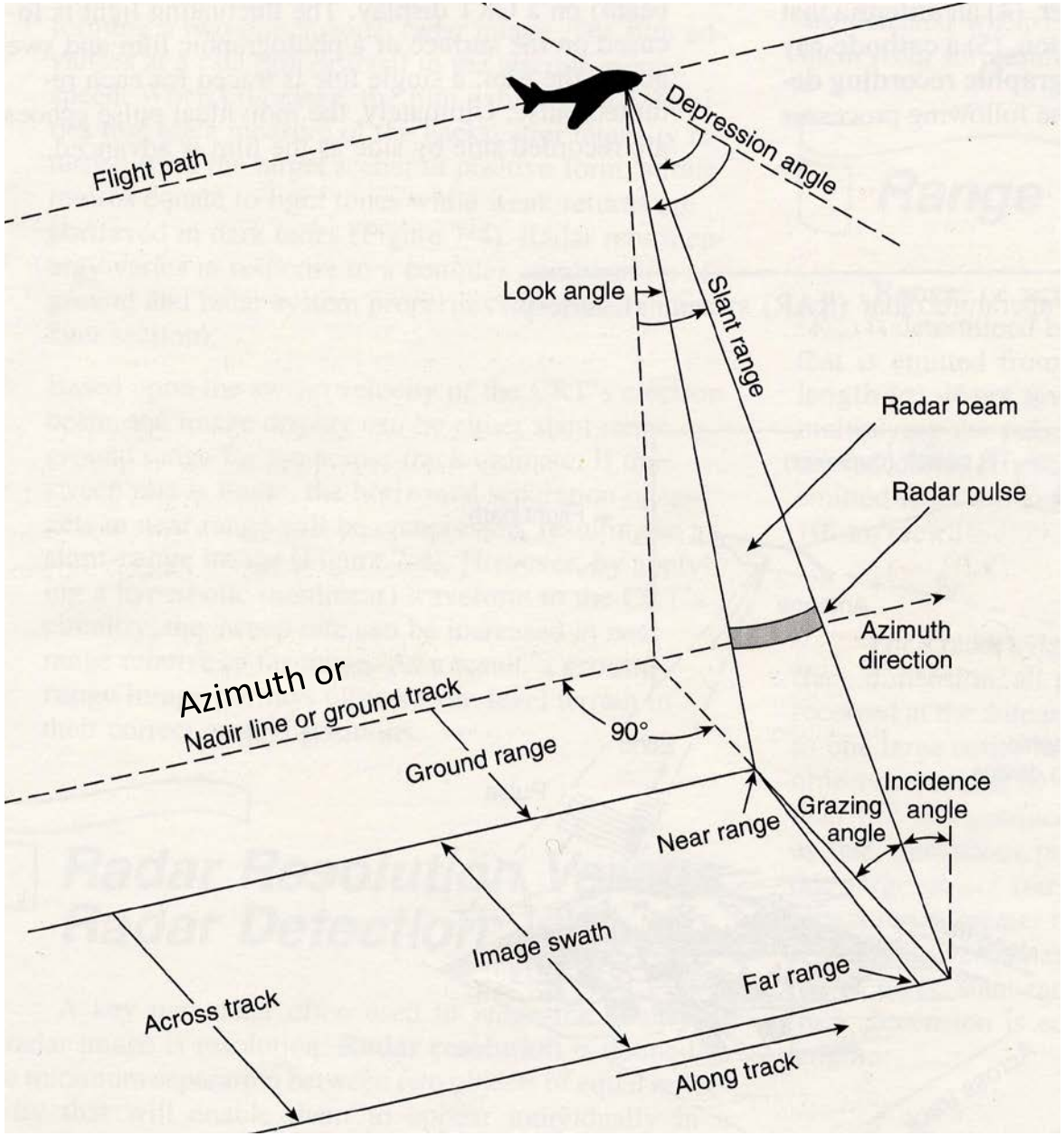

Azimuth direction: the direction the airplane/satellite is moving

Slant Range direction: direction of radar illumination

Ground Range: Slant range projected on the ground

Incidence angle or **Look angle** (ϑ): the angle between the slant range and nadir

Depression or **grazing angle** (γ or ε): the angle between the horizontal plane (containing azimuth and ground range) and the slant range

For a flat surface $\gamma = 90 - \vartheta$

The angles ϑ and γ vary between **near-range** and **far-range**

Real Aperture Radar

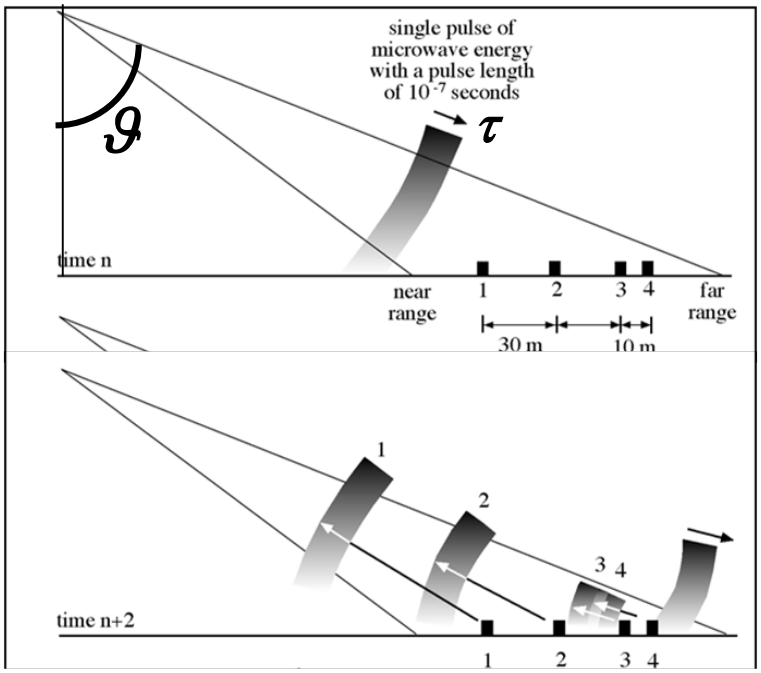

τ is the pulse length.

The echoes from two different objects will arrive with different time delays.
The two objects will be recognized if their distance is larger than

$$R_r = \frac{c\tau}{2\sin\vartheta}$$ which is the **ground range resolution**

(the echo signal from 4 overlaps the echo from 3 since 4 and 3 are closer than R_r)

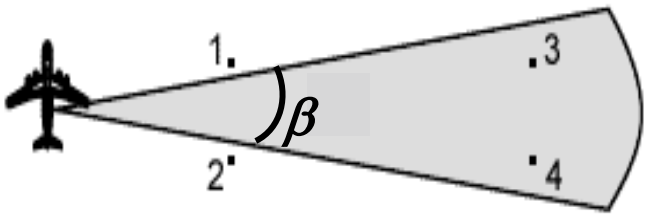

Beamwidth $\beta = \lambda/D$

Two objects can be separated in azimuth if their azimuth distance is larger than

$$R_a = \frac{h}{\cos\vartheta}\beta$$ which is the **azimuth resolution**

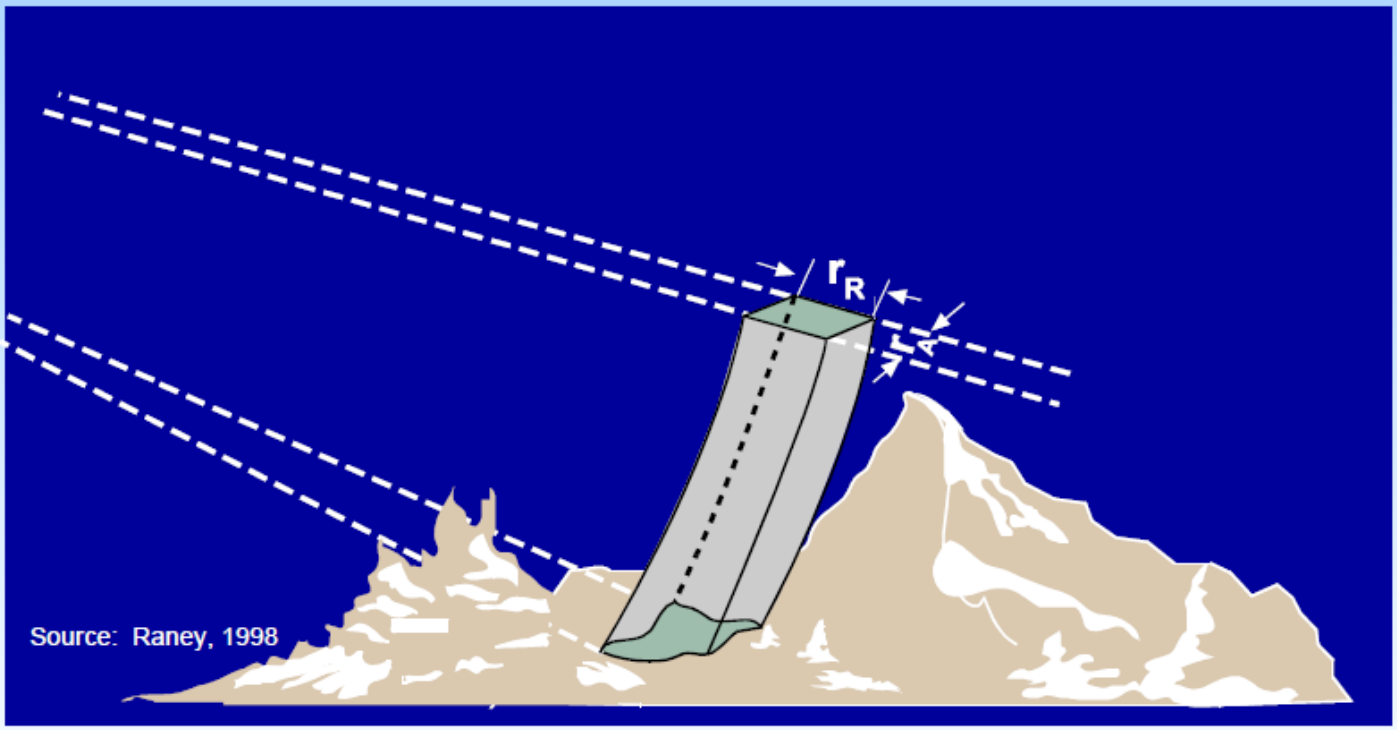

r_R = range resolution

r_A = azimuth resolution

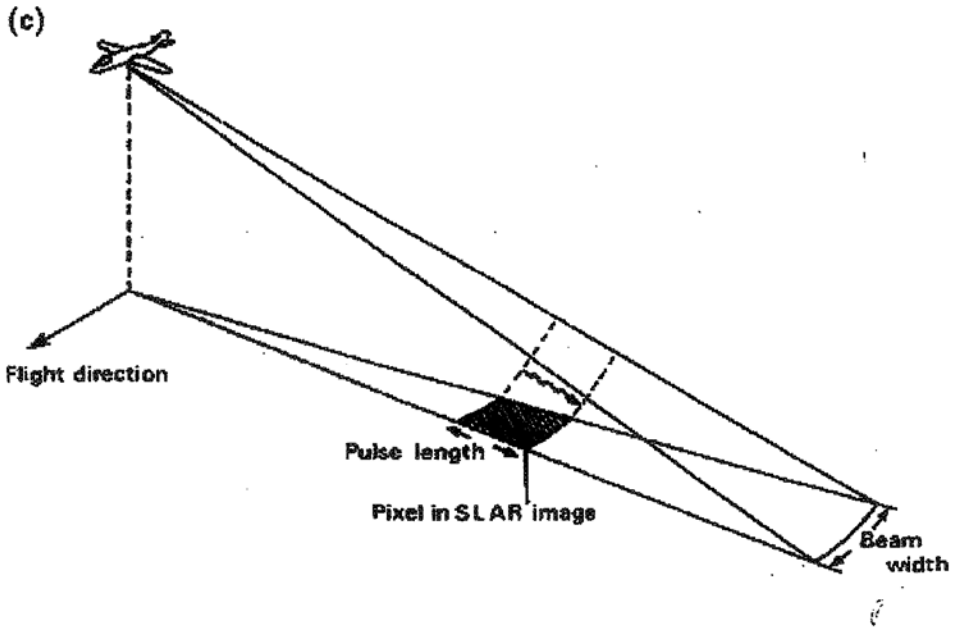

The range resolution of a Radar depends on the pulse length τ: shorter pulses result in higher resolution.

For a real aperture radar, azimuth resolution is determined by the angular beamwidth containing the radar illumination, and it improves as the antenna length gets larger and larger.
However, there is a practical limit to antenna dimension on board satellites.

A Synthetic Aperture Radar (SAR) uses signal processing to refine azimuth resolution to smaller values than those fixed by the antenna length.

The SAR signal processing uses measurements acquired in successive positions of a small antenna to simulate a large antenna.

Synthetic Aperture RADAR

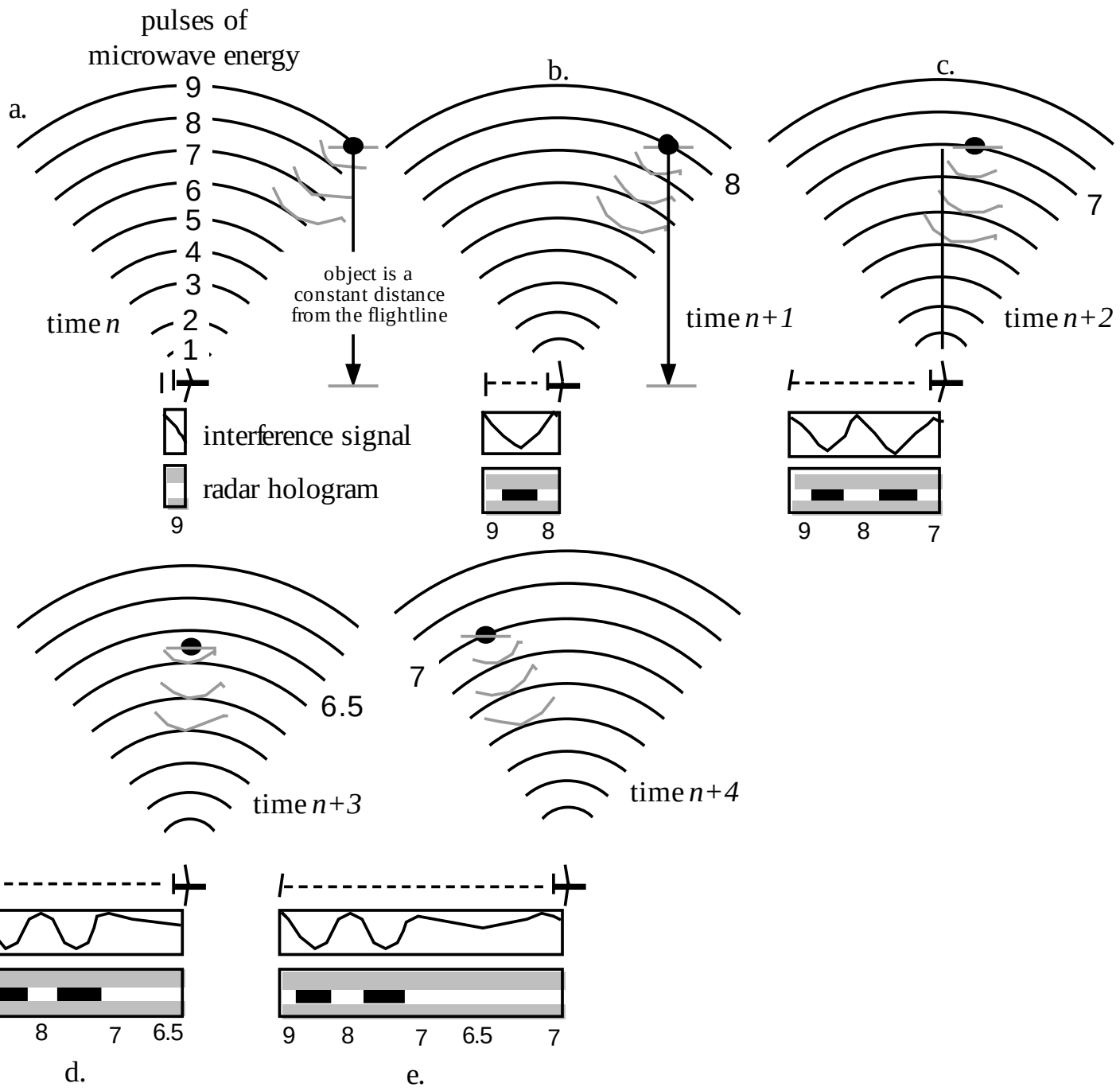

During radar motion, the same object is viewed multiple times. The image is assembled from multiple looks from different angles (sorted by frequency).

To perform SAR processing, you need not only the echo time delay, but its frequency as well. Based on the Doppler history of the object, its position is located with a high resolution (Doppler shift: lower frequency behind the sensor, higher ahead).

SAR (Azimuth resolution)

The motion of the aircraft is used to generate a long synthetic antenna

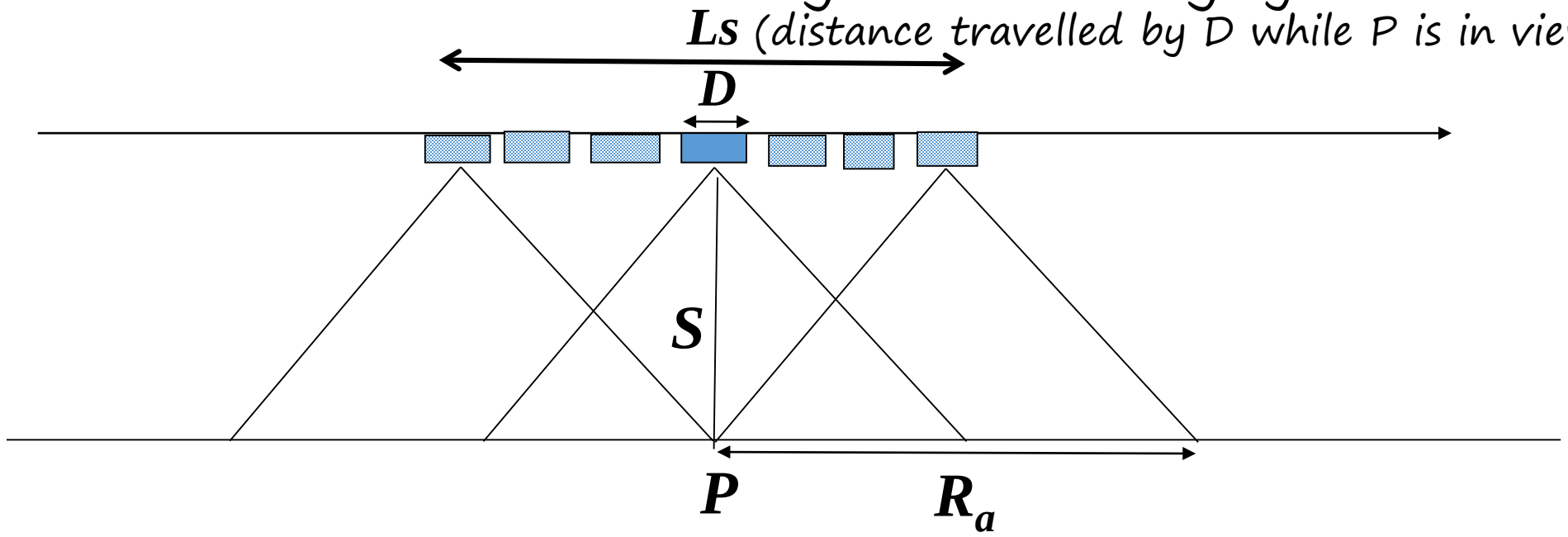

Azimuth resolution of a RAR is $R_a = S\lambda/D = H/\sin\gamma \cdot \lambda/D$, where H = height.

An antenna array of length Ls has a beamwidth $\beta_s = \lambda/(2\,Ls)$.

So, for synthetic aperture of length Ls, and slant range $S = H/\sin\gamma$, we have

$Ls = R_a = S\lambda/D$, and $R_{a,\,SAR} = S \cdot \beta_s = S \cdot \lambda/(2\,Ls) = S \cdot \lambda/2 \cdot D/(\lambda S) = D/2$

So $R_{a,\,SAR}$ is independent of H, and improves as D gets smaller

Synthetic Aperture RADAR

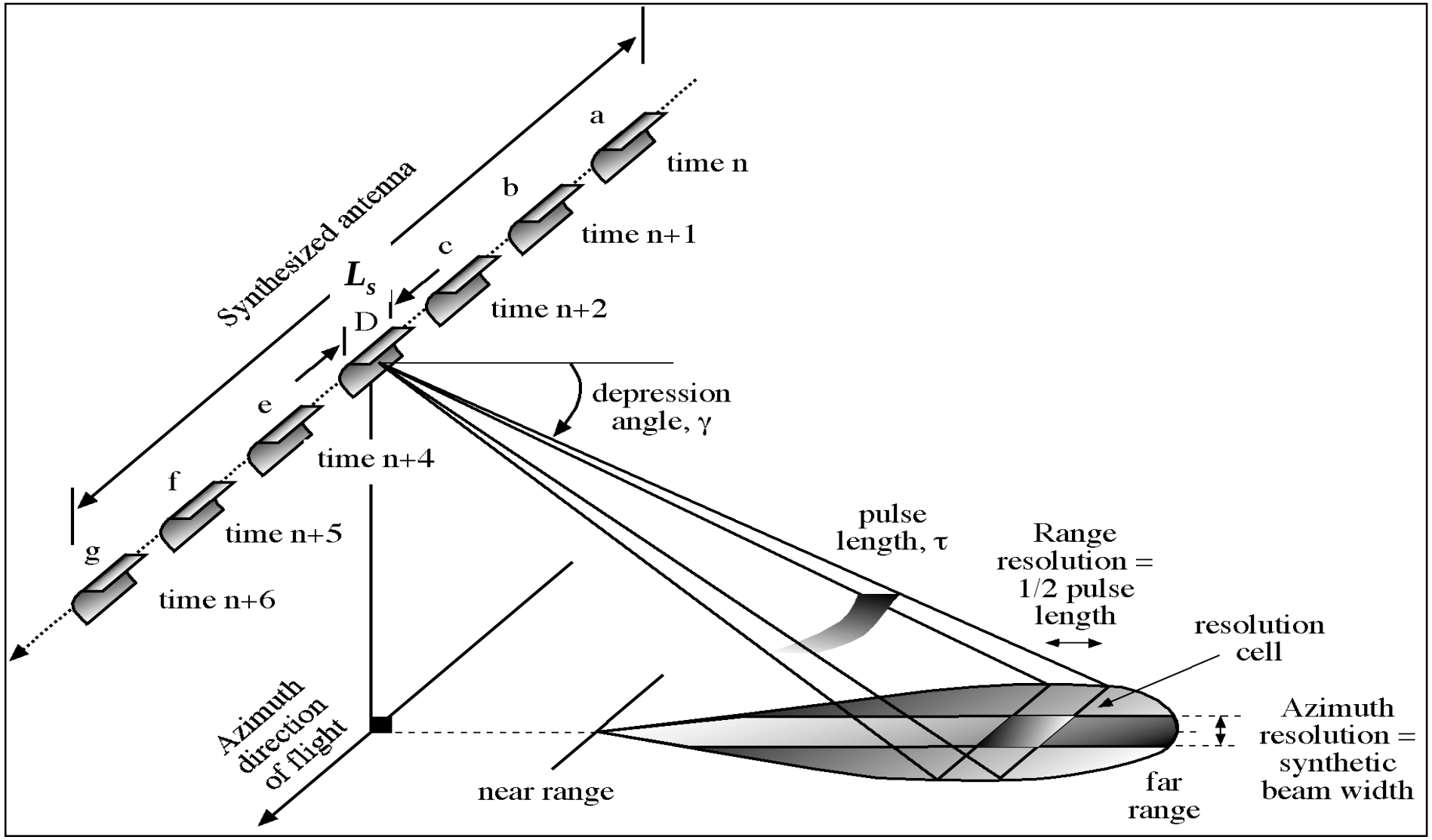

Jensen, 2000

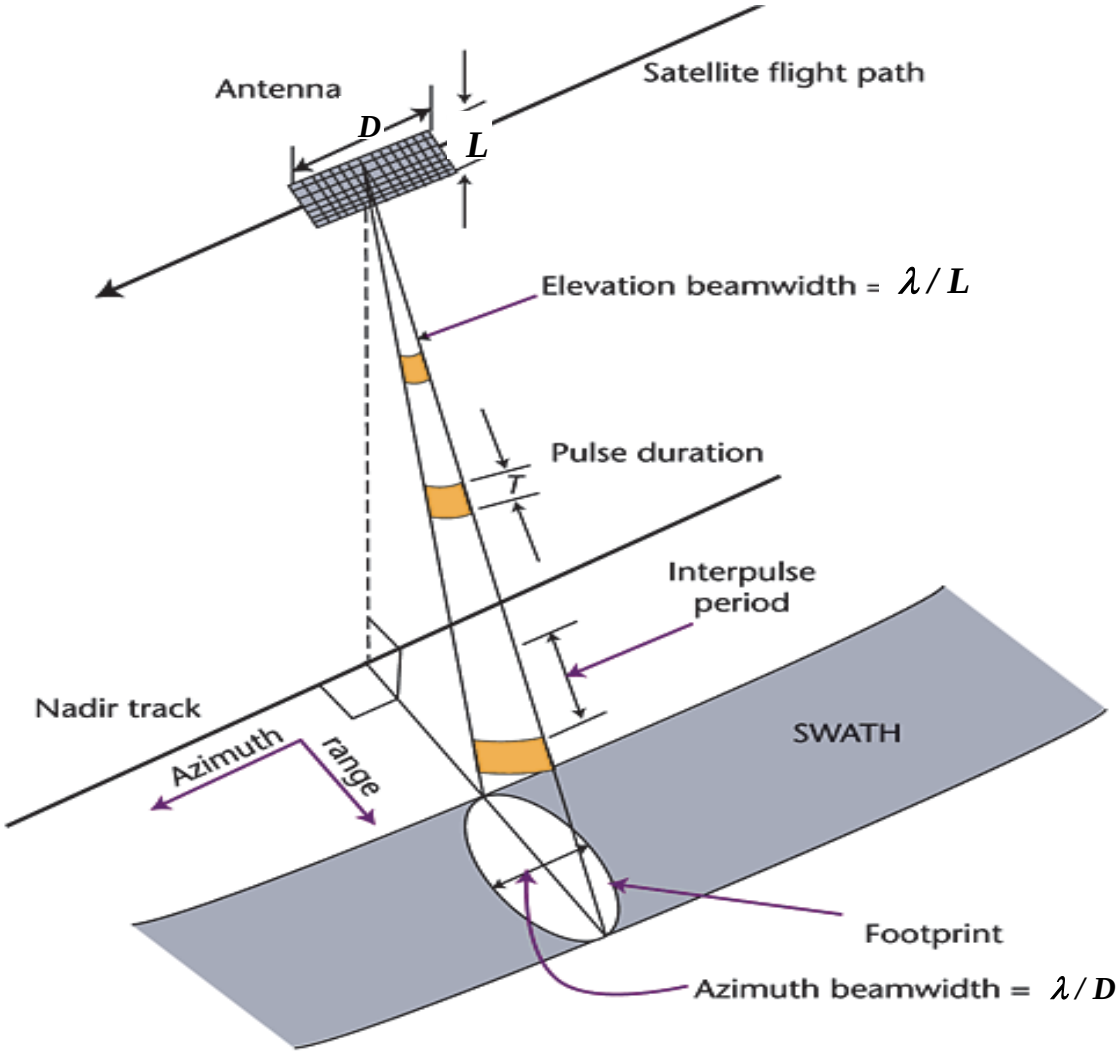

D=antenna length in the along-track direction
L=orthogonal antenna length

The swath of a RAR is:

$$W = \frac{h}{\cos^2 \vartheta} \frac{\lambda}{L}$$

no fundamental difference between light we can see and light we can't see

- Our eyes are fairly limited – very narrow range of EM spectrum!
- Near infrared is a much wider band, behaves similarly to visible, but we can't see it.
- Infrared and microwaves also useful for remote sensing of the Earth

Visible

Near IR

Photos by Andzrej Wrozniak

More Terms

Along with radiance, radiant flux, etc., more terms are needed to discuss the interaction of radiation with matter. One of them is ***Reflectance***

Surfaces viewed by a sensor at optical wavelengths are *illuminated* by the Sun, and the incident flux density – the irradiance – is reflected by the surfaces.

The reflected portion allows the object to be seen!

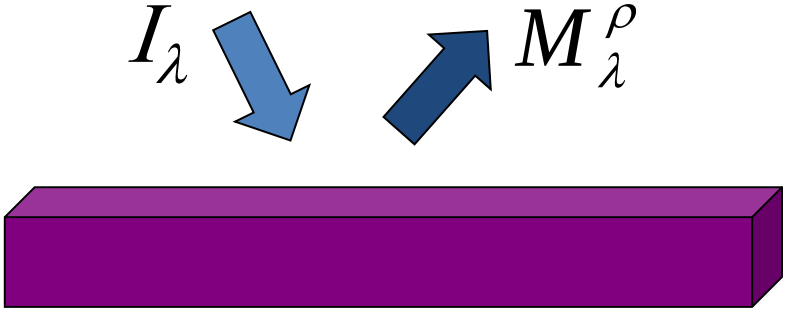

$$\rho_\lambda = \frac{M_\lambda^\rho}{I_\lambda}$$

Spectral Reflectance ρ_λ: ratio of the spectral reflected exitance M_λ^ρ to the spectral incident irradiance I_λ (spectral quantities are required to make measurement independent of the instrument bandwidth)

Note differences between bands at different locations

Why do differences exist?

- different materials reflect differently
- different wavelengths interact with materials differently

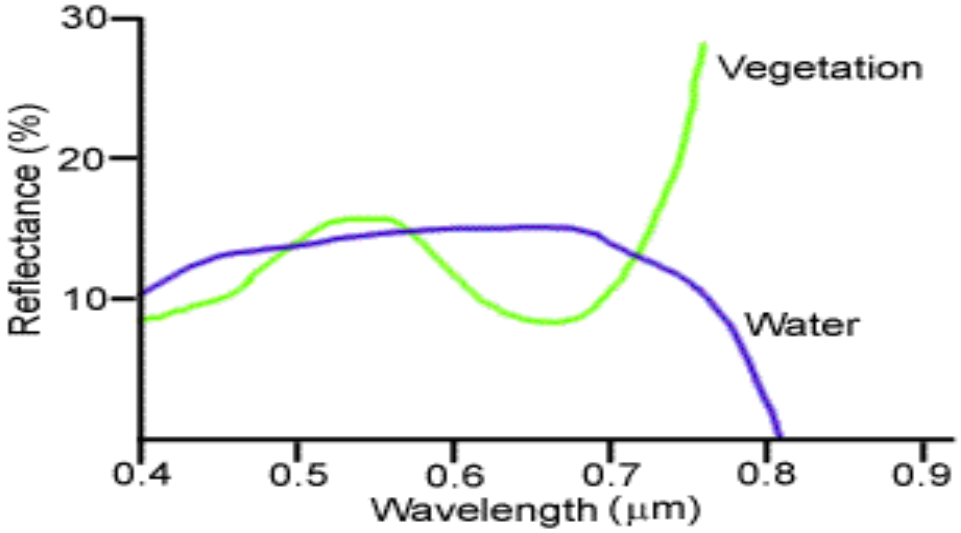

spectral reflectance curves
or, better,
SPECTRAL SIGNATURES
for
vegetation and water

- maximum in IR for vegetation
- minimum in IR for water

Spectral Signatures

pinewoods, grasslands, sand pit similar (not good choice)

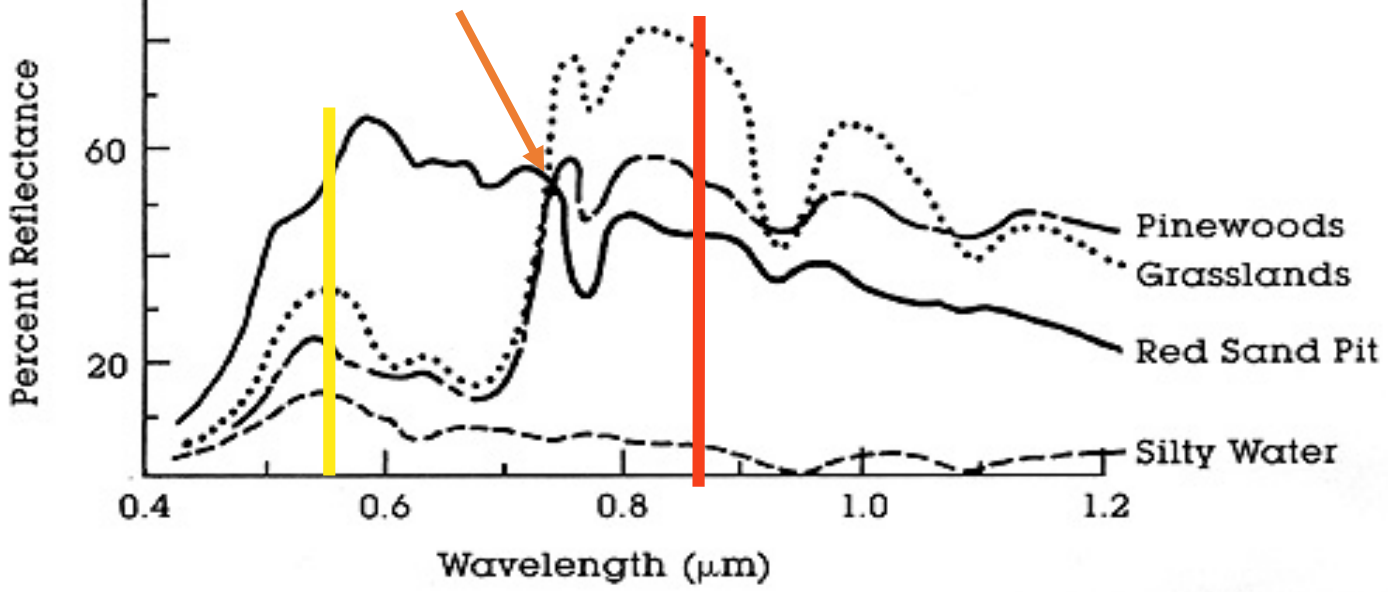

RS instruments will only cover certain wavelength regions depending upon sensor

You need to pick a channel in which features may be discriminated

For example, you can compare reflectances for 2 bands

...idea is to have maximum separation of reflectances for different objects

Detectors are designed to measure specific parts of the spectrum

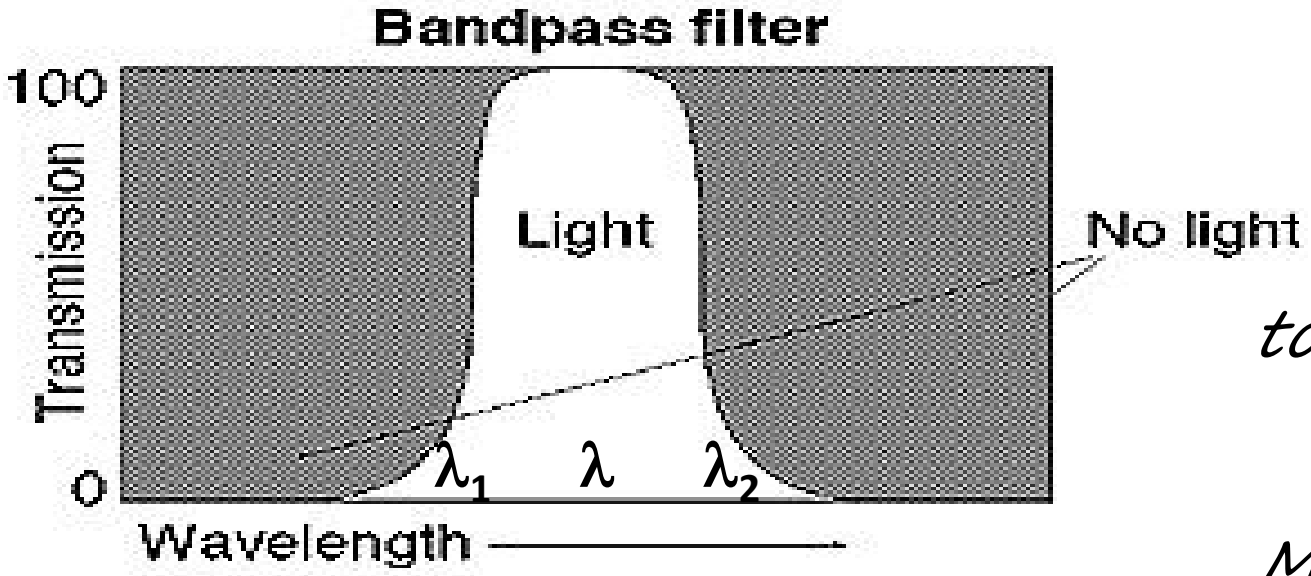

this leads to concept of
spectral resolution

each detector corresponds
to a "band" or wavelength region
$\Delta\lambda=\lambda_2-\lambda_1$ around λ

More detectors yield more bands,
which give rise to greater
spectral resolution

$$T(\lambda) = \frac{\Phi^{measured}}{\Phi}$$

(also called Responsivity or
Sensor Response Curve)

Detector designed for different portions of the
EM spectrum use different materials.

The radiant flux measured by a RS instrument is:

$$\Phi = \int \pi D^2 L_\lambda \sin^2 \frac{IFOV}{2} T_\lambda d\lambda$$

T_λ can be assumed ~1 inside $\Delta\lambda$, so that for a Lambertian surface

$$\Phi = \pi L_\lambda D^2 \sin^2 \frac{IFOV}{2} \Delta\lambda$$

Now remind the relationship between exitance and radiance for a Lambertian surface ($M_\lambda = \pi L_\lambda$), and the expression for the Solar Irradiance on Earth (I_λ^{sun})

$$\rho_\lambda = \frac{M_\lambda^{refl}}{I_\lambda^{sun}} = \frac{\Phi}{D^2 \sin^2 \frac{IFOV}{2} \Delta\lambda} \Big/ B_\lambda(6000) \cos\theta_s \frac{\pi R_s^2}{d_{ST}^2}$$

Spectral resolution is determined by:

- The number of spectral bands of the sensors (channels)
- the amplitude of spectral bands (bandwidth) of the sensor, which is indicated with

$\Delta\lambda$ in μm, or νm

Δf in Hz

A high spectral resolution is necessary when discrimination of objects is based upon the spectral response.

Panchromatic band

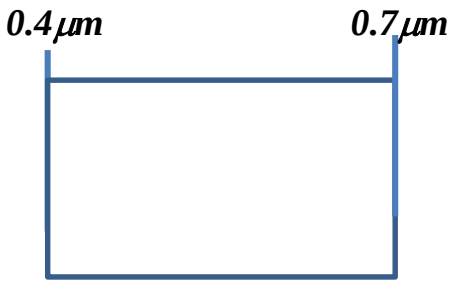

1 channel

$\Delta\lambda$=0.3μm

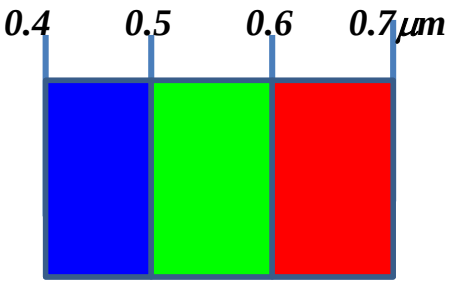

3 channels

$\Delta\lambda$=0.1μm

Spectral resolution

- The incoming energy is separated into several spectral components that are independently sensed
  - Multispectral – few bands, defined using optical filters
  - Hyperspectral – many bands, split using a prism or diffraction grating

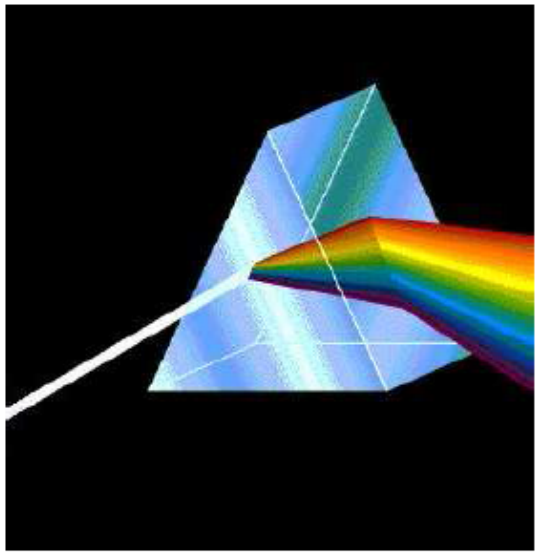

- Filters, dichroic gratings to separate thermal forms but detectors themselves can be varied to be sensitive to particular wavelength ranges (varying HgCdTe)

Cross-Track scanner (whiskbroom)

Scanning mirror, multiple discrete detectors and dispersing element: instead of a band filter for each detector, a **dispersing element** (a prism) breaks the incoming light into component wavelengths. Light is dispersed across a linear array of detectors.
A rotating mirror and forward movement create the spatial arrangement of pixels.

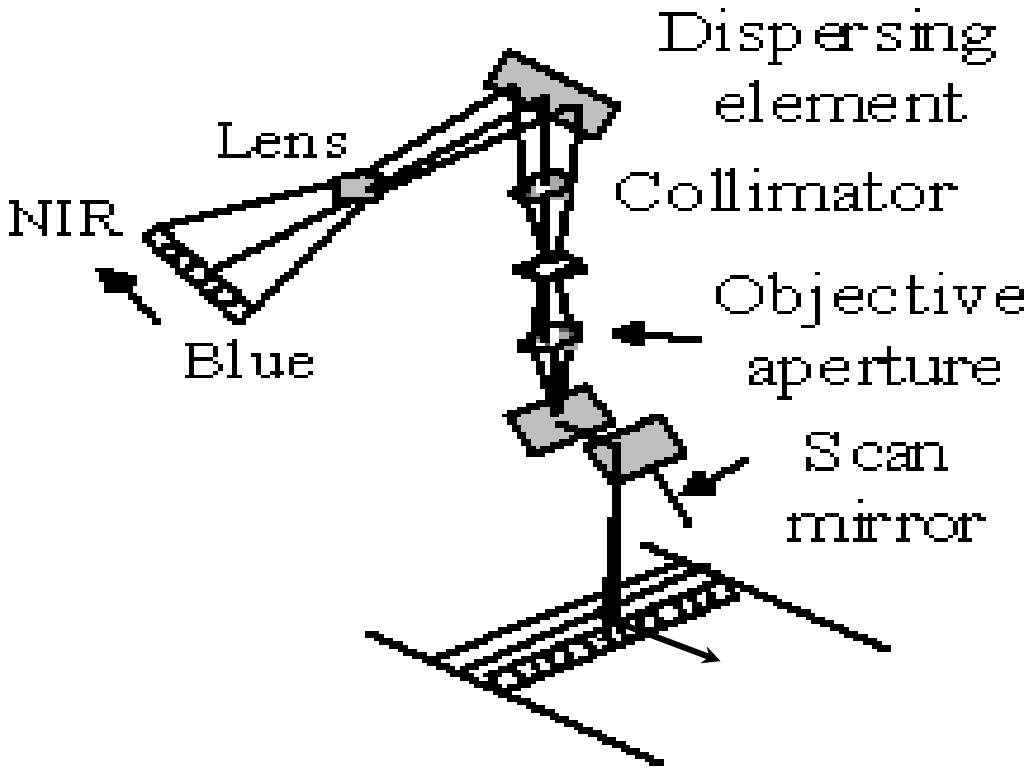

The advantage of a dispersing element vs. filters is that narrow bands can be detected in a small instrument

- ***Sensor spectral response curves***
  - ***several multispectral systems*** *(Fig. 3-8, p79)*

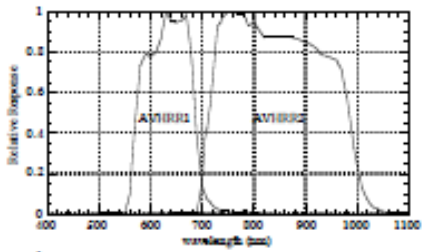

AVHRR

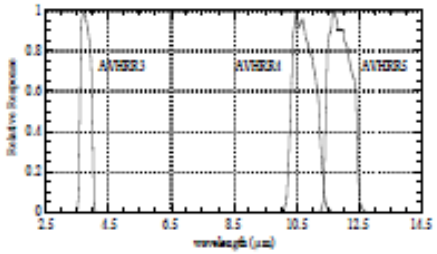

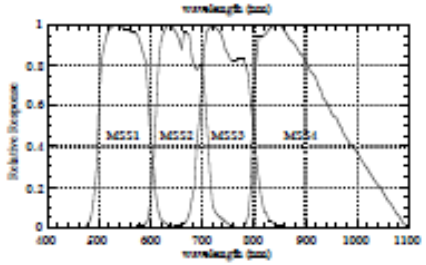

Landsat MSS

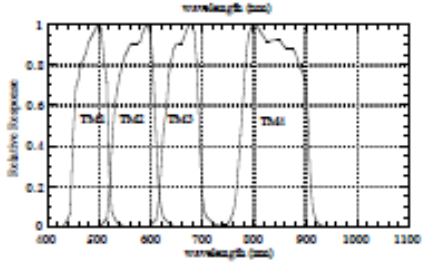

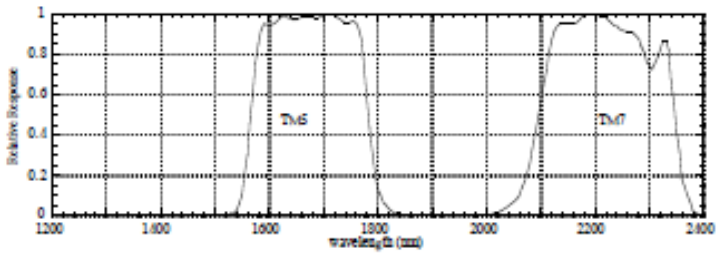

Landsat TM

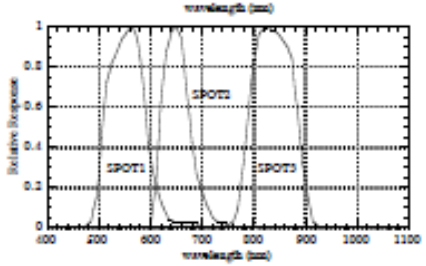

SPOT

Spectral Resolution

- As in the spatial case, the width of the instrument spectral response determines its ability to record detail in the spectral signal
- Hyperspectral systems with narrow spectral responses (typically about 10nm) are useful for detecting fine spectral detail

Simulation of spectral doublet measurement with two different spectral resolutions

TM

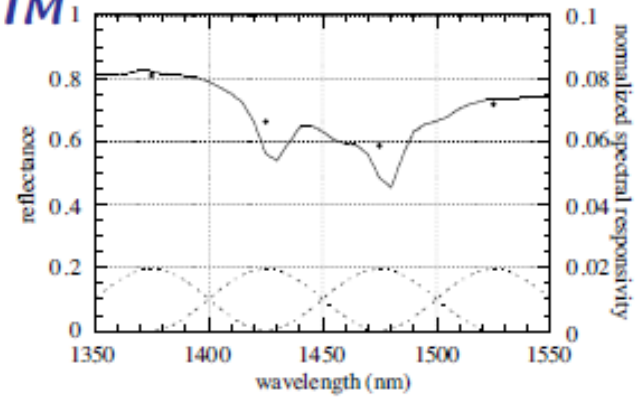

AVIRIS

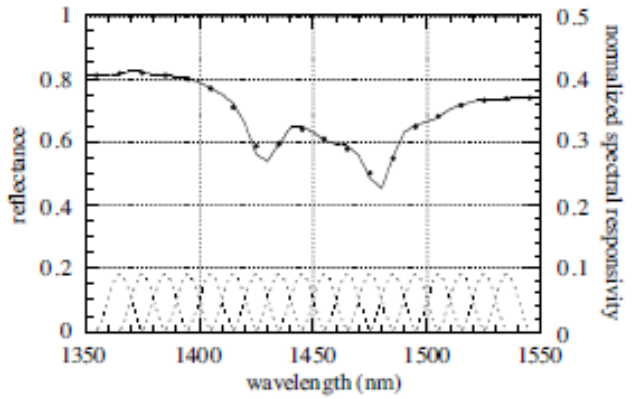

Radiometric resolution concerns the sensitivity of the instrument to electromagnetic radiation, and it represents the minimum power difference that can be detected by the sensor.

Radiometric resolution is often indicated with NEP (Noise Equivalent Power) or with NEΔL (Noise Equivalent Radiance), i.e., the power (or radiance) developed by the background noise intrinsic in the instrument: radiometric resolution gets better as NEP gets lower.

For a typical photodetector, radiometric resolution is given by

$$NEP = \frac{1}{D^*}\sqrt{\frac{D_f^2}{2\tau}} \qquad \text{for} \qquad \lambda > 1\mu m$$

and with

$$NEP = 4.61\frac{hf}{\tau} \qquad \text{for} \qquad \lambda < 1\mu m$$

where D_f is the detector linear dimension, D^* its detectivity (which is a function of temperature and of wavelength).

τ Is the observation duration, i.e., the time lapse during which the sensor performs the single measurement within ***IFOV***.

Generally, in radiometric measurements, the minimum detectable power is inversely proportional to the observation duration (integration time).

Another parameter that is often used to evaluate radiometric resolution is the

Signal to Noise Ratio (SNR).

In the case of optical sensors, ***SNR*** in the spectral interval $\Delta\lambda$ is

$$\mathrm{SNR} = \frac{\phi}{\mathrm{NEP}} = \frac{\pi L_\lambda D^2 \sin^2 \frac{IFOV}{2} \Delta\lambda D^* \sqrt{2\tau}}{\sqrt{D_f^2}}$$

Radiometric resolution gets better
- as IFOV gets bigger,
- as the spectral bandwith gets larger and
- as the integration time gets longer

Dwell Time τ (Integration time)

is the time employed by the instrument to perform a single measurement, i.e., to look at a resolution cell

For a Cross-Track Scanner (whiskbroom) the time τ depends on the tangential velocity of the satellite v projected on the ground

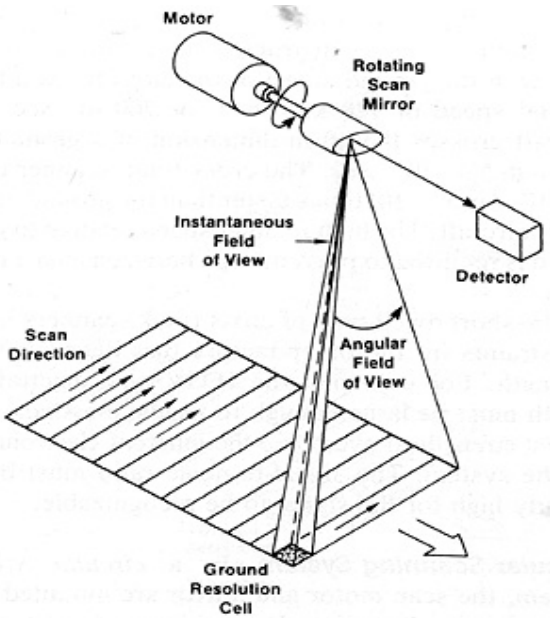

A. CROSS–TRACK SCANNER.

$$v_p = v\frac{R_T}{R_T + h}$$

and on the number N of resolution cells that the sensor must observe while the satellite advances along its nadir track by a distance Δx

$$\tau = \xi\frac{\Delta x}{v_p}\frac{1}{N} = \xi\frac{\Delta x}{v_p}\frac{\Delta x}{W}$$

with $0.5<\xi<1$

In order to increase τ, it is necessary to increase Δx. That is, in order to get a high spatial resolution, it is necessary to decrease τ, with a consequent degradation of radiometric resolution

Along-track scanners (pushbroom) have a higher dwell time:

N photodetectors are placed at the aperture focus, each one of them being dedicated to observation of a single resolution cell

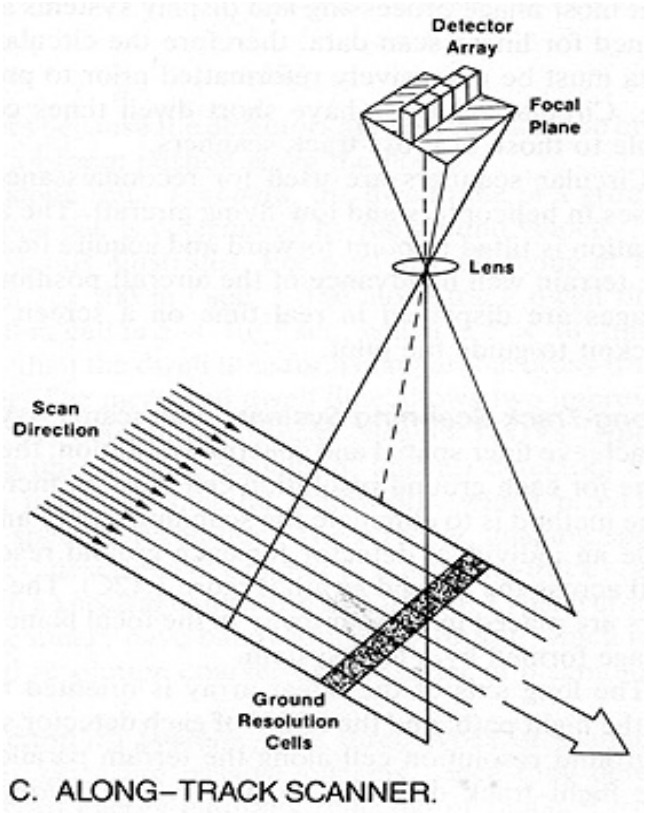

C. ALONG–TRACK SCANNER.

$$\tau_{AT} = \frac{\Delta x}{v_p}$$

$$\tau_{AT} = \frac{W}{\xi \Delta x}\tau_{CT} \approx 10^4 \tau_{CT}$$

Also in this case, a bigger τ means a bigger Δx, but

wrt Cross-Track sensors

For equal spatial resolution, radiometric resolution is better

That is

For equal radiometric resolution, along track sensors have a higher spatial resolution

AT scanners have a smaller swath than CT scanners

Sensor Comparison

- whiskbroom: Landsat Enhanced Thematic Mapper ETM+
- pushbroom: Earth Observer - 1 Advanced Land Imager ALI

Signal-to-Noise Ratio (SNR) - Alaska low-light image , both 30m GIFOV

Landsat ETM+ (November 2000)

EO-1 ALI (December 2000)

When they are recorded, the radiance measurements are discretized, i.e., they are transformed into Digital Numbers (**DN**) that can take on integer values between **0** and 2^M-1.
The discretization interval Δ that separates two adjacent radiance values is defined as:

$$\Delta = \frac{L_{\max} - L_{\min}}{2^M - 1} \geq NE\Delta L$$

L_{max} and L_{min} are the maximum and minimum radiance measurable by the instrument.
The difference $L_{max} - L_{min}$ is called dynamic range of the sensor

All radiance values that differ by a value < Δ, will have the same **DN**. Then, Δ represents the minimum radiance difference that can be sensed.

For a given dynamic range of the instrument, Δ gets smaller as **M** gets larger.
For this reason, radiometric resolution is often indicated with the number of bits **M** of the discretized signal

4 bit image

8 bit image

The higher the number of quantization levels, the greater the sensitivity of the sensor

A special low-light sensor on NOAA satellite can distinguish night lights with 250 times better radiometric resolution than before. It took 312 satellite orbits and 2.5 terabytes of clear, cloud-free data to create this composite view of Earth at night.

Building a Remote Sensor

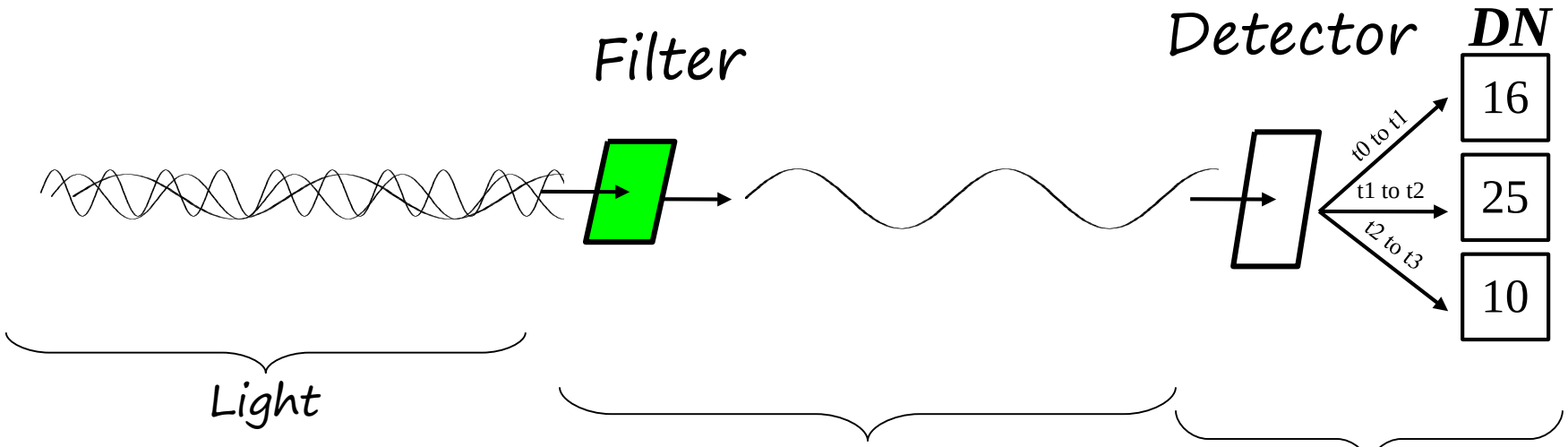

A subset of wavelengths is allowed to pass to the detector. This subset is referred to as a **spectral band**.

Light generates a voltage when it hits the sensor plate. The voltage is sampled for a discrete amount of time (τ), and is "quantized" and recorded as a **digital number** (***DN***).

Important: the detector has a set field of view, and therefore measures **RADIANCE** (in $W/(m^2 \cdot sr \cdot \mu)$).

The **temporal resolution** is the time interval after which the same area is re-observed

Temporal resolution is equal to the Revisit Time

It is measured in days (or hours)

Trade-offs between resolutions

In order to have a high spatial resolution, IFOV must be small but, in this way, radiometric resolution is degraded.

You can increase radiometric resolution increasing the spectral bandwidth but, in this way, spectral resolution is degraded.

On the contrary, a low spatial resolution allows a good radiometric and spectral resolution.

A good time resolution can overcome the drawbacks of a low spatial or spectral resolution.

The fundamental radar equation

$$P_r = \frac{P_t G_t}{4\pi R^2} \sigma \frac{A_r}{4\pi R^2}$$

relates characteristics of the radar, the target, and the received signal

Consider an antenna that approximates a **point source**, radiating in all directions.

P_t is the power transmitted toward the target that is at distance R.

The power density on the target is $\frac{P_t}{4\pi R^2}$

All real antennas are **directional**, i.e., they emit radiation into a fixed solid angle. The concentration of power into a (relatively) small solid angle is described by the gain.

G_t is the gain of the transmitting antenna in the direction of the target,

σ is the effective backscatter area of the target, and A_r is the area of the receiving antenna. (Note that $A/G=\lambda^2/4\pi$)

P_r is the power received by the antenna

Finally, it is the effects of terrain on the radar signal that we are most interested in, i.e. the amount of *radar cross-section*, σ, per unit area A on the ground. This is called the ***radar backscatter coefficient*** and is computed as :

$$\sigma^0 = \frac{\sigma}{A}$$

The *radar backscatter coefficient* determines the percentage of electromagnetic energy reflected back to the radar from within a resolution cell.

The σ^0 of a surface depends on a number of terrain parameters like geometry, surface roughness, moisture content, and the radar system parameters (wavelength, incidence angle, polarization, etc.).

Scattering Mechanisms

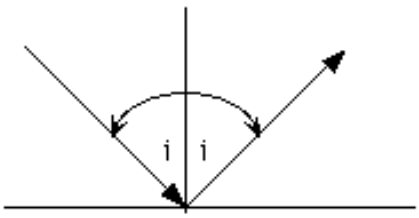

Reflection off a smooth surface
The angle of incidence, i, equals the angle of reflection.

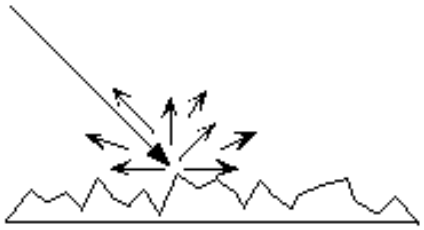

Scattering off a rough surface
The variation in surface height is on the order of the incoming signal's wavelength.

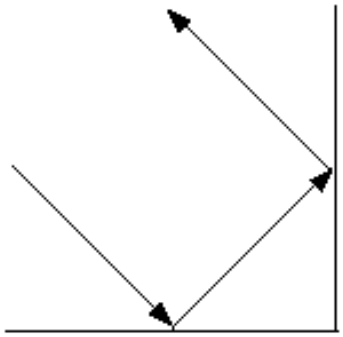

Double Bounce
(Corner Reflector)

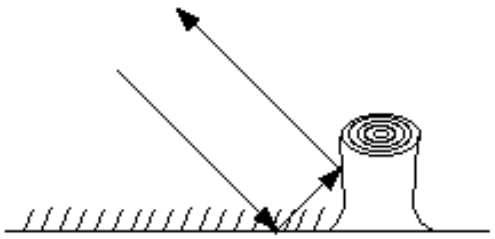

Double Bounce
One possible natural occurence - reflecting off two smooth surfaces, grass and a freshly-cut tree's stump

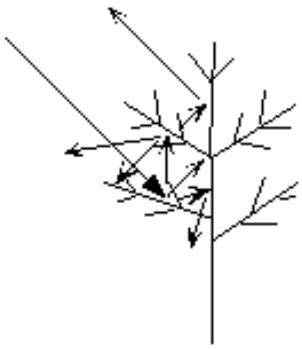

Volumetric Scattering
Example scattering in a tree

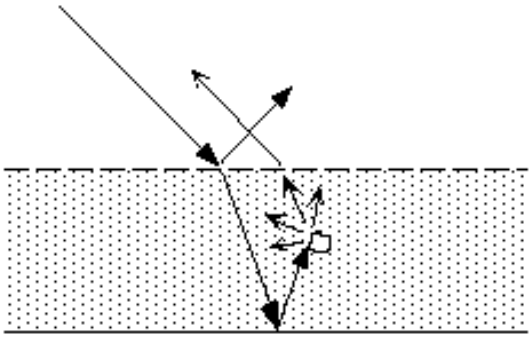

Volumetric Scattering
In this example the incident radiation is both reflected and refracted/transmitted through a layer of dry snow. The refracted radiation then reflects off underlying ice, scatters off a chunk of ice in the snow, and finally refracts back toward the receiver.

Foreshortening

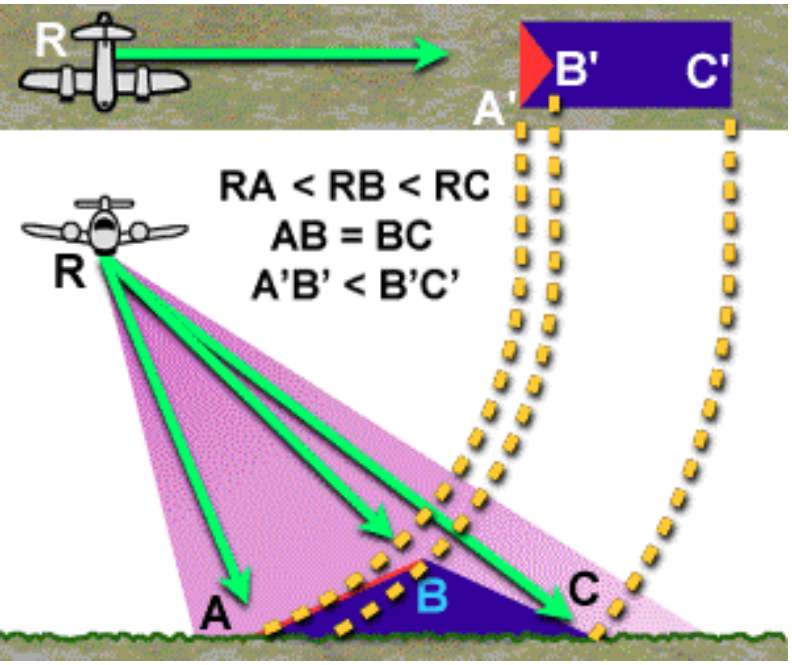

While the hill slopes ***AB*** and ***BC*** are equal, the foreslope (***AB***) is compressed (***A'B'***) much more than the backslope (***BC***) is compressed (***B'C'***), due to the radar imaging geometry.

Layover

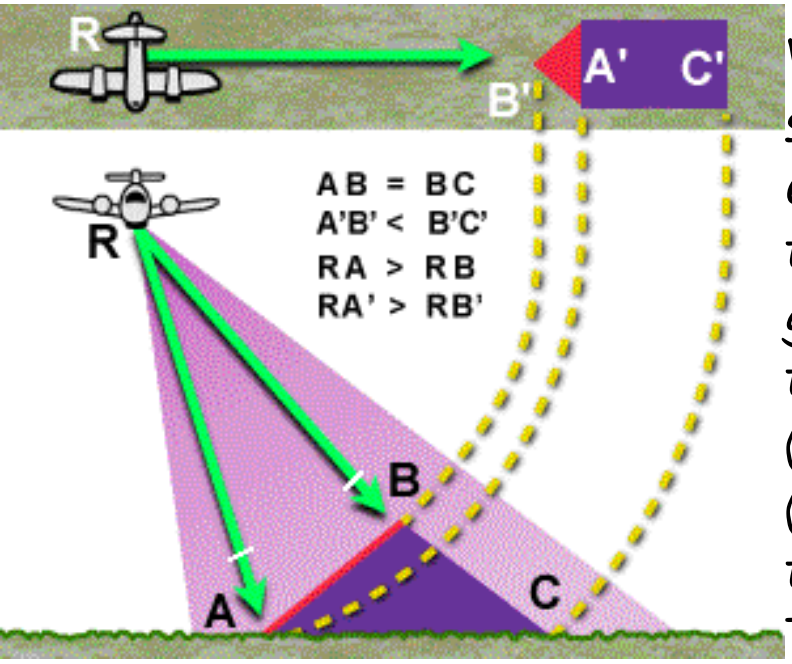

While the mountain slopes ***AB*** and ***BC*** are equal,
the radar imaging geometry dictates that the radar-facing slope (***AB***) will be imaged (***B'A'***) as leaning toward the radar.
This is due to ***RA*** > ***RB***.

The slant geometry of radar leads to foreshortening and layover

foreshortening (moderate slopes)

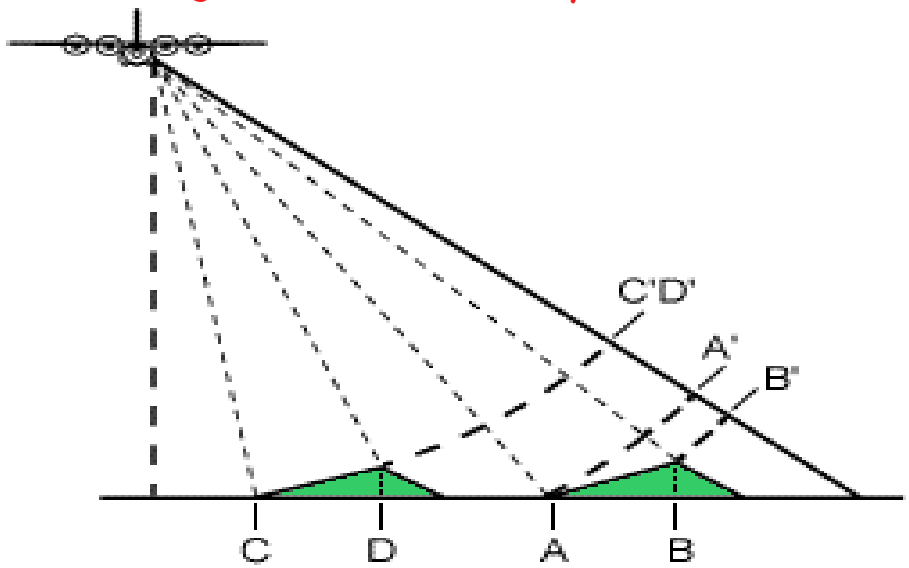

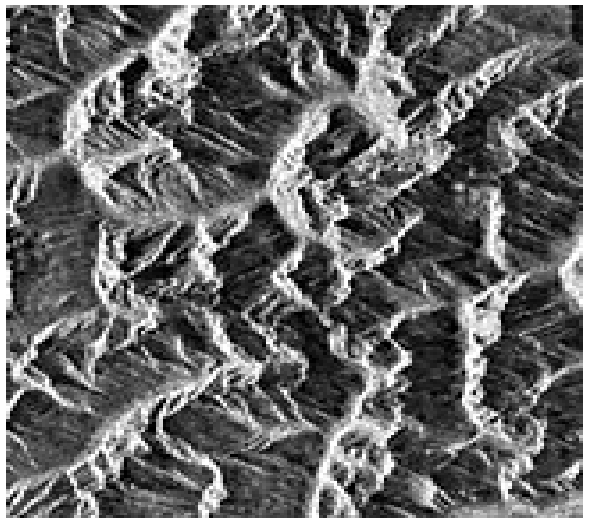

slopes appear shorter than they are

layover (steep slopes; tall objects)

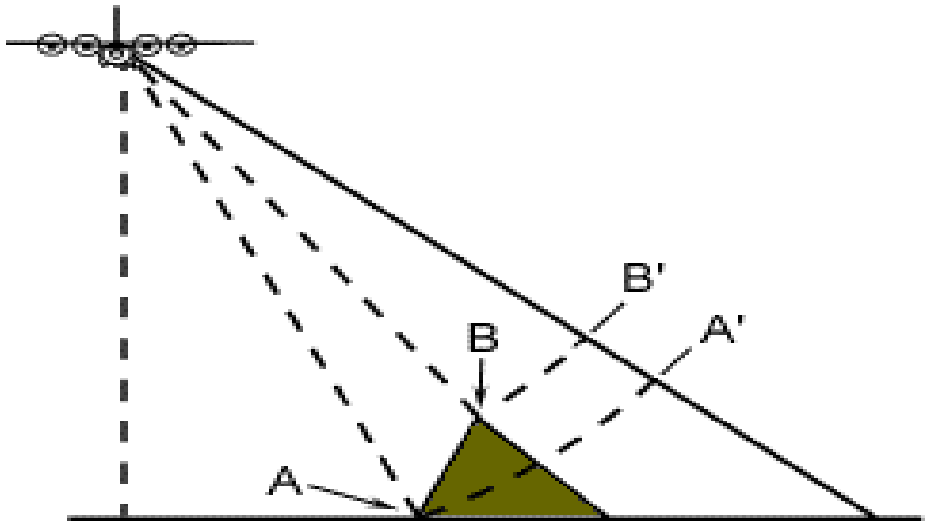

later pulse reaches top of peak before earlier pulse reaches base;

peaks appear to lean toward sensor

The slant geometry of radar leads to shadows also

shadow

geometry prevents signal from reaching area behind tall feature

...dark area (shadow) occurs where no signal reaches

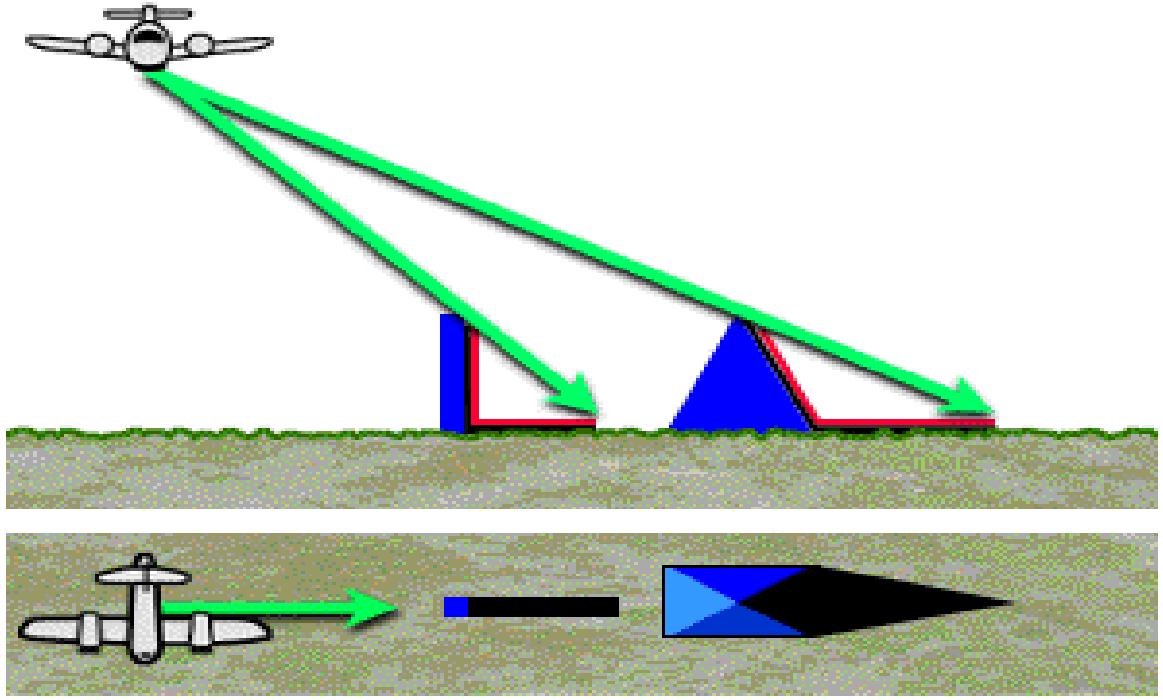

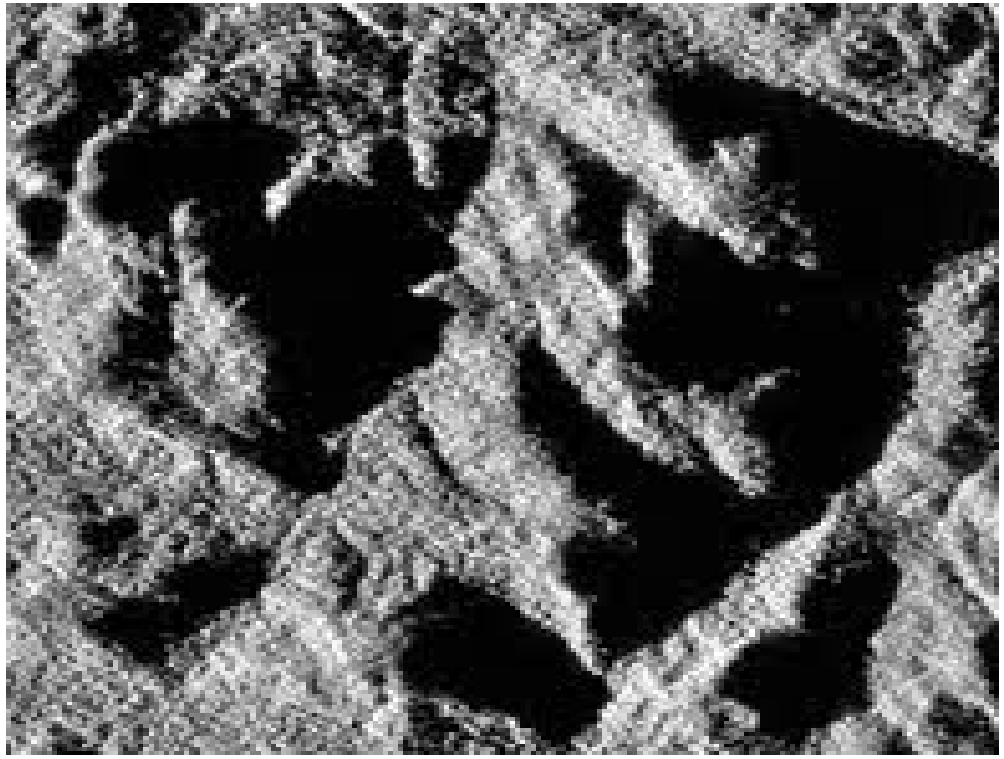

is instrument to left or right?

Link between depression angle and terrain features

as depression angle decreases, amount of shadow increases for objects of same height

depression angle not constant in image

on image: succession of highlights and shadows; different in near and far ranges

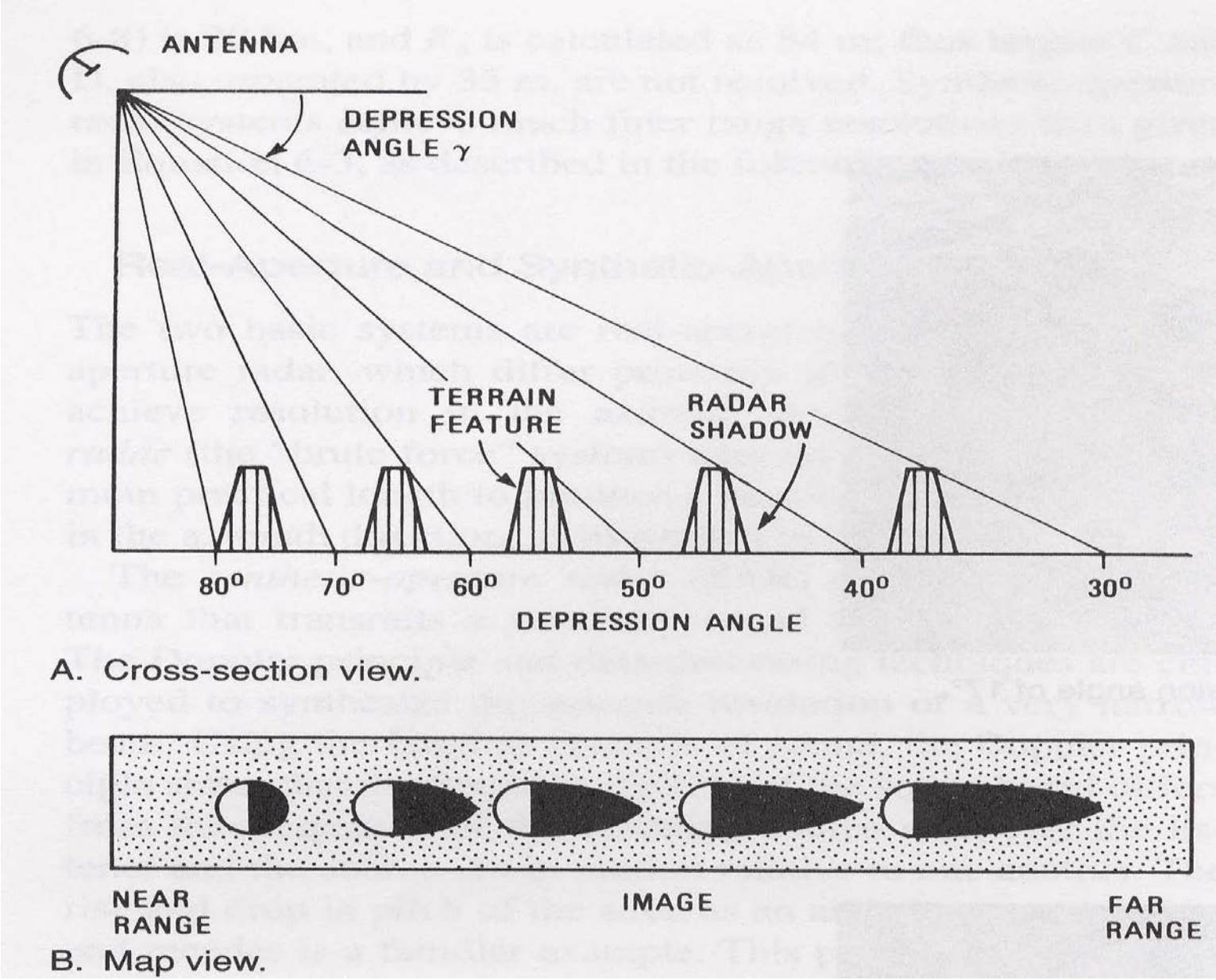

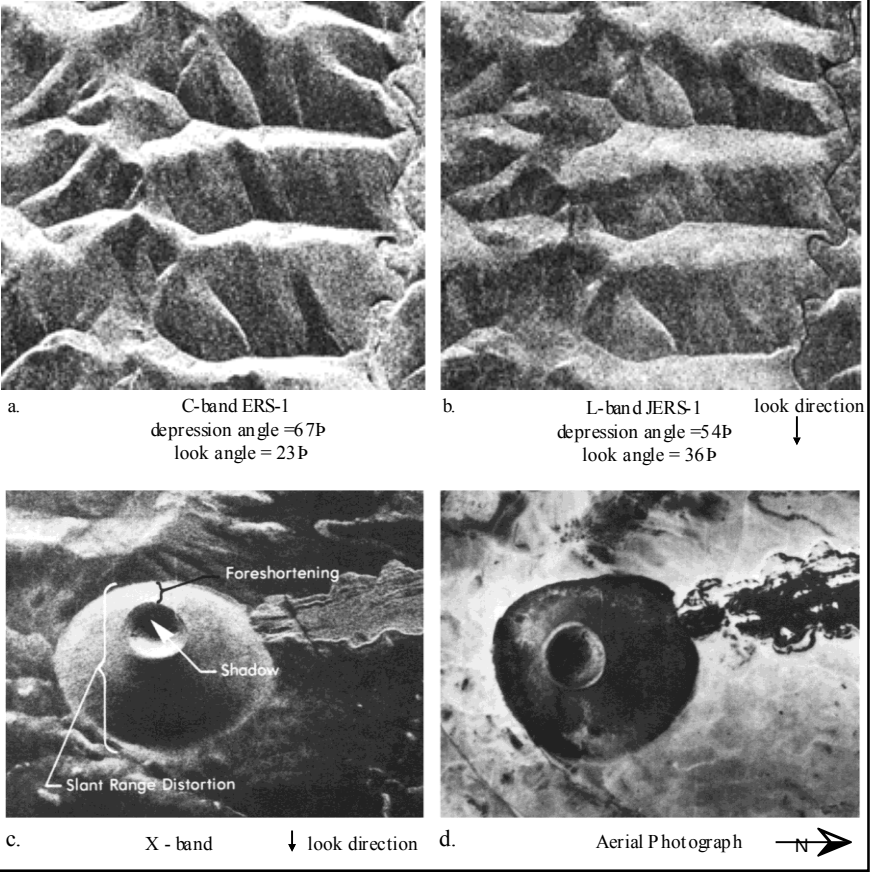

Foreshortening

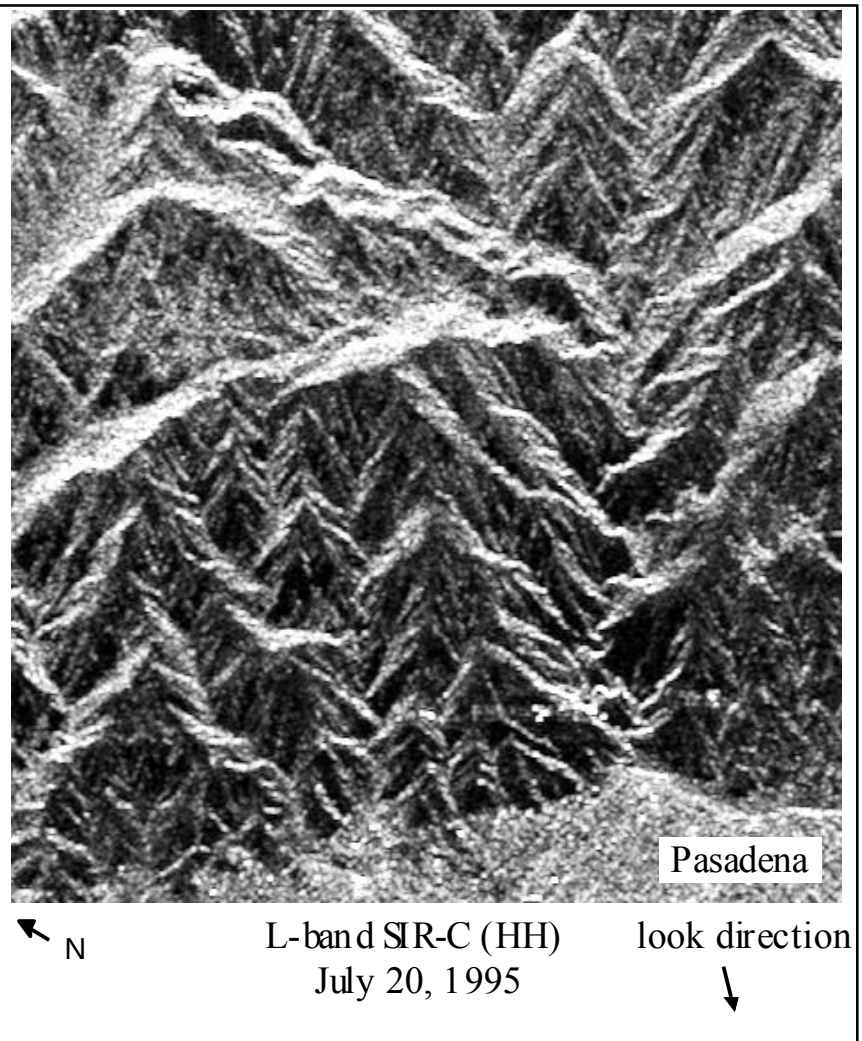

Layover

A

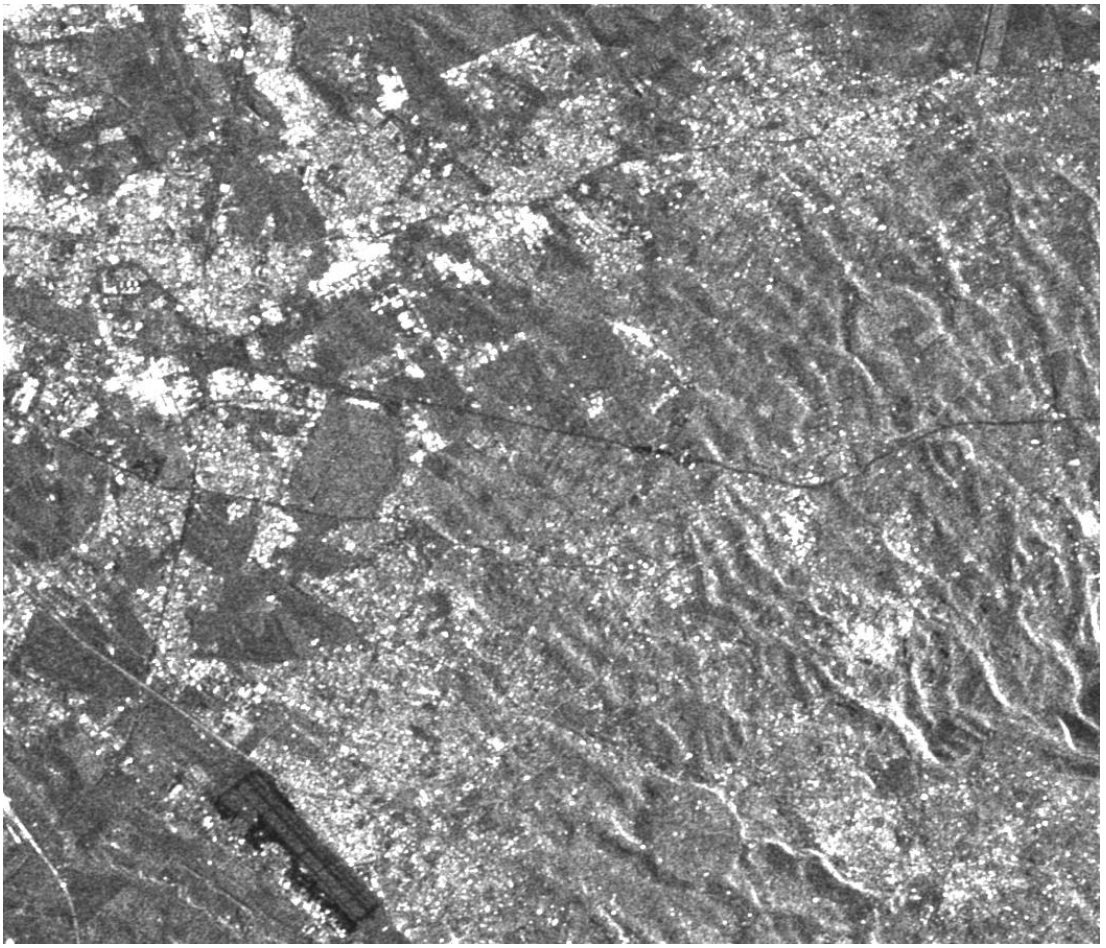

D

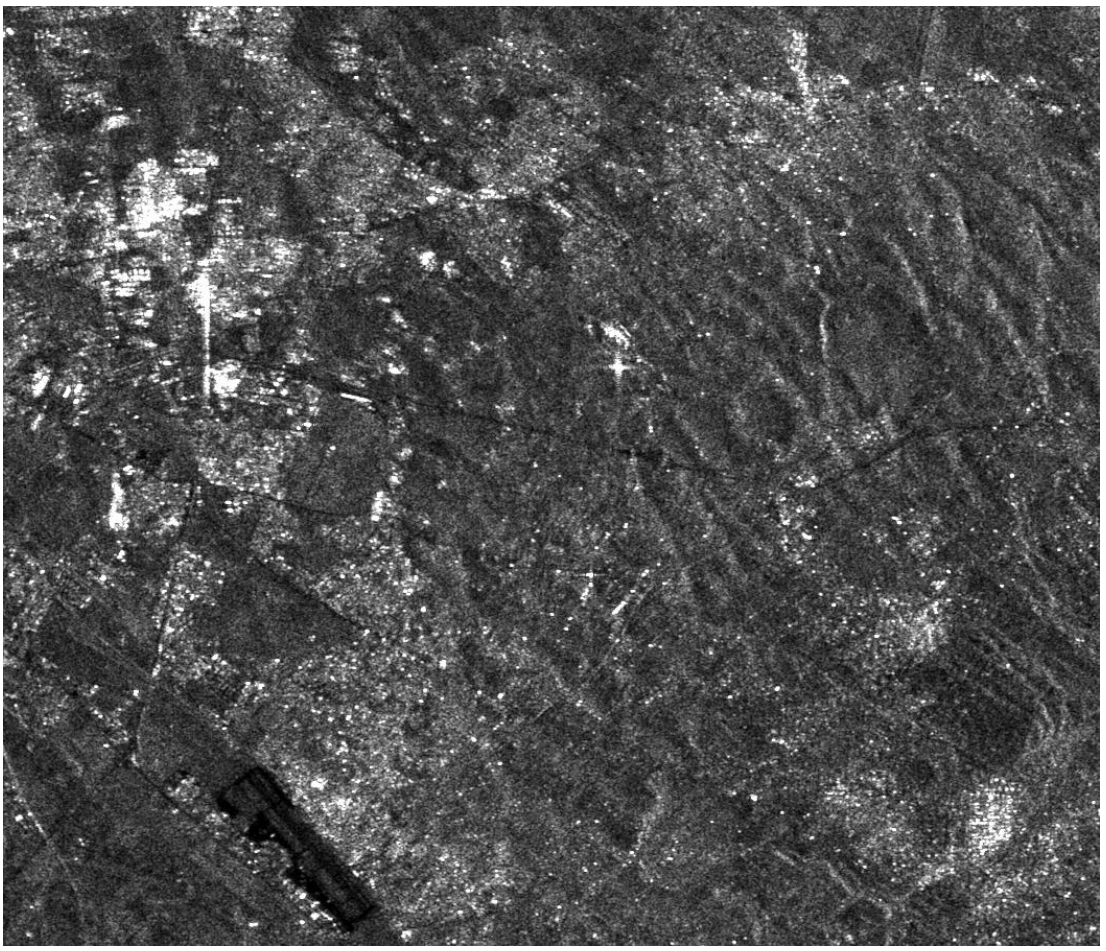

Image (Contrast) enhancement

Includes techniques that modify images in order to improve their quality
and allows an easier interpretation.
Image enhancement improves visual content, but it does not add information to data

Stretch

Raw images usually are very dark and lack constrast because the sensor dynamic range is not exploited at maximum in an individual scene.

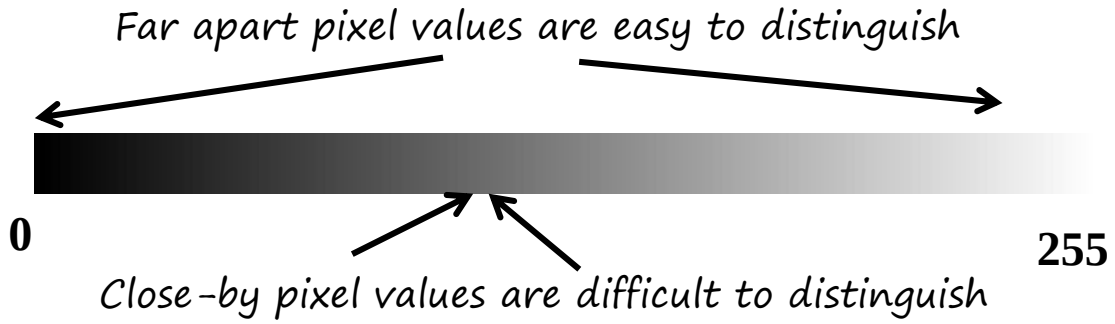

The contrast stretching techniques change the image value distribution to cover a wider range

Contrast of an image can be revealed by its histogram

The histogram of an image is a graphical representation of the distribution of **DN** (radiance) in the image.

The **DN** values are displayed along x axis.
The frequency of occurrence of each **DN** in the image is shown on the y axis

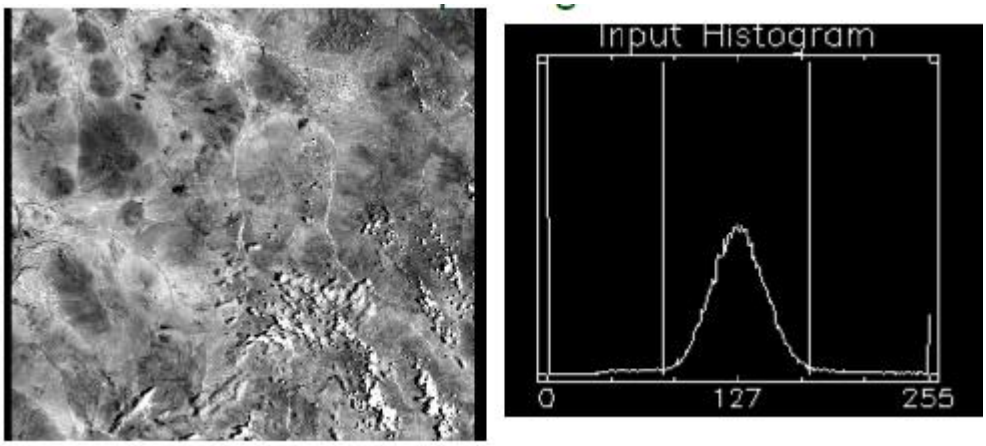

Histograms tipically show a unimodal distribution. But image histograms may be bi-modal, or multi-modal, due to the fact that there are two, or more, dominant materials in the scene with different reflectance values.

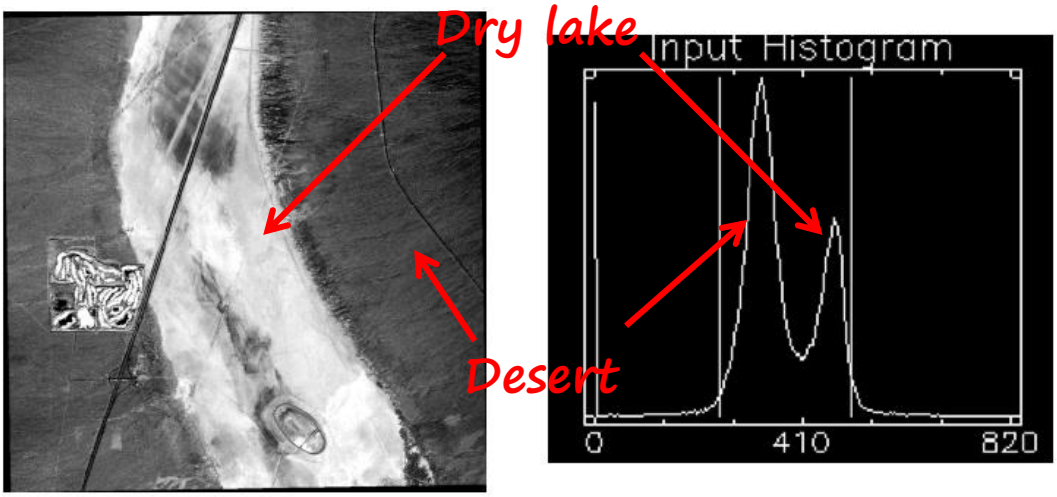

Linear Stretching

A $DN'=0$ is assigned to the lowest DN in the image,
$DN'=2^M - 1$ is assigned to the highest DN, where M is the number of available bits for display.
To each intermediate DN, a new value is assigned according to a linear transformation:

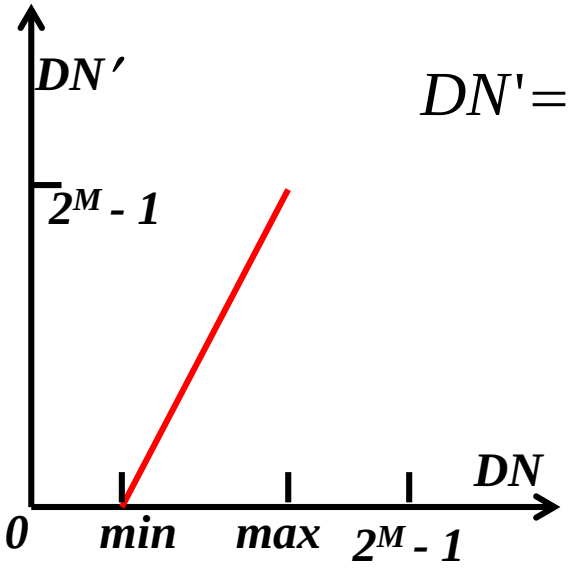

$$DN' = aDN + b = \frac{DN - \min}{\max - \min}(2^M - 1)$$

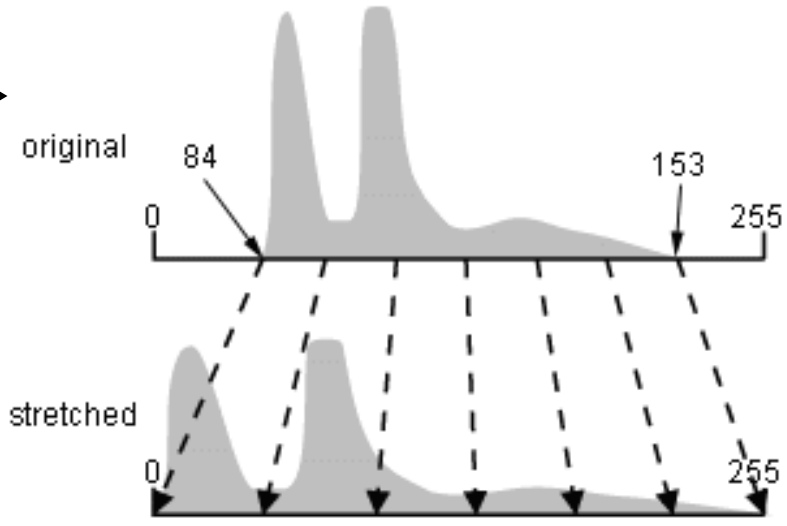

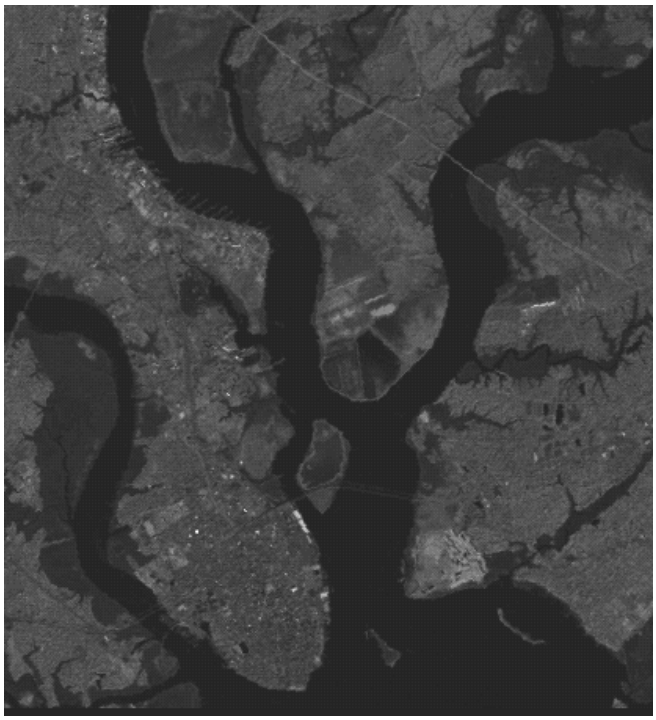

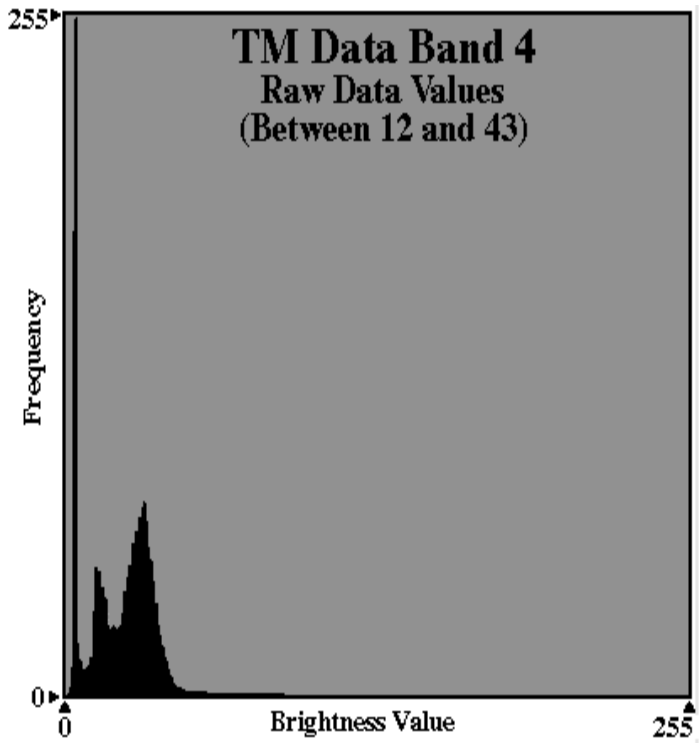
255
TM Data Band 4
Raw Data Values
(Between 12 and 43)
Frequency
0
0
Brightness Value
255

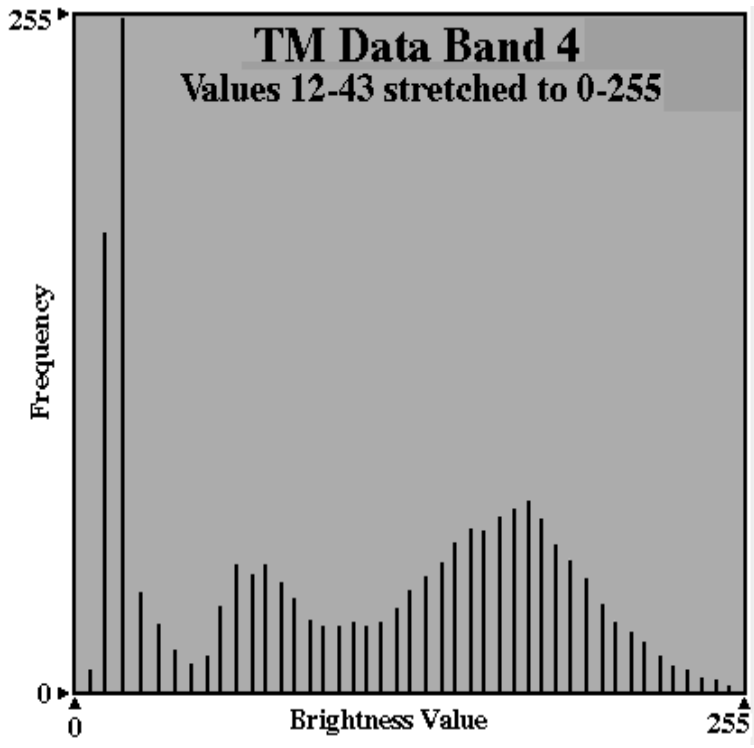
255
TM Data Band 4
Values 12-43 stretched to 0-255
Frequency
0
0
Brightness Value
255

Percentage, standard deviation, threshold linear stretch

It is possible to enhance contrast on a limited portion of DN's, applying contrast stretching on a restricted part of the histogram

X percentage (say 5%) top or/and low values of the image will be set to 0 or 2^M-1, rest of values will be linearly stretched to 0 to 2^M-1.

Low $X\%$ or/and top $X\%$ will be saturated to 0 or/and 2^M-1, respectively.

If the percentage coincides with a standard deviation percentage, then it is called a standard deviation contrast stretch. For a normal distribution, 68%, 95.4%, 99.73% values lie in $\pm1\sigma$, $\pm2\sigma$, $\pm3\sigma$. So 16% linear contrast stretch is the $\pm1\sigma$ contrast stretch.

Threshold stretch is applied to create masks: select a DN value for which all larger (or smaller) values are saturated

LUT

Since the correspondence between old and new DN are known (through the transformation) usually Look Up Tables are built in advance and then applied on image values.

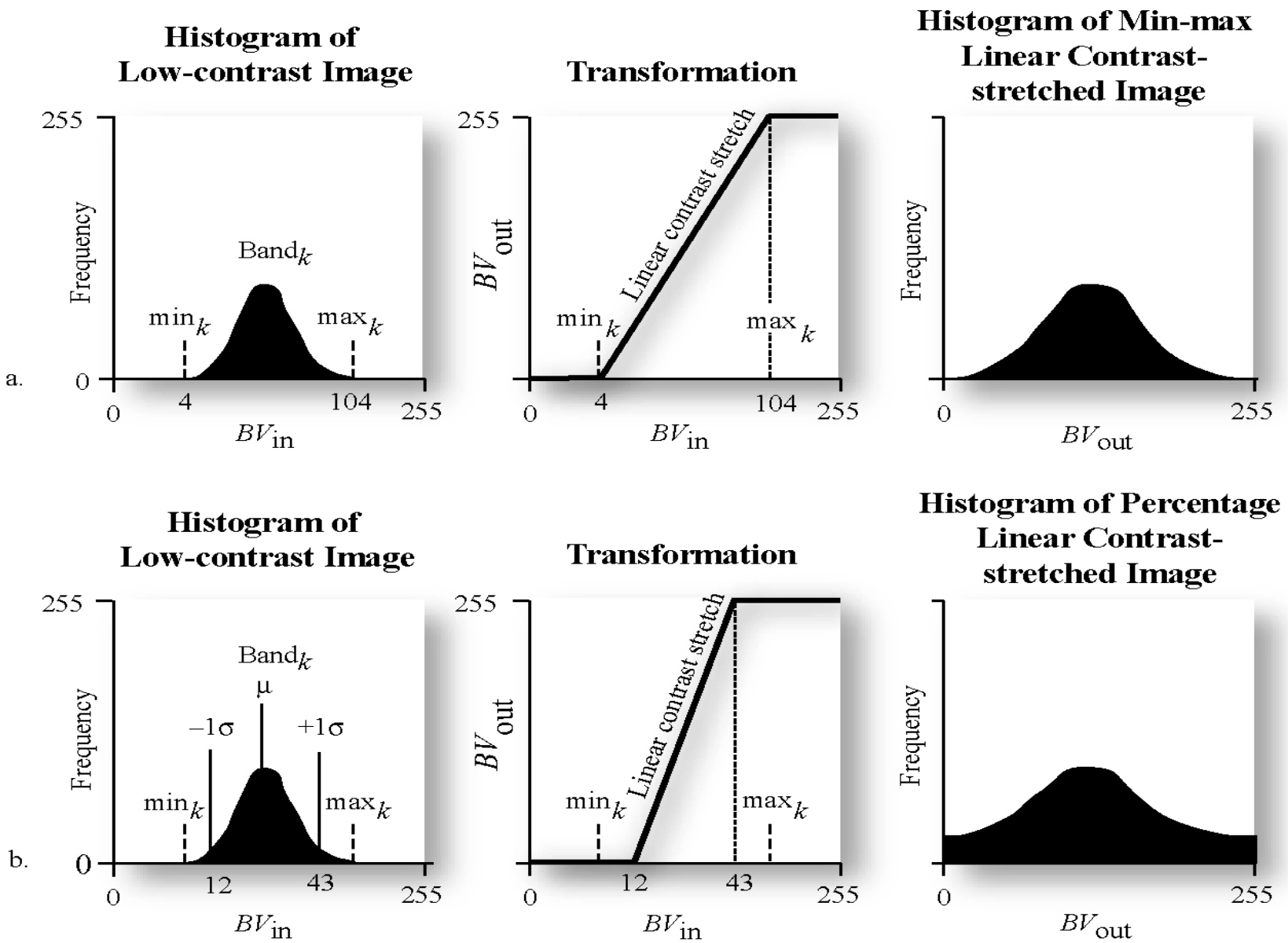

Min-Max Contrast Stretch

±1 Standard deviation contrast Stretch

In this case the transformation function is steeper than in the min-max case

original

Saturating the water
Stretching the land

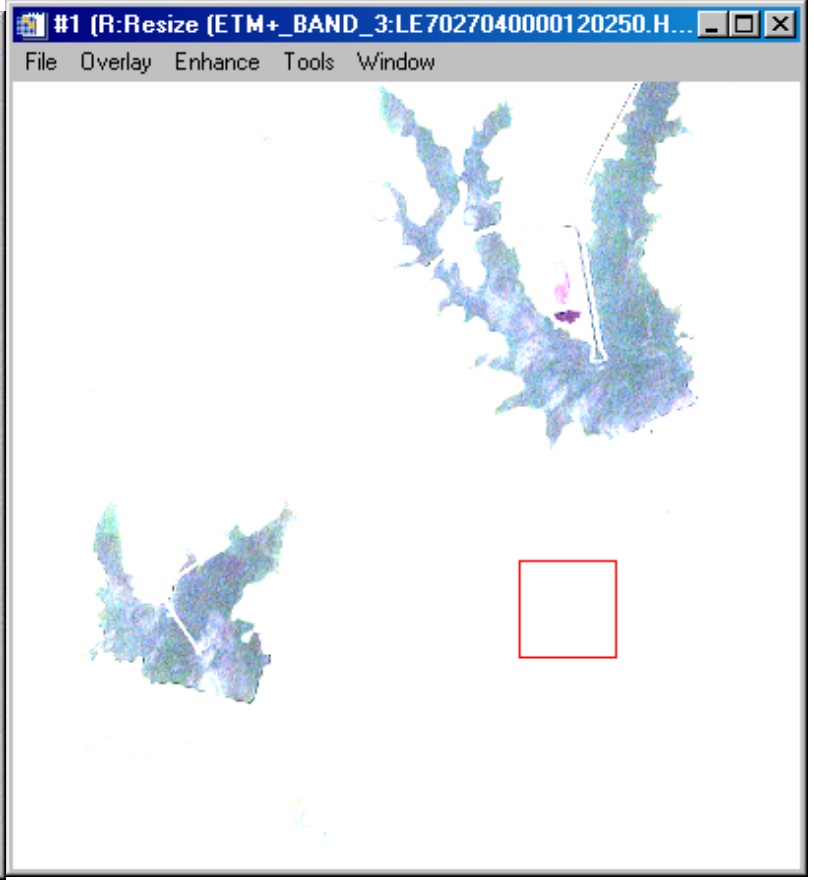

Saturating the land
Stretching the water

Threshold linear contrast stretch

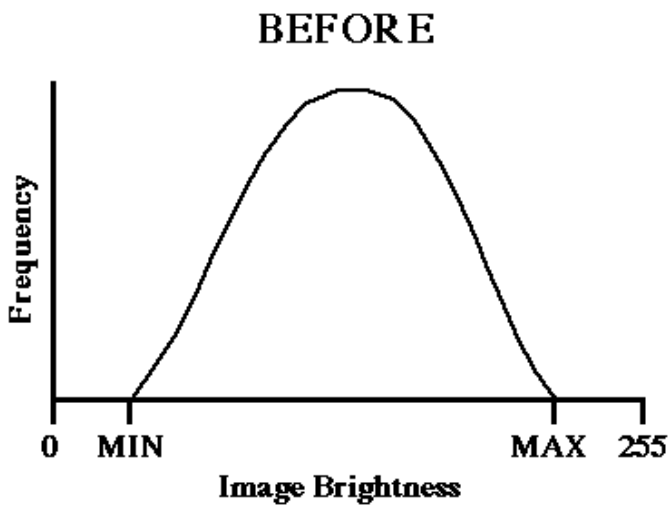

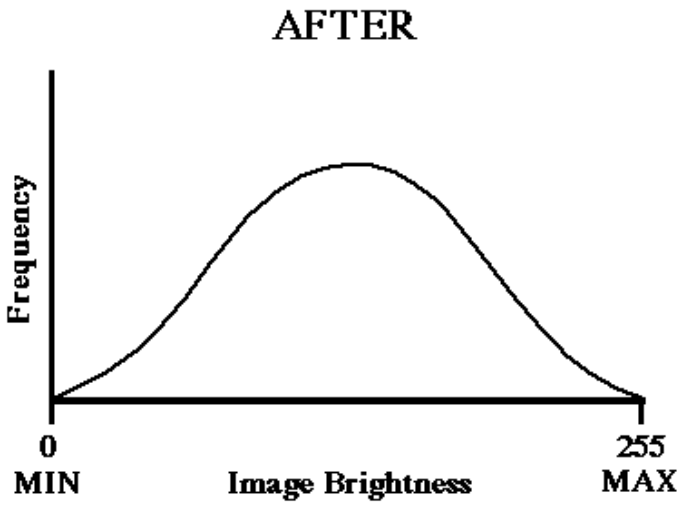

The transformation function that modifies contrast is:

$$y=f(x)$$

The original histogram is $h(x)$

The final histogram is $h'(y)$

By definition, the number of pixels in the range between x and $x+dx$ of the original histogram must be equal to the number of pixels between y and $y+dy$ in the final histogram.

$$h(x)dx = h'(y)dy$$

$$x = f^{-1}(y)$$

$$h'(y) = h(f^{-1}(y))\frac{d(f^{-1}(y))}{dy}$$

Histogram Equalization

This technique modifies the image histogram in order to make it uniform.
An image with a uniform histogram gives the same frequency to all available **DN** values.

In practice, a histogram with a perfectly uniform distribution cannot be obtained from a digital image but, with this technique, it is possible to make it almost uniform.

In this case, we do not know the transformation function $y=f(x)$, but we know the final histogram $h'(y)$.

$$h'(y)\cdot dy = \frac{N}{L}, \quad \mathrm{dy} = \frac{\mathrm{L}-1}{\mathrm{L}}$$

$$y = \frac{L-1}{N}\int h(x)dx$$

The integral above is the cumulative histogram.

$\frac{L-1}{N}$ is a normalization and scale factor

N= number of pixels in the image
L= number of possible DN (usually $2^M - 1$)

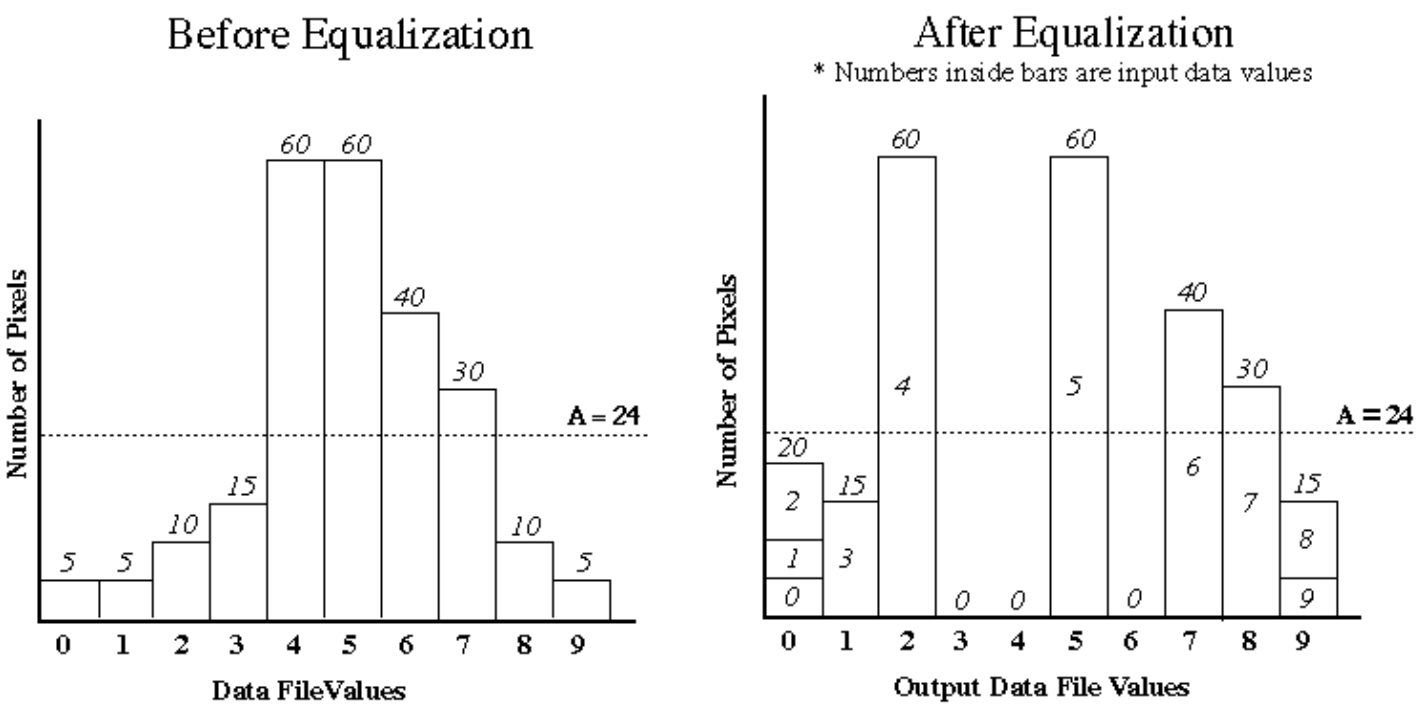

L=10

N=240

The most frequent ***DN***'s of the original image will be distributed in a wider range of ***DN*** in the equalized image (they will have higher contrast).
Whereas the contrast is reduced for the ***DN***'s in the tails (less frequent ***DN***).

Some pixels that originally have different values are now assigned the same value (perhaps loss of information).

Contrast Stretch of Thematic Mapper Band 4 Data Charleston, SC

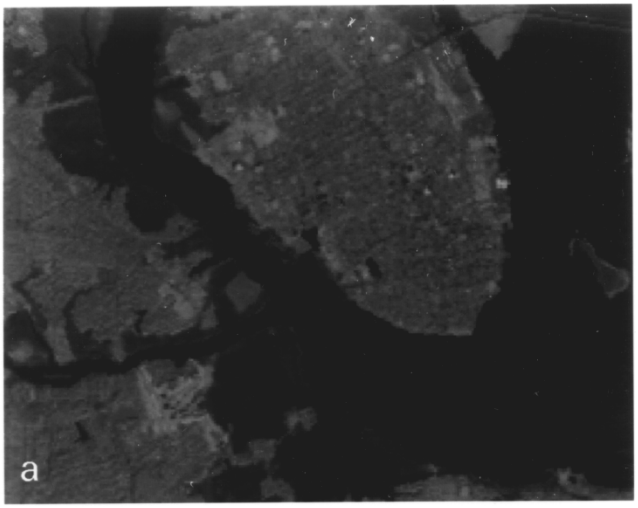

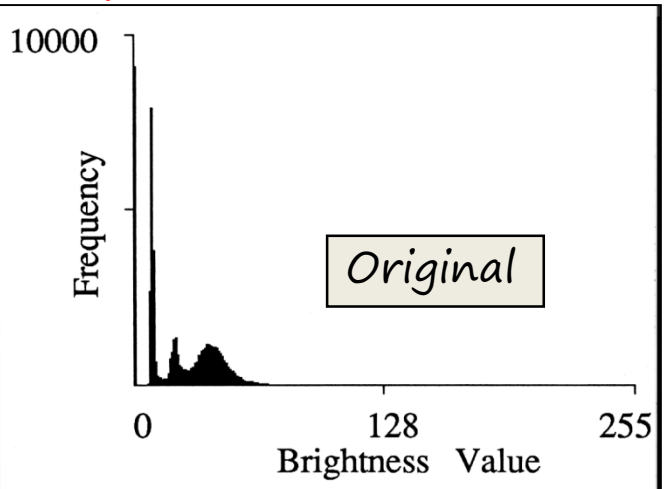

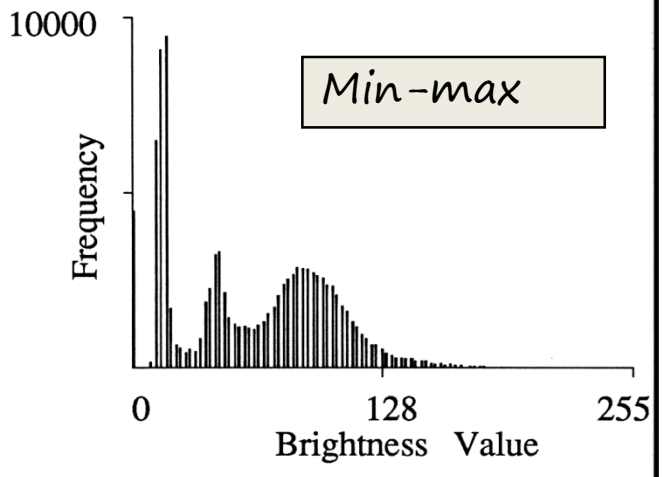

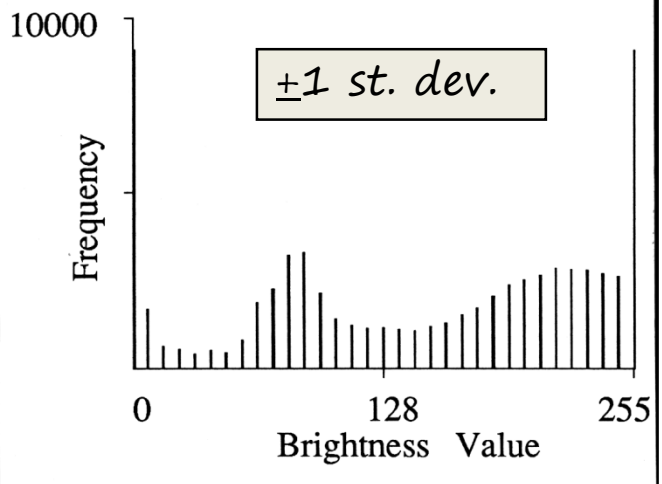

Contrast Stretching of Charleston, SC Landsat Thematic Mapper Band 4 Data

Specific percentage linear contrast stretch designed to highlight wetland

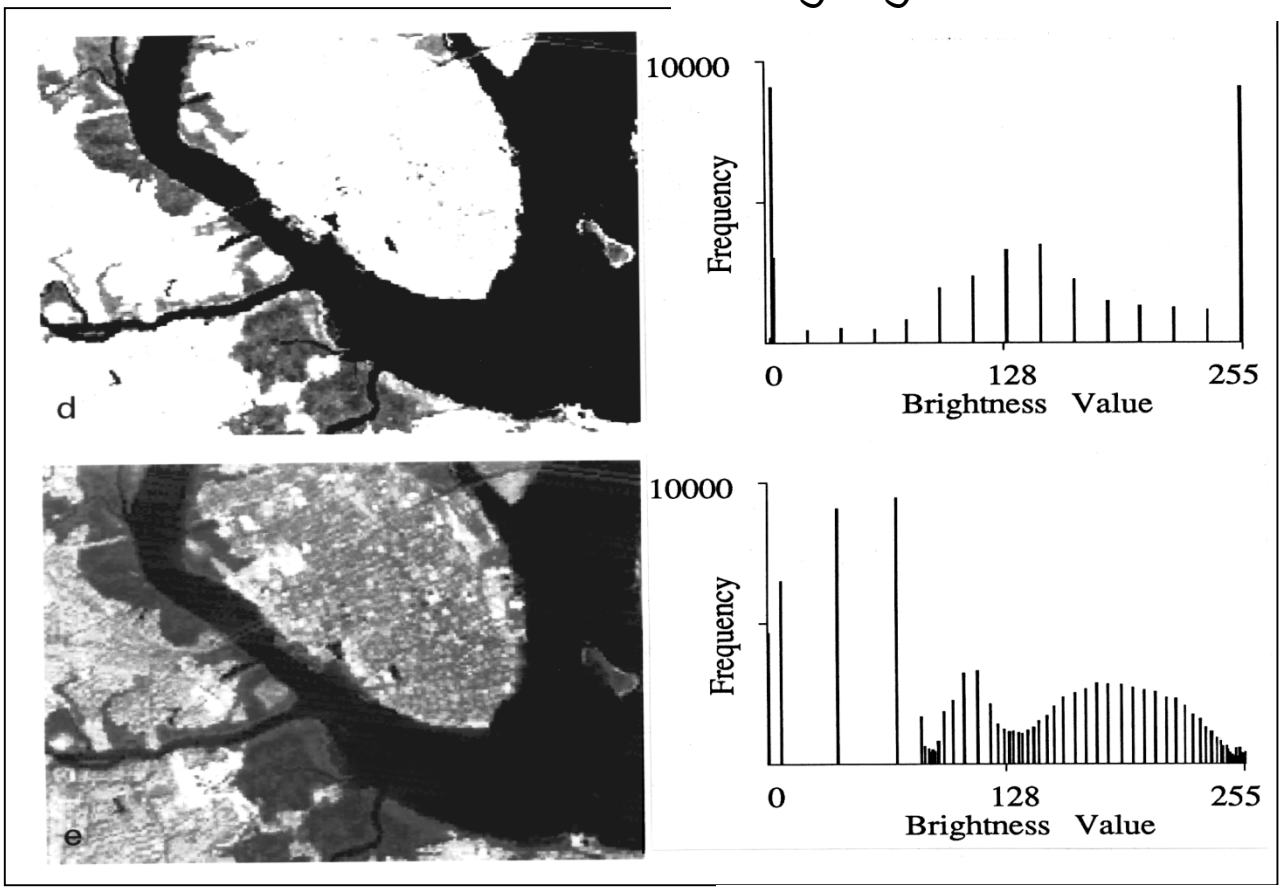

Histogram Equalization

- *Reference stretch*
  - *match the CDF of the image being processed to a reference CDF, for example from another image*
  - *useful for*
    - *multitemporal or multisensor radiance matching*
    - *matching image to reference contrast*

graphical depiction of CDF reference stretch (Fig. 5-23)

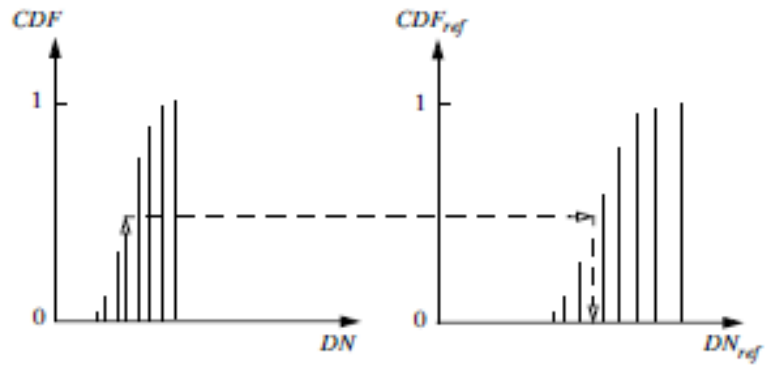

TM band 3, December 31, 1982

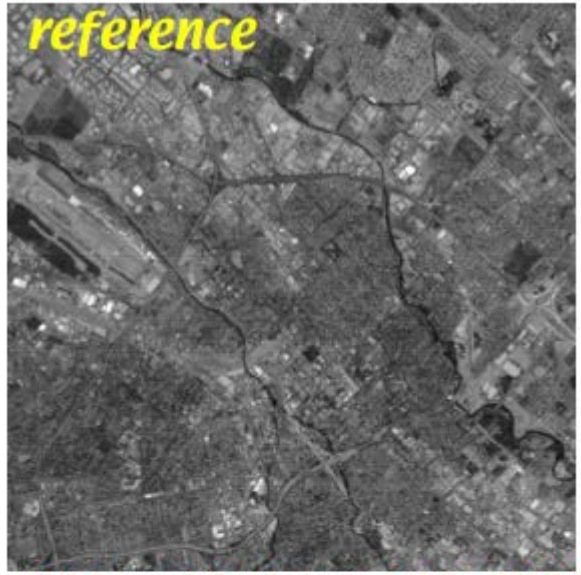

TM band 3, August 12, 1983

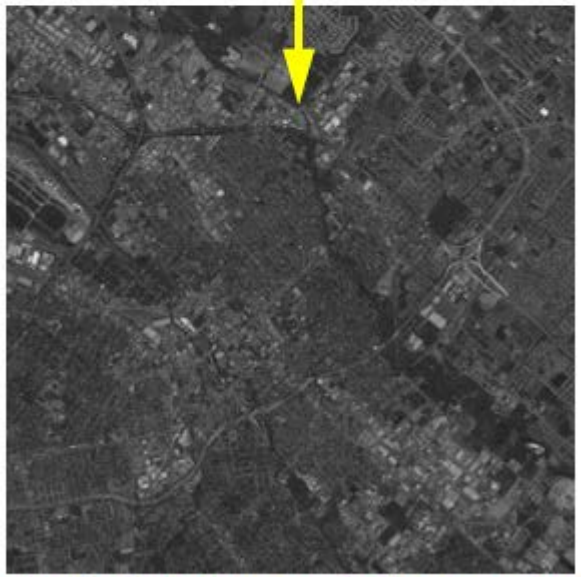

dark-light target linear stretch

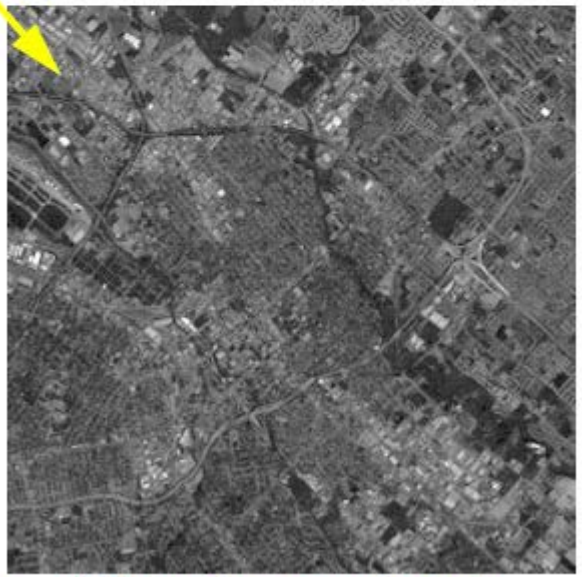

CDF reference stretch

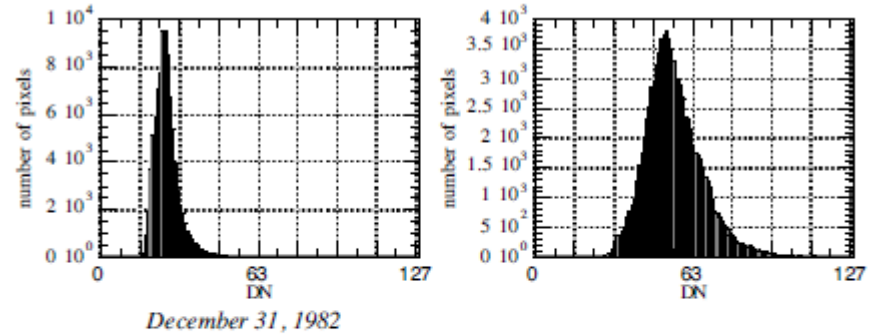

December 31, 1982

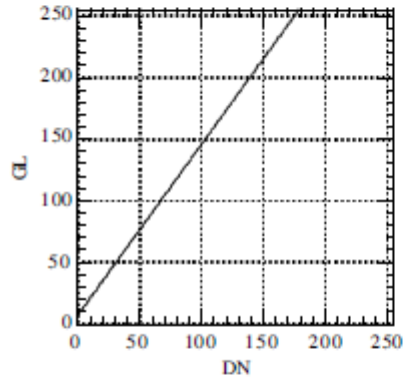

dark-light linear stretch

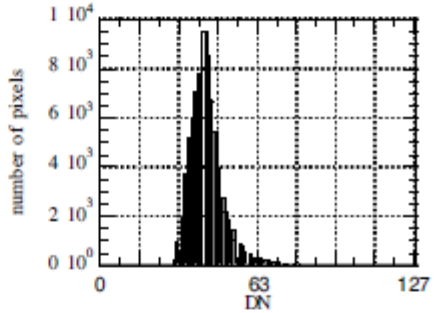

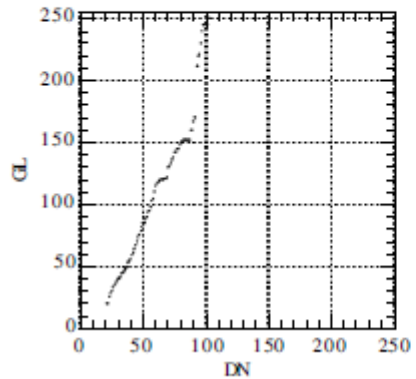

CDF reference stretch

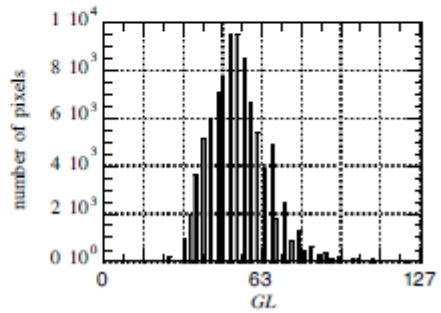

Before being used for information extraction, images undergo some processing procedures.

Ideally, the radiance recorded by a remote sensing system is an accurate representation of the radiance actually leaving the feature of interest (e.g., soil, vegetation, water, or urban land cover) on the Earth's surface. Unfortunately, *noise* (error) can enter the data-collection system at several points. For example, it may be introduced by the sensor system itself when the individual detectors do not function properly or are improperly calibrated.

Image Restoration

Corrects mistakes, noise and geometric distortions introduced in the data during acquisition and transmission.

Measurements can be degraded by sensor malfunctioning, and by recording and transmission systems

Line Dropouts

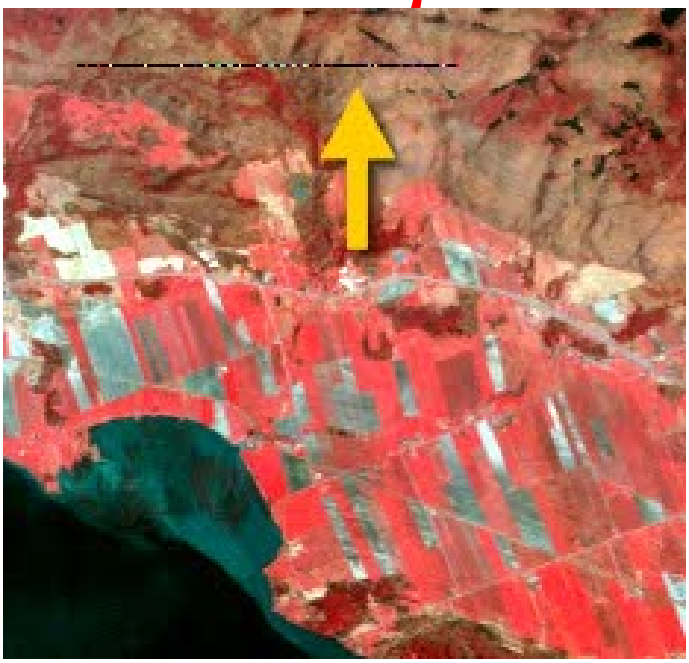

The defective line has a **DN** average ~**0** (or much lower than the one of adjacent lines).
The line (or part of it) contains no information due to a malfunctioning of the sensor.
There is no way to restore data that were never acquired. However, it is possible to improve the visual interpretability of the data by introducing estimated **DN**'s.

Pixels of the defective line are replaced by the **DN** average of the above and below pixels

$$DN_{ij} = \frac{DN_{i-1,j} + DN_{i+1,j}}{2}$$

i = row index
j = column index

MSS / Landsat

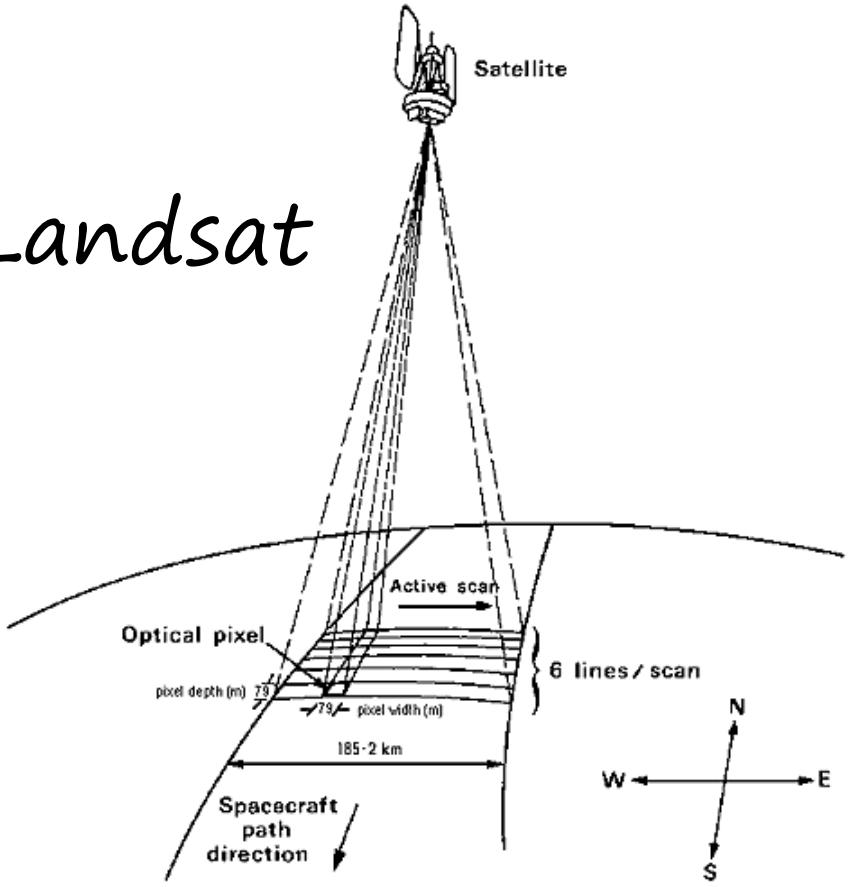

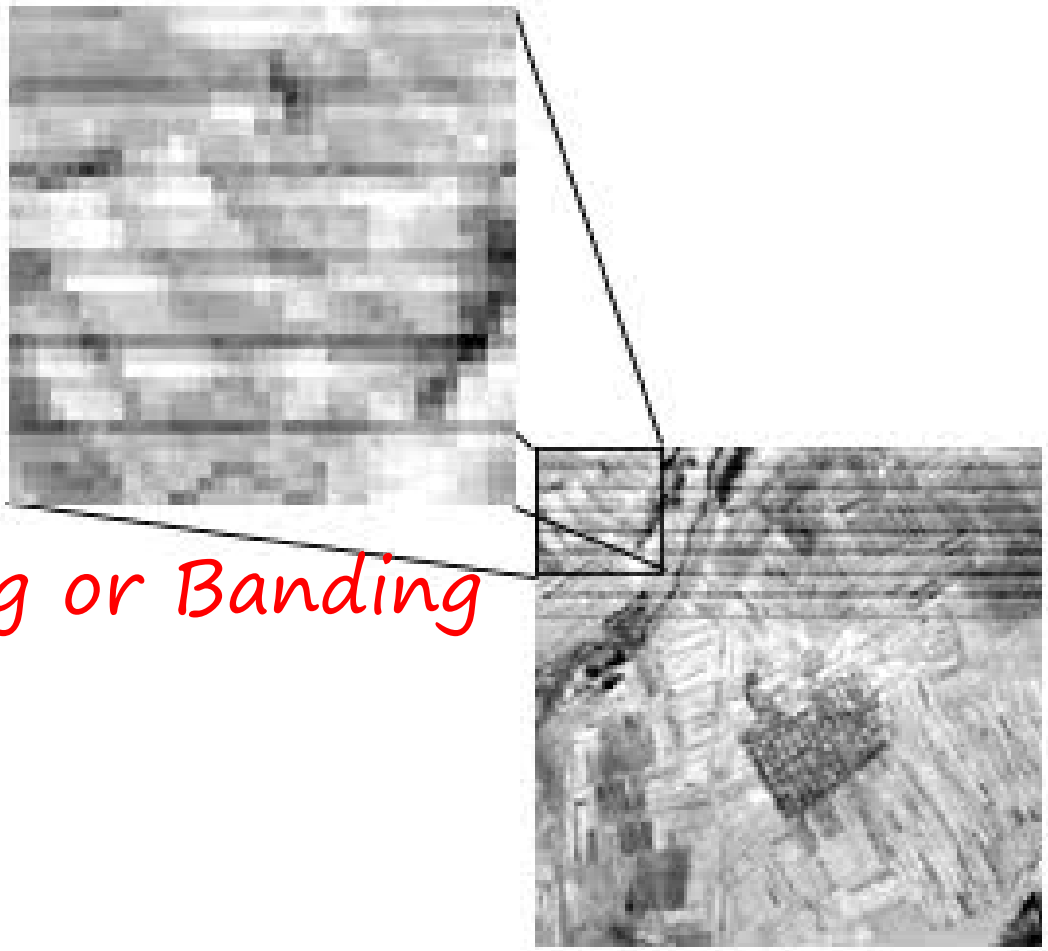

Striping or Banding

SPOT

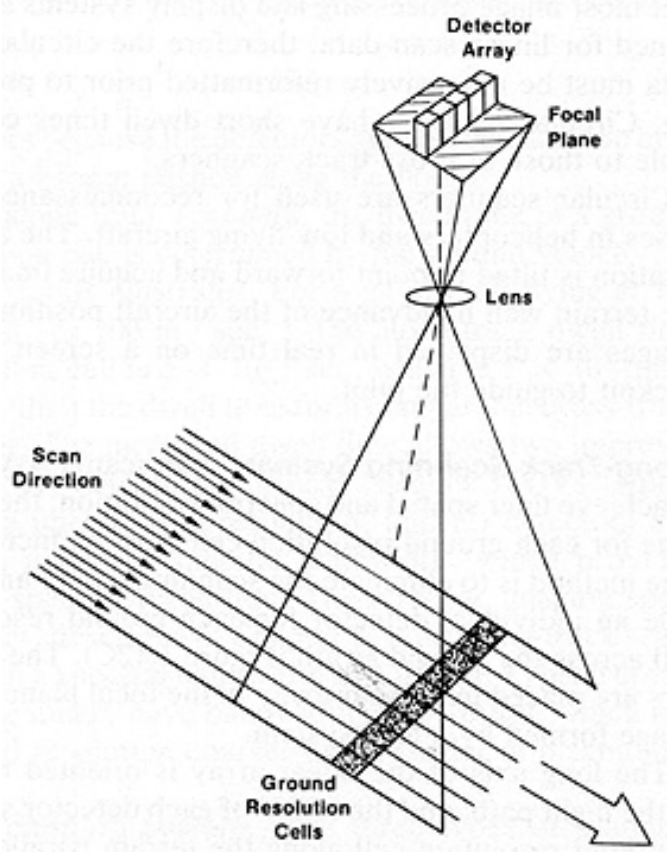

C. ALONG–TRACK SCANNER.

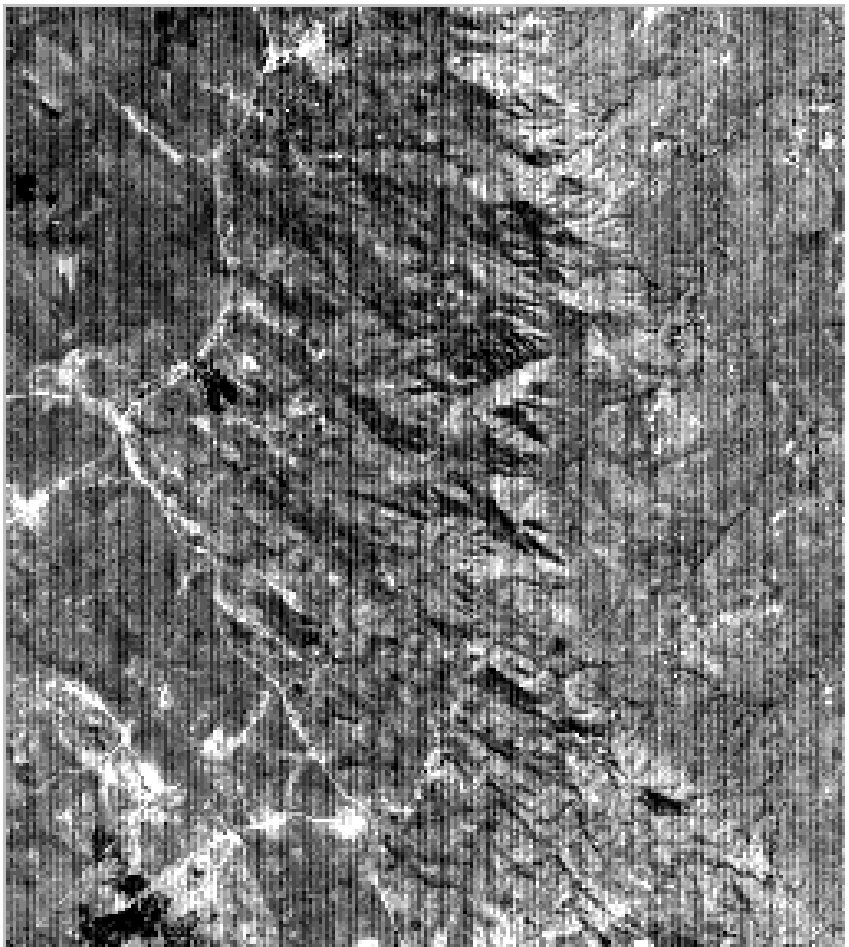

Destriping

Contrarily to line drop-out, in presence of striping the bad lines contain valuable information, but should be repaired. This may be accomplished by the following procedure:

- A homogeneous area is selected in the image (for example, a body of water)
- The average of pixels in the selected area is calculated, and then the separate averages of individual detectors
- If the average related to a certain detector is very different from the total one, that detector is out of adjustment (mis-calibrated)
- Pixels acquired by the defective detector are "scaled" in order to have the same average of the others

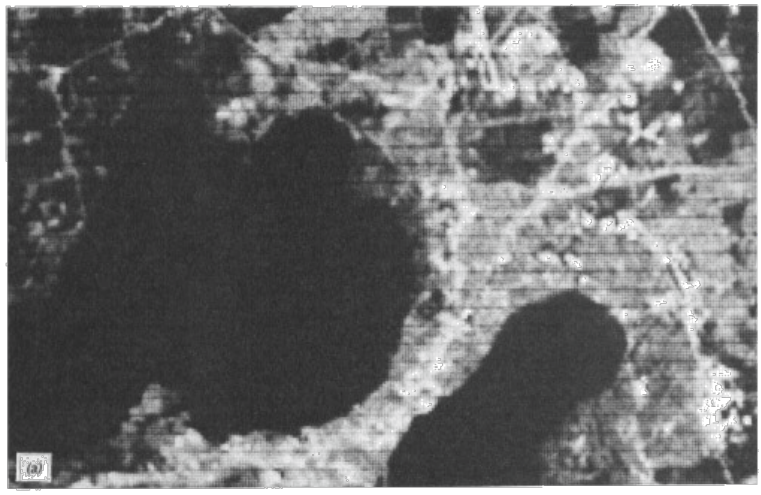
(a)

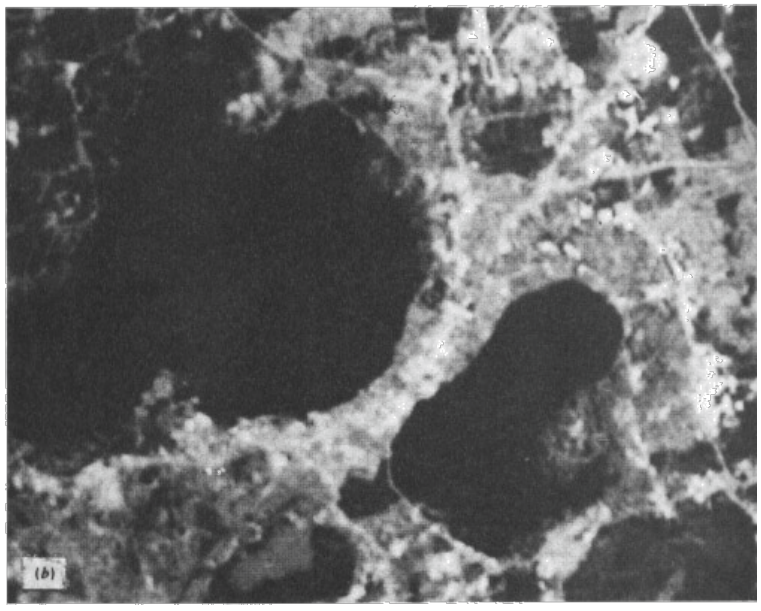
(b)

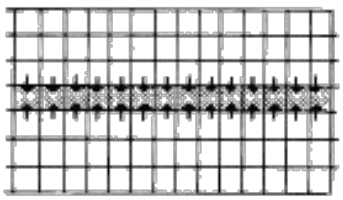

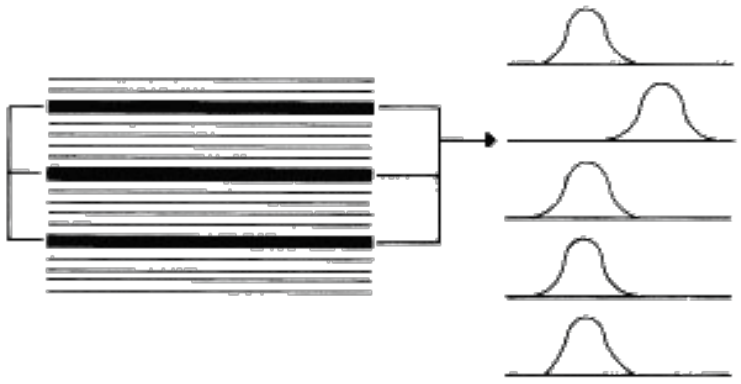

Remote sensed imagery always exhibits geometric errors that are inherent to the acquisition geometry of data, or to the satellite platform motion, or to the Earth movement.
It is usually necessary to *preprocess* remotely sensed data and remove geometric distortion so that individual pixels are in their proper planimetric (x, y) map locations.

Non systematic errors

- Attitude changes
- Height variations
- Velocity variations

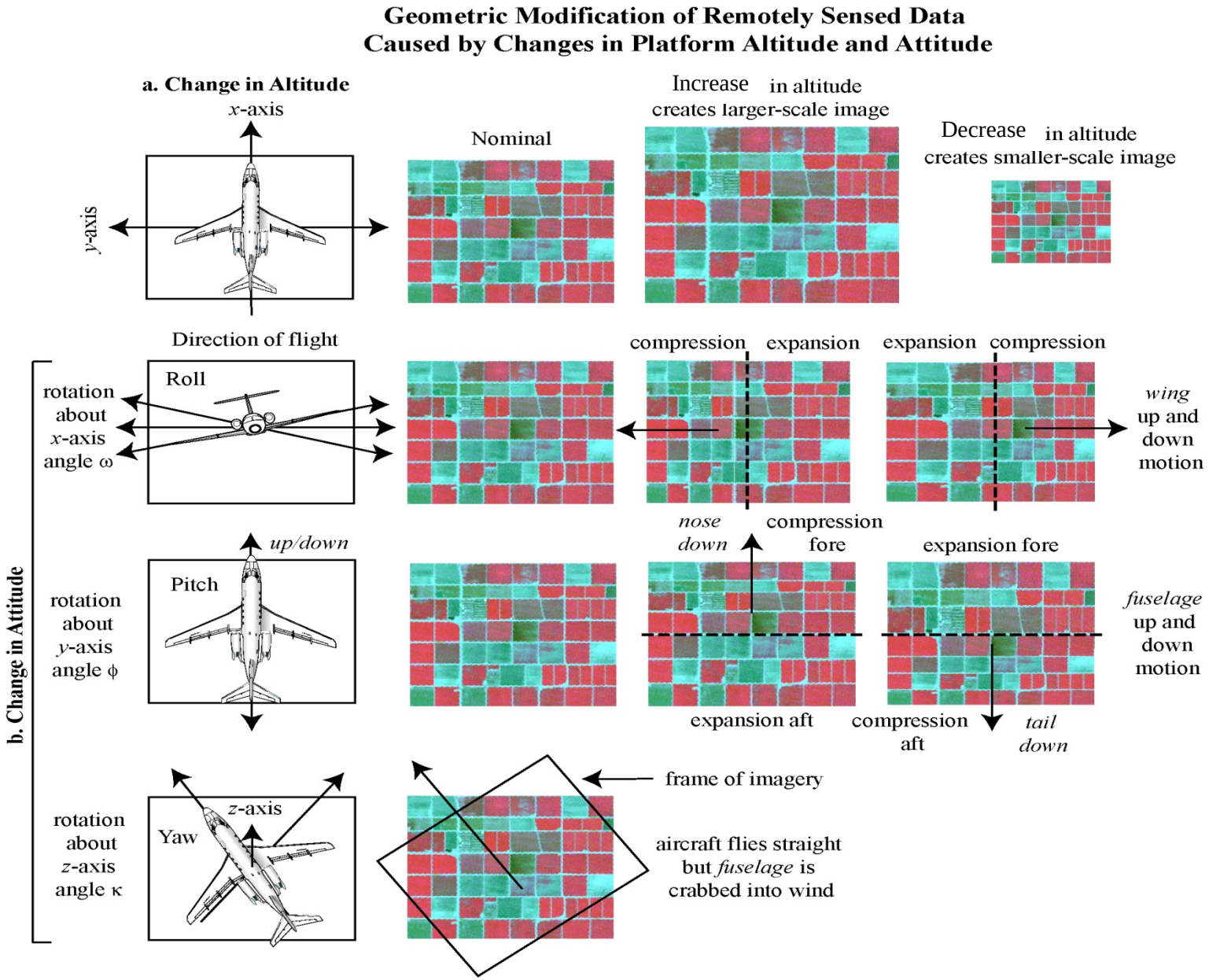

Roll occurs when the aircraft or spacecraft fuselage maintains directional stability but the wings move up or down, i.e. they rotate about the x-axis.
Pitch occurs when the wings are stable but the fuselage nose or tail moves up or down, i.e., they rotate about the y-axis.
Yaw occurs when the wings remain parallel but the fuselage is forced by wind to be oriented some angle to the left or right of the intended line of flight, i.e., it rotates about the z-axis.

Remote sensing data (mainly airborne) often are distorted due to a combination of changes in *altitude* and *attitude* (roll, pitch, and yaw).

Systematic errors

Earth rotation
(image skew)

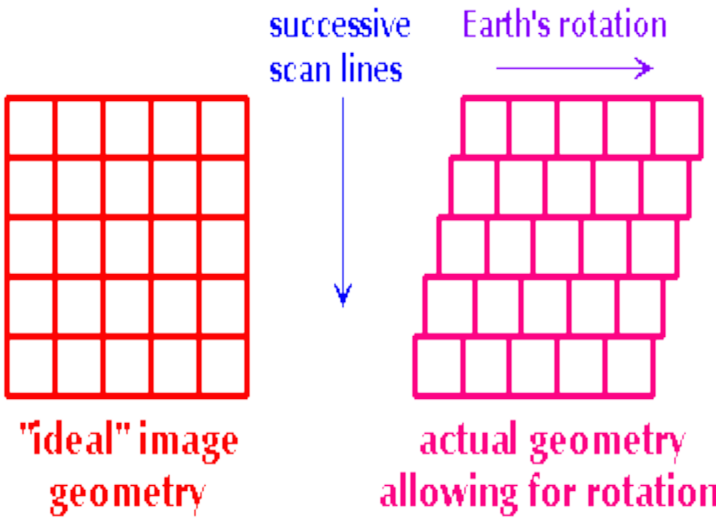

In Landsat images

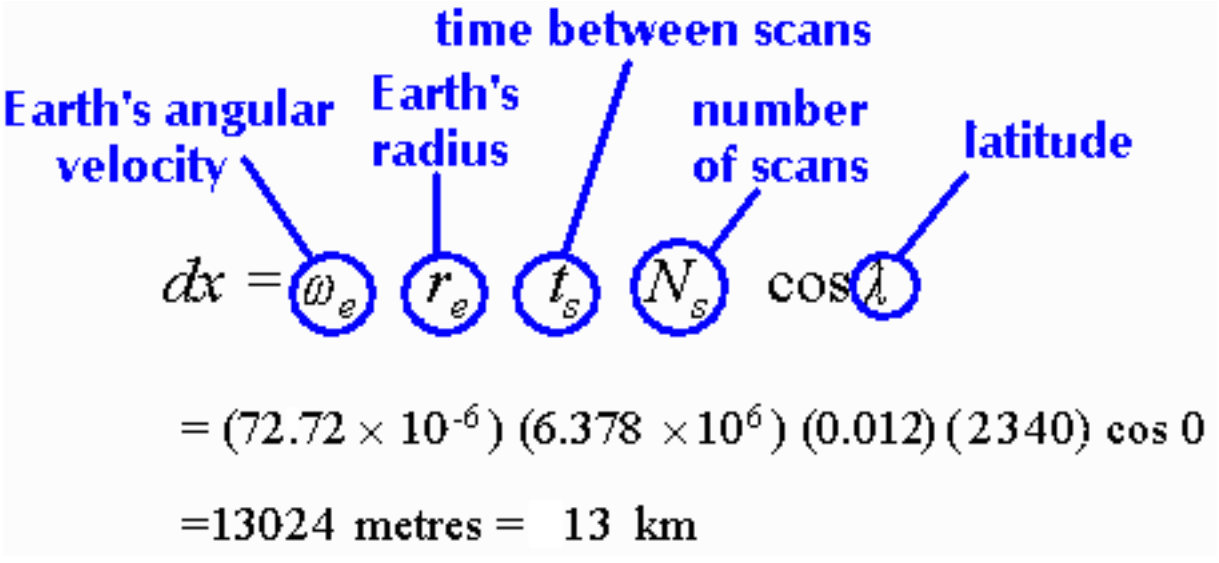

Image Skew

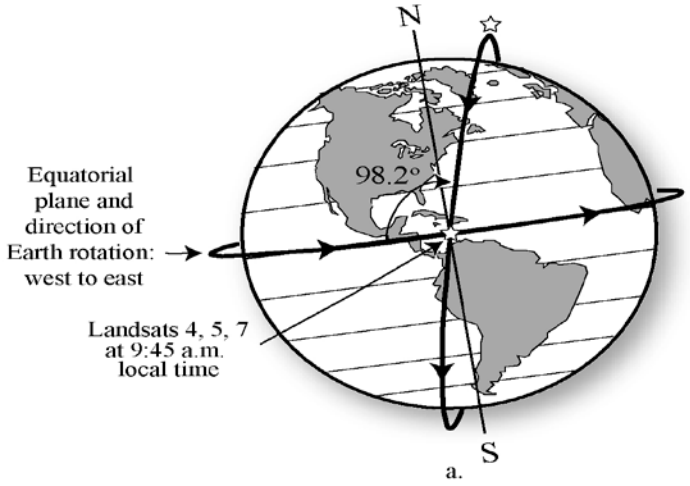

a.

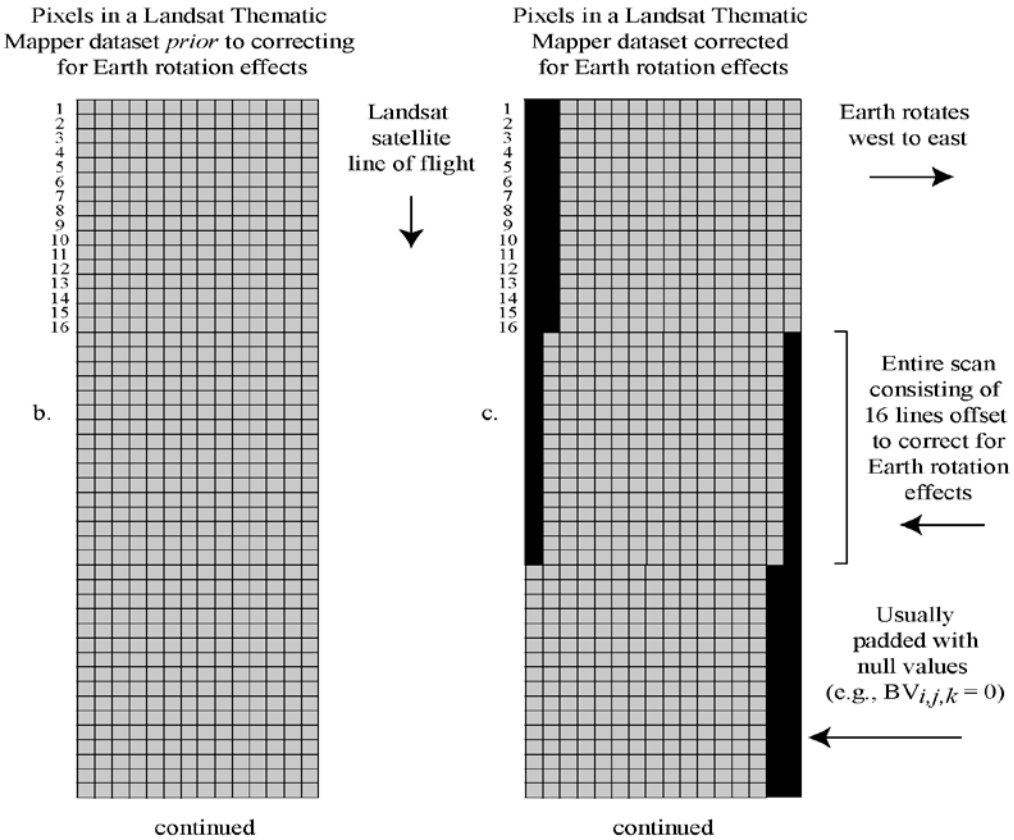

a) Landsat satellites 4, 5, and 7 are in a Sun-synchronous orbit with an angle of inclination of 98.2°. The Earth rotates on its axis from west to east as imagery is collected.

b) Pixels in three hypothetical scans (consisting of 16 lines each) of Landsat TM data. While the matrix (raster) may look correct, it actually contains systematic geometric distortion caused by the angular velocity of the satellite in its descending orbital path in conjunction with the surface velocity of the Earth as it rotates on its axis while collecting a frame of imagery.

c) The result of adjusting (*deskewing*) the original Landsat TM data to the west to compensate for Earth rotation effects. Landsats 4, 5, and 7 use a bidirectional cross-track scanning mirror.

Panoramic distortion

Pixels on the swath edges are larger than those at the center

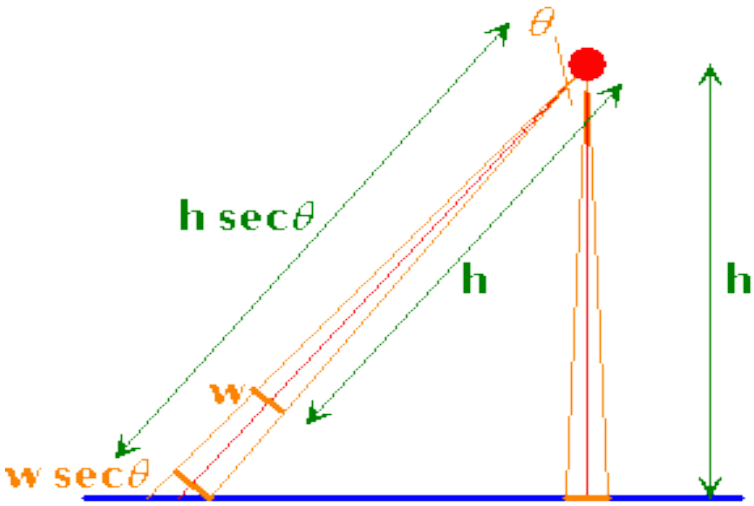

$w \cdot \sec^2\theta$

w= spatial resolution

If the swath is very big, also Earth curvature distorts pixels

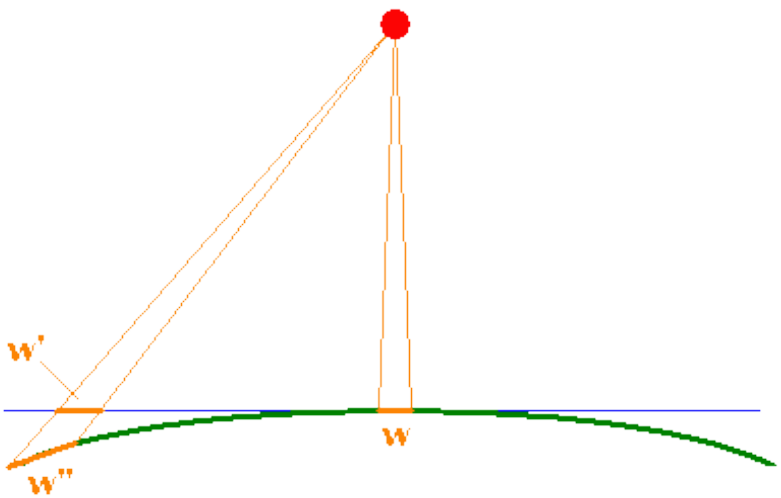

The pixel dimensions are:

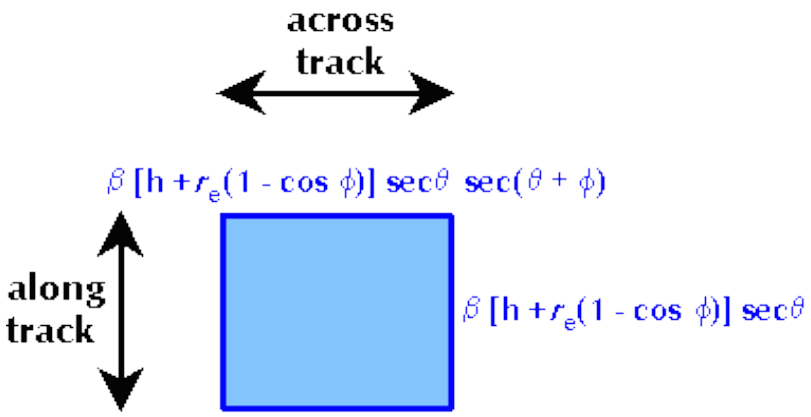

β = IFOV
ϕ = angle from the Earth center to the pixel
θ = observation angle ($0 < \theta < FOV/2$)

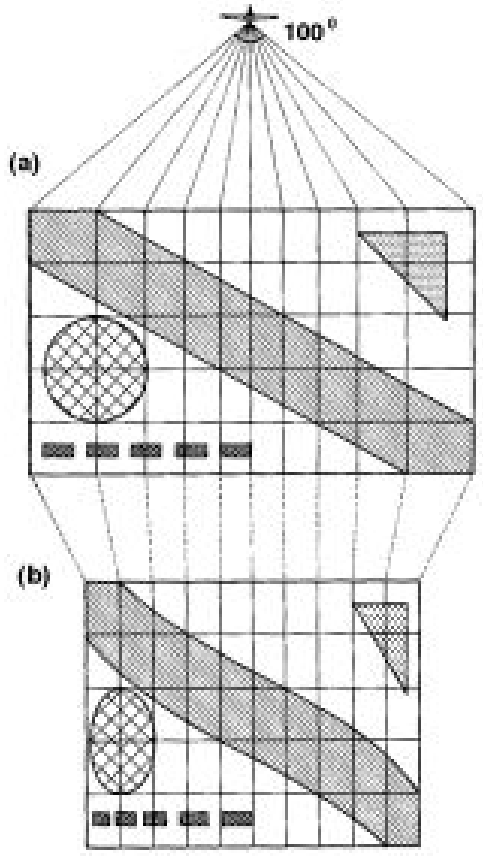

Geometric distortion must be corrected in order to associate the information content of each pixel to the right geographical location.

The geometric correction procedures are called:
Rectification or Georeferentiation: alignement of an image to a geographic map. It is the process by which the geometry of an image is made planimetric.
Registration: alignement of one image to another image. Two images of like geometry and of the same geographic area are made coincident, so that corresponding elements of the same ground area appear in the same place.
Geocoding: rectification of the image on a map with standard pixel. Allows for easier use of data in software packages (GIS).

Systematic errors are corrected establishing the mathematical relationship between the distorted pixel and the corrected one. It is necessary to know the platform position and the geometry of the acquisition. Commercially remote sensor data already have much of the systematic errors removed.

Non systematic errors are corrected using
Ground Control Points,
i.e., points whose position (in geographic or image coordinates) are known.

GCP's are easily locatable points both in the distorted image and in the reference image (or map): road or river intersections, airports, small islands, field or building corners

GCP's must not change with time and must be equally distributed all over the image.

The paired coordinates from many GCP's can be modeled to derive geometric transformation coefficients.

Let $X^{ref}Y^{ref}$ be the coordinates of a point in the reference (master) image. Let's assume that the coordinates X'Y' of the same point in the distorted image (slave) are described by the functions:

$$X' = f(X^{ref}, Y^{ref})$$
$$Y' = g(X^{ref}, Y^{ref})$$

Usually, to correct satellite images quadratic polynomials are employed

$$X' = a_{00} + a_{01}X^{ref} + a_{10}Y^{ref} + a_{11}X^{ref}Y^{ref} + a_{02}(X^{ref})^2 + a_{20}(Y^{ref})^2$$

$$Y' = b_{00} + b_{01}X^{ref} + b_{10}Y^{ref} + b_{11}X^{ref}Y^{ref} + b_{02}(X^{ref})^2 + b_{20}(Y^{ref})^2$$

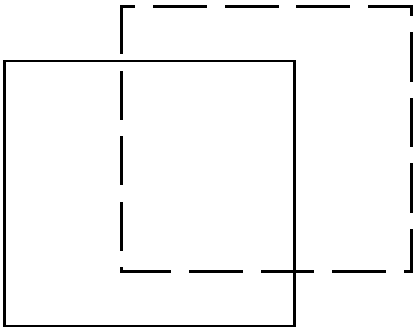

$$X' = a_{00} + X^{ref}$$

$$Y' = b_{00} + Y^{ref}$$

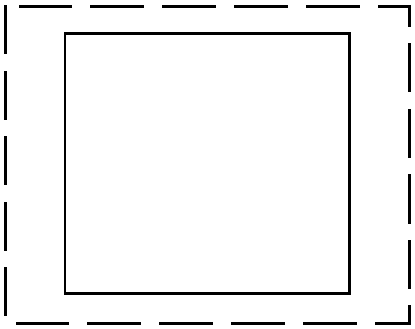

$$X' = a_{01} X^{ref}$$

$$Y' = b_{00} + Y^{ref}$$

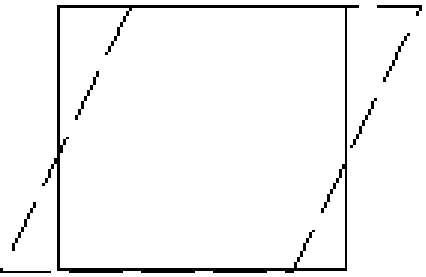

$$X' = X^{ref} + a_{10} Y^{ref}$$

$$Y' = Y^{ref}$$

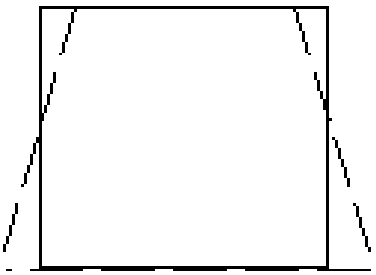

$$X' = a_{11} X^{ref}$$

$$Y' = Y^{ref}$$

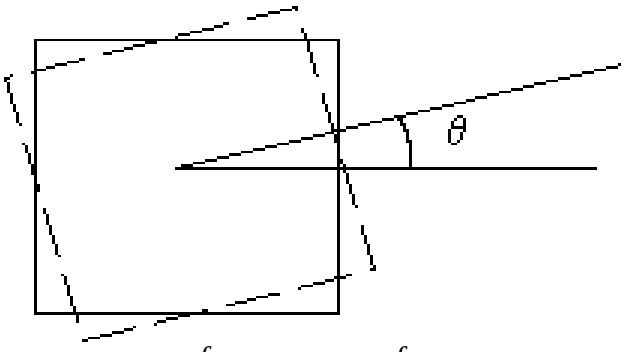

$$X' = a_{01} X^{ref} + a_{10} Y^{ref}$$

$$Y' = b_{01} X^{ref} + b_{10} Y^{ref}$$

The right coefficients of the correction functions f and g must be found

1. GCP's are located on the original image using a map or GPS.

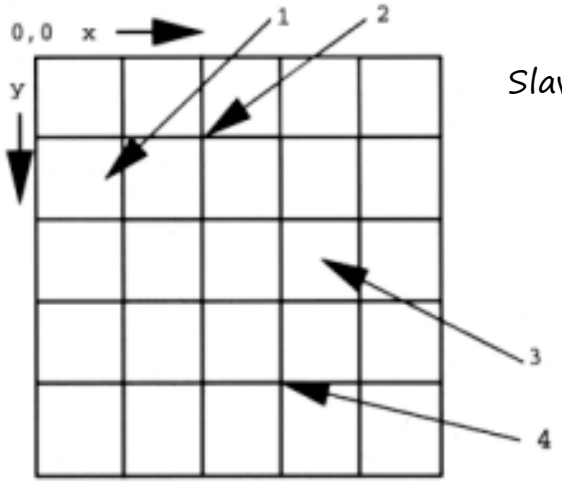

Slave image in terms of cols and rows

1. (0.75, 1.5) = lat1, long1
2. (2.0 , 1.0) = lat2, long2
3. (3.5 , 2.5) = lat3, long3
4. (3.0 , 4.0) = lat4, long4

2. GCP's are located on the l , geometrically correct grid.

Reference image in terms of lat and lon

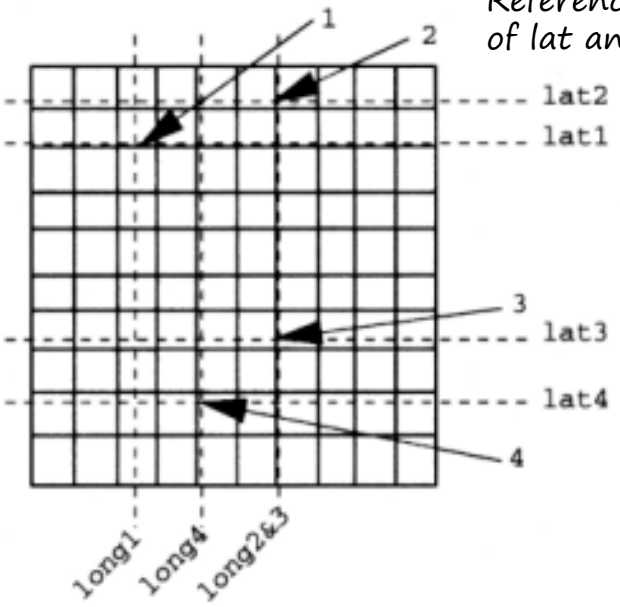

3. A transformation function is calculated to "stretch" the uncorrected image to fit the grid.

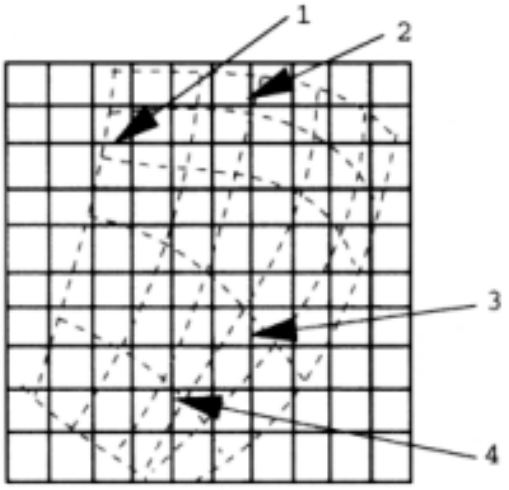

☞ *Fig. 7-31, p339: Location of GCPs*

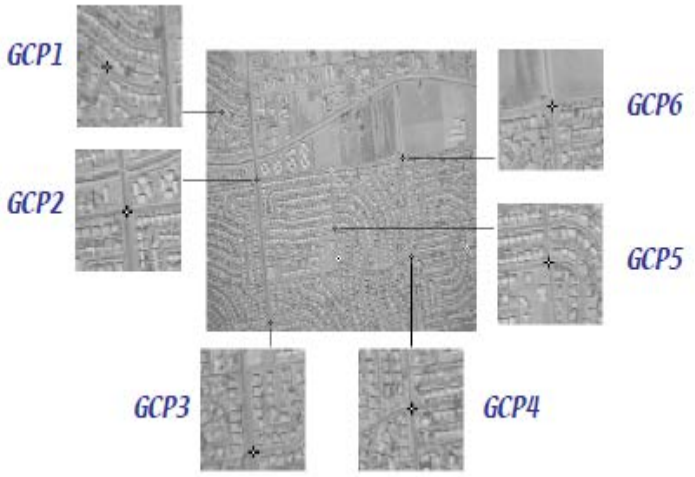

aerial photo (x,y)

SLAVE

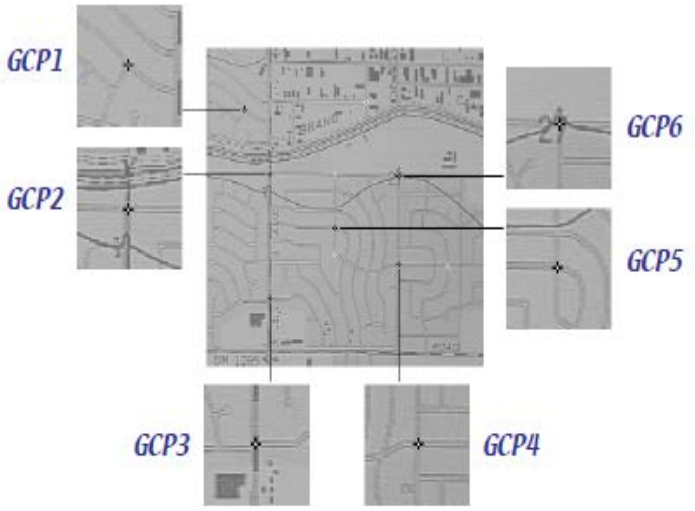

map reference (x_{ref},y_{ref})

MASTER (Reference)

☞ Fig. 7-32, p340: Mapping of GCPs

GCP coordinates in the two images are known:

$(X_{GCP}^{slave}, Y_{GCP}^{slave})$ and $(X_{GCP}^{ref}, Y_{GCP}^{ref})$

Which are the functions

$$X' = f(X^{ref}, Y^{ref})$$
$$Y' = g(X^{ref}, Y^{ref})$$

that better model the displacement from $(X_{GCP}^{ref}, Y_{GCP}^{ref})$ to $(X_{GCP}^{slave}, Y_{GCP}^{slave})$?

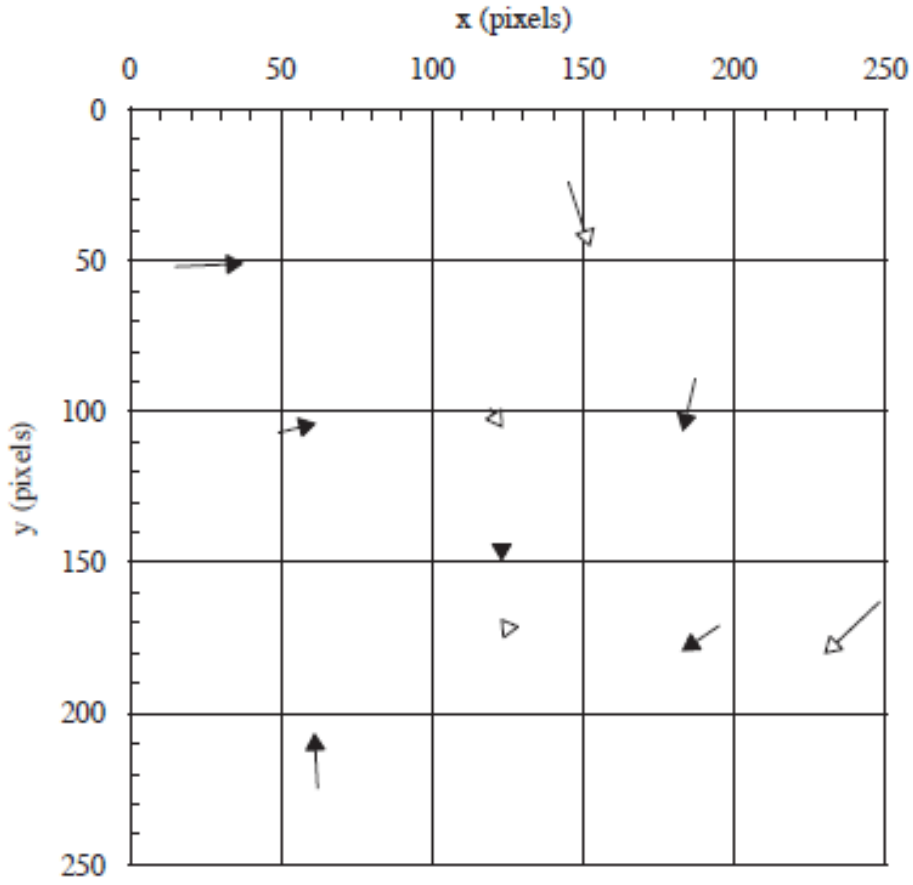

The polynomial coefficients may be found applying the error minimization techniques, and exploiting the GCP coordinates in the Master $(X_{GCP}^{ref}, Y_{GCP}^{ref})$ and the Slave $(X_{GCP}^{slave}, Y_{GCP}^{slave})$

$$RMSE = \sqrt{\frac{1}{N_{GCP}} \sum_{i=1}^{N_{GCP}} (X_{GCPi}^{'} - X_{GCPi}^{slave})^2 + (Y_{GCPi}^{'} - Y_{GCPi}^{slave})^2}$$

$(X_{GCP}^{'}, Y_{GCP}^{'})$ are the GCP coordinates obtained through the functions

$$f(X_{GCP}^{ref}, Y_{GCP}^{ref}) \text{ and } g(X_{GCP}^{ref}, Y_{GCP}^{ref}).$$

The polynomial coefficients in the f and g functions are selected in such a way as to minimize the RMS Error.

☞ Fig. 7-34, p341: Refinement of GCPs by error analysis

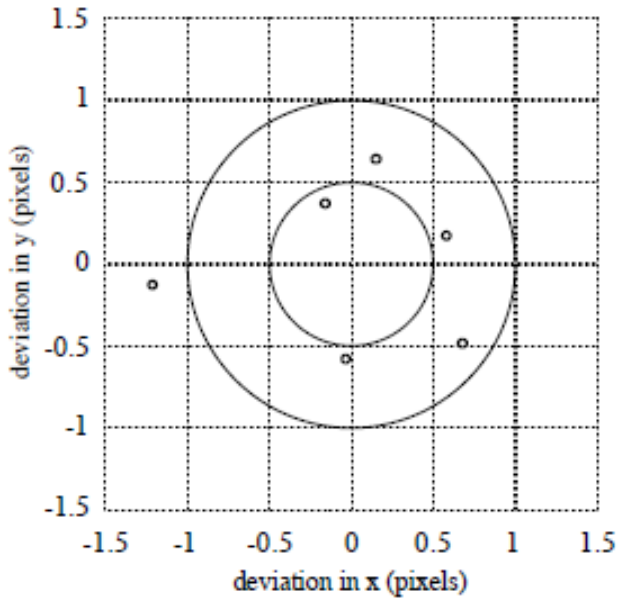

original six GCPs

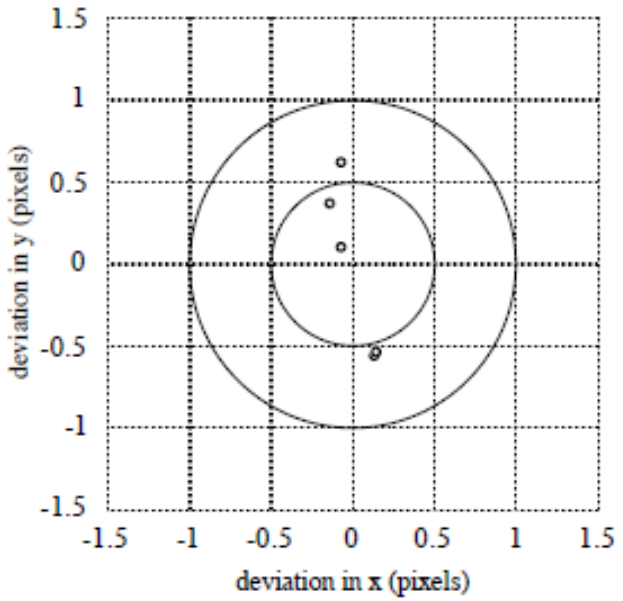

five GCPs, with outlier deleted

There is an iterative process that takes place.
First, all of the original GCPs (e.g., 6 GCPs) are used to compute an initial set of coefficients. The root mean squared error (RMSE) associated with each of these initial 6 GCPs is computed. Then, the individual GCPs that contributed the greatest amount of error are determined and deleted. After the first iteration, this might only leave 5 of 6 GCPs.
A new set of coefficients is then computed. The process continues until the RMSE reaches a user-specified threshold (e.g., $\leq$1 pixel error in the x-direction and $\leq$1 pixel error in the y-direction).

The goal is to remove the GCPs that introduce the most error into the coefficient computation. When the acceptable threshold is reached, the final coefficients are used to rectify the slave image to an output image, as previously discussed.

FCC SPOT Morocco

June image

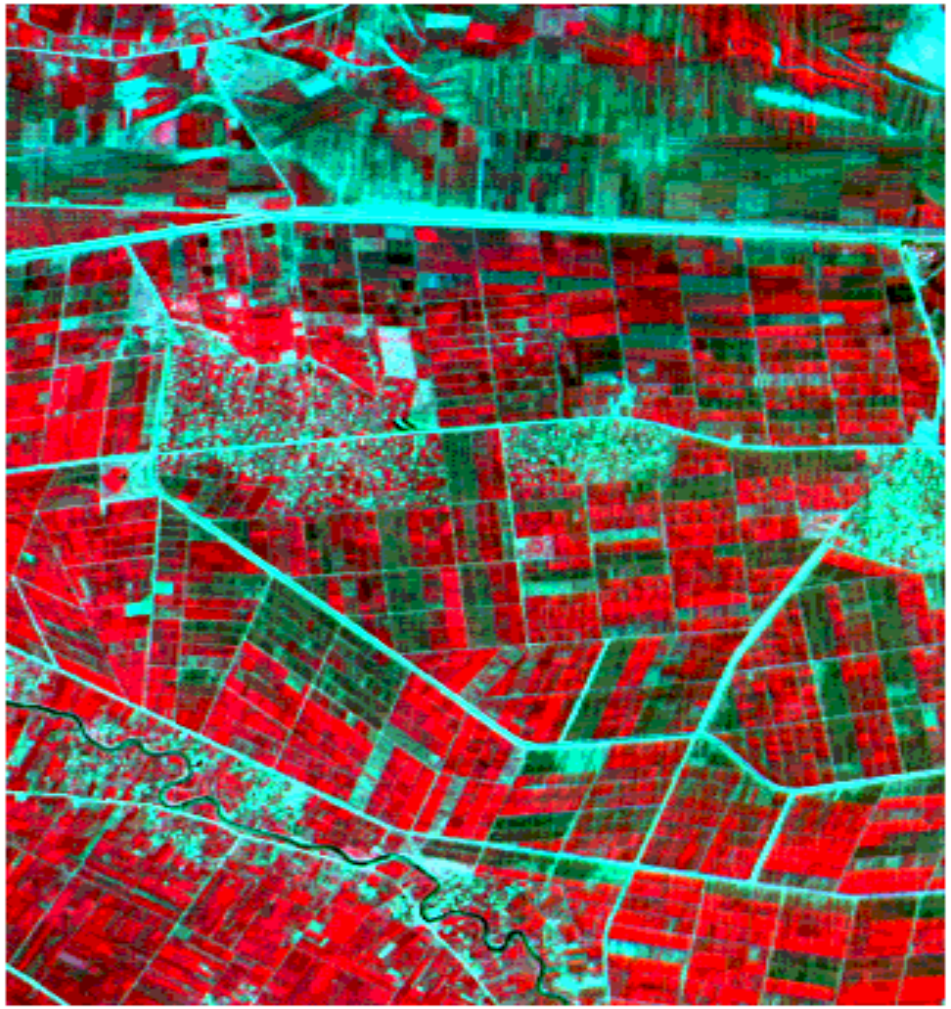

May image

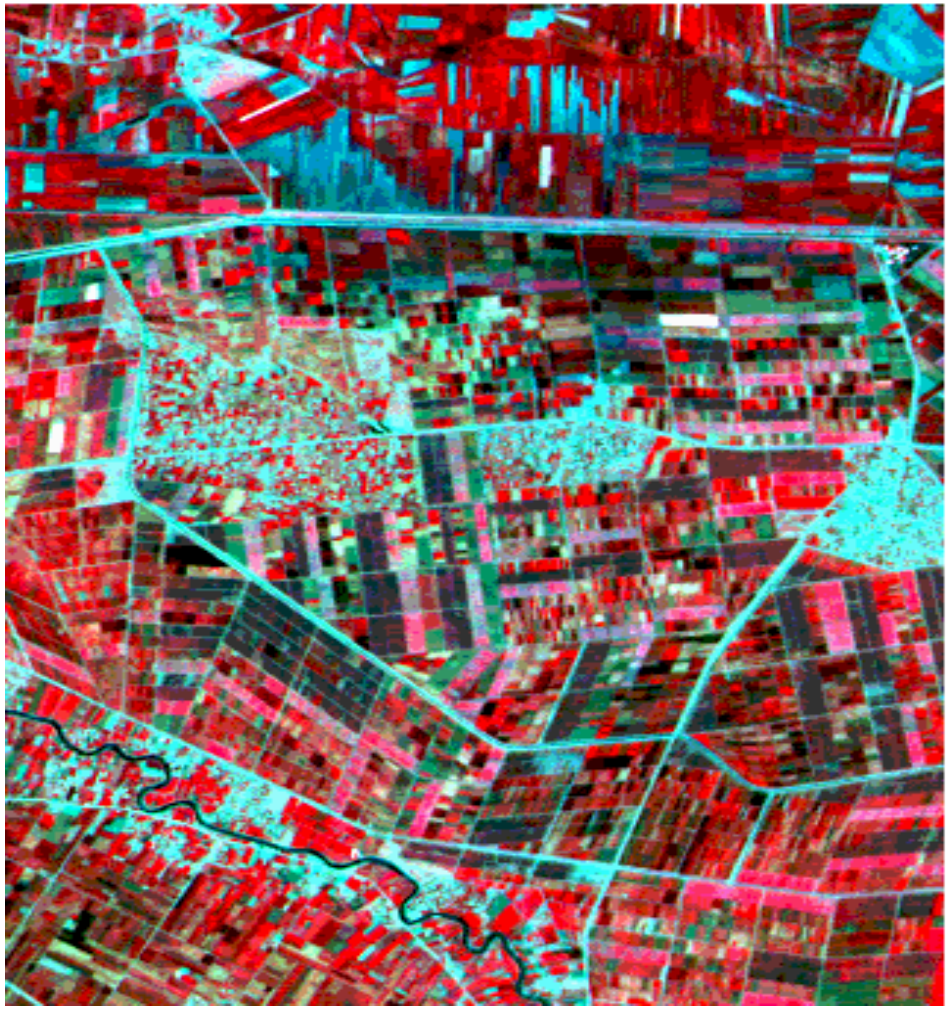

May image with 12 control points

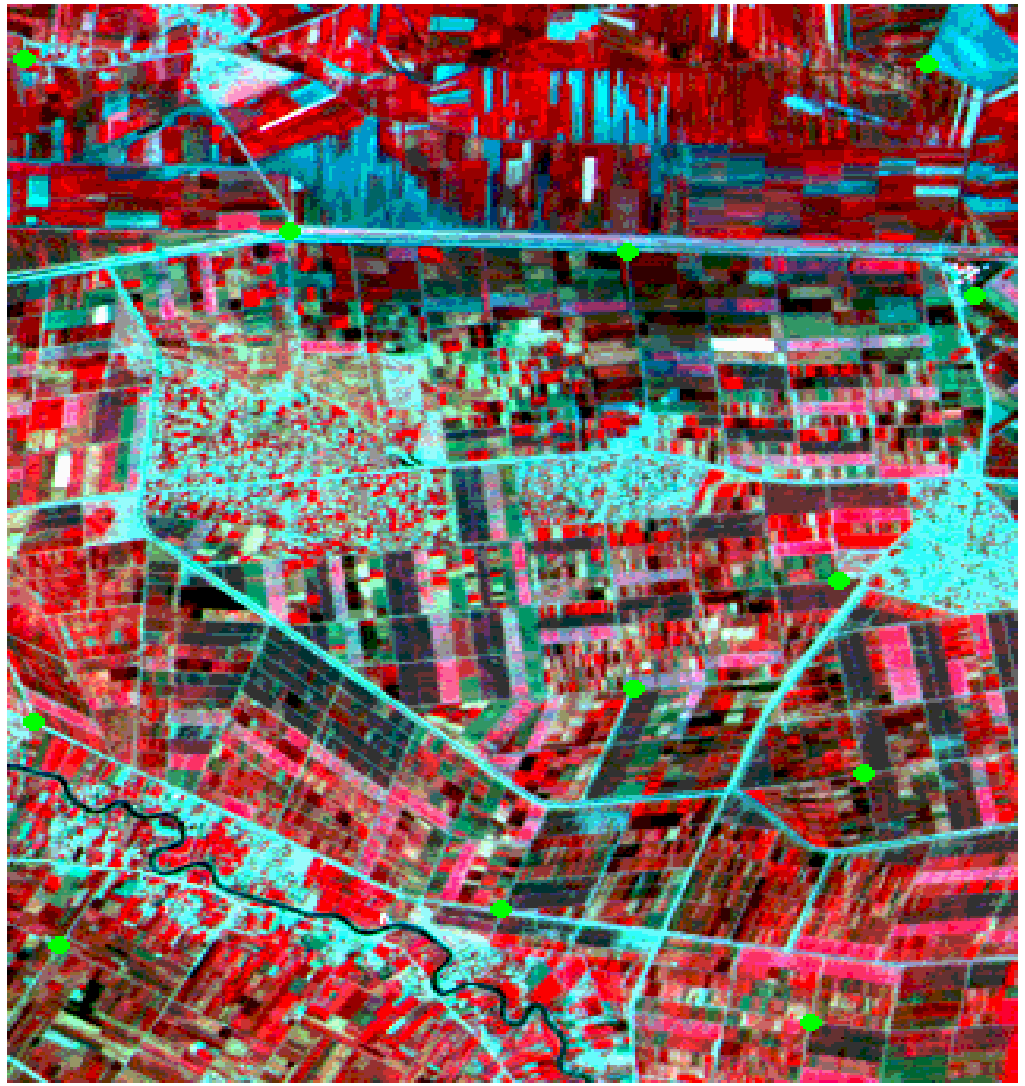

June image

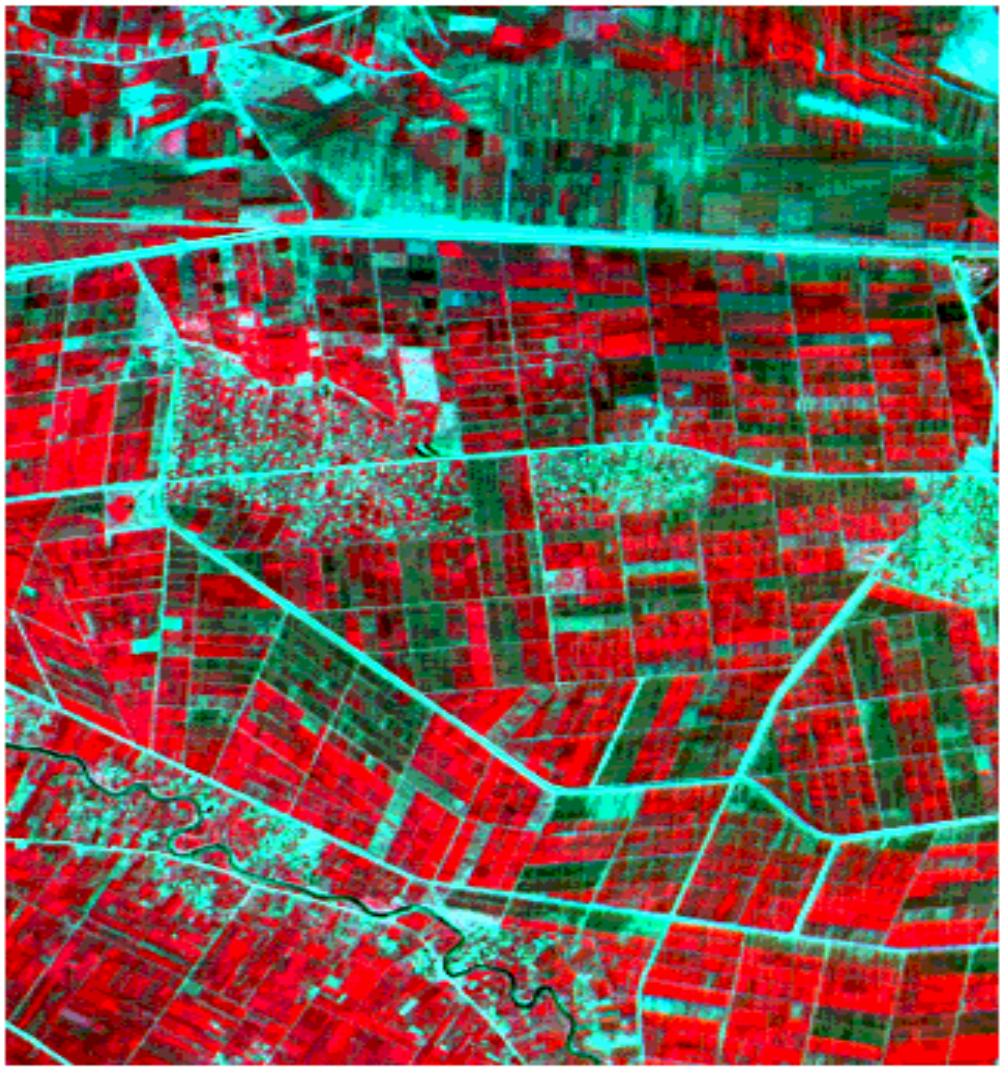

Resampled May image

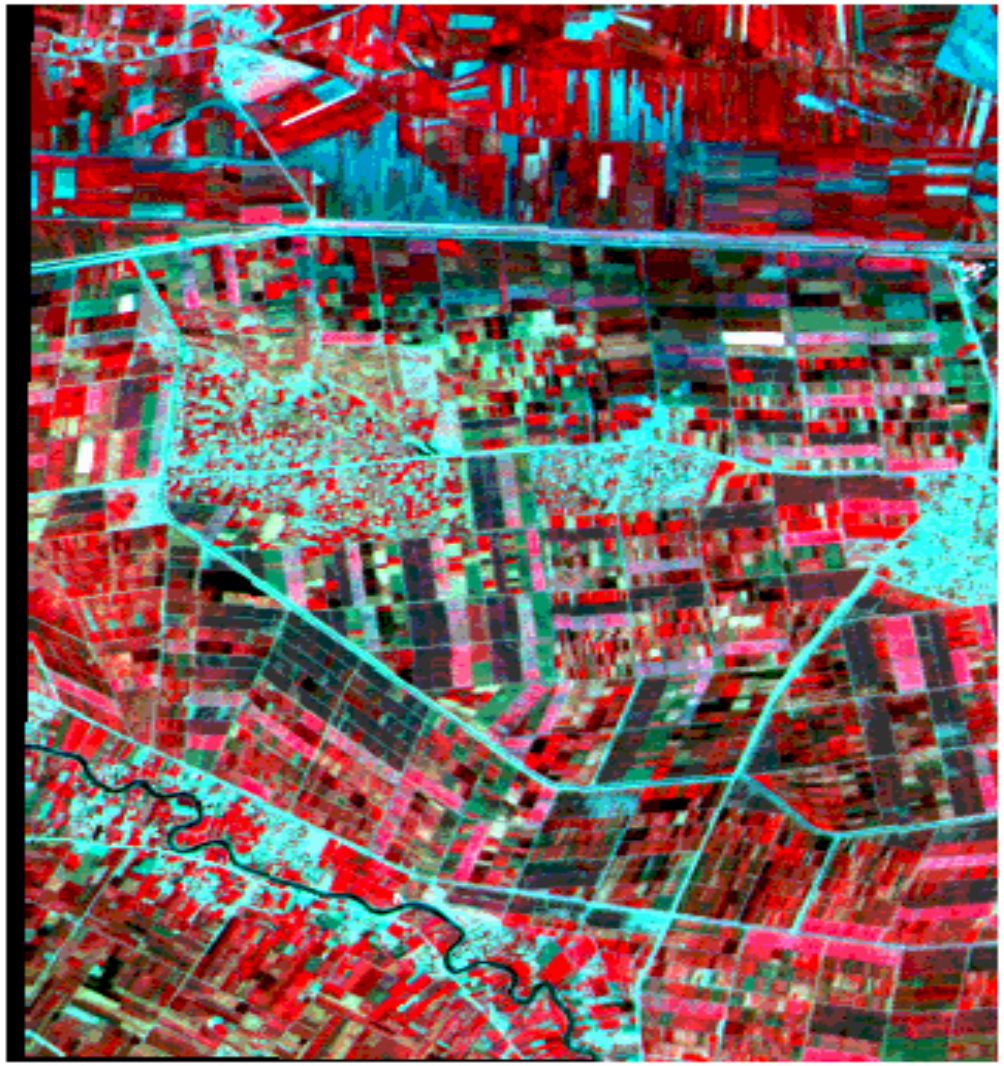

The XY coordinates in the corrected image are integer numbers that correspond to the real numbers $X'Y'$ in the distorted image.

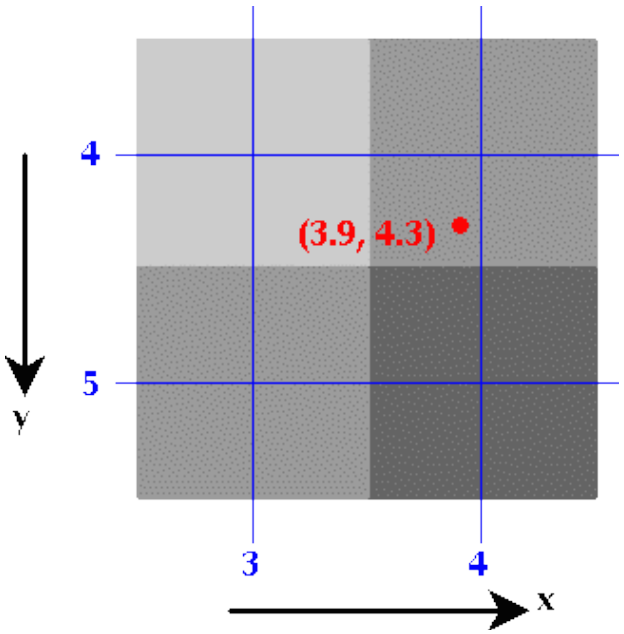

Then, it is necessary to establish how and what value assign to the coordinates XY
This process is called Resampling or Warping.

What **DN** will we assign to pixel **X,Y** in the corrected image, that corresponds to coordinate **X′, Y′** in the distorted image?

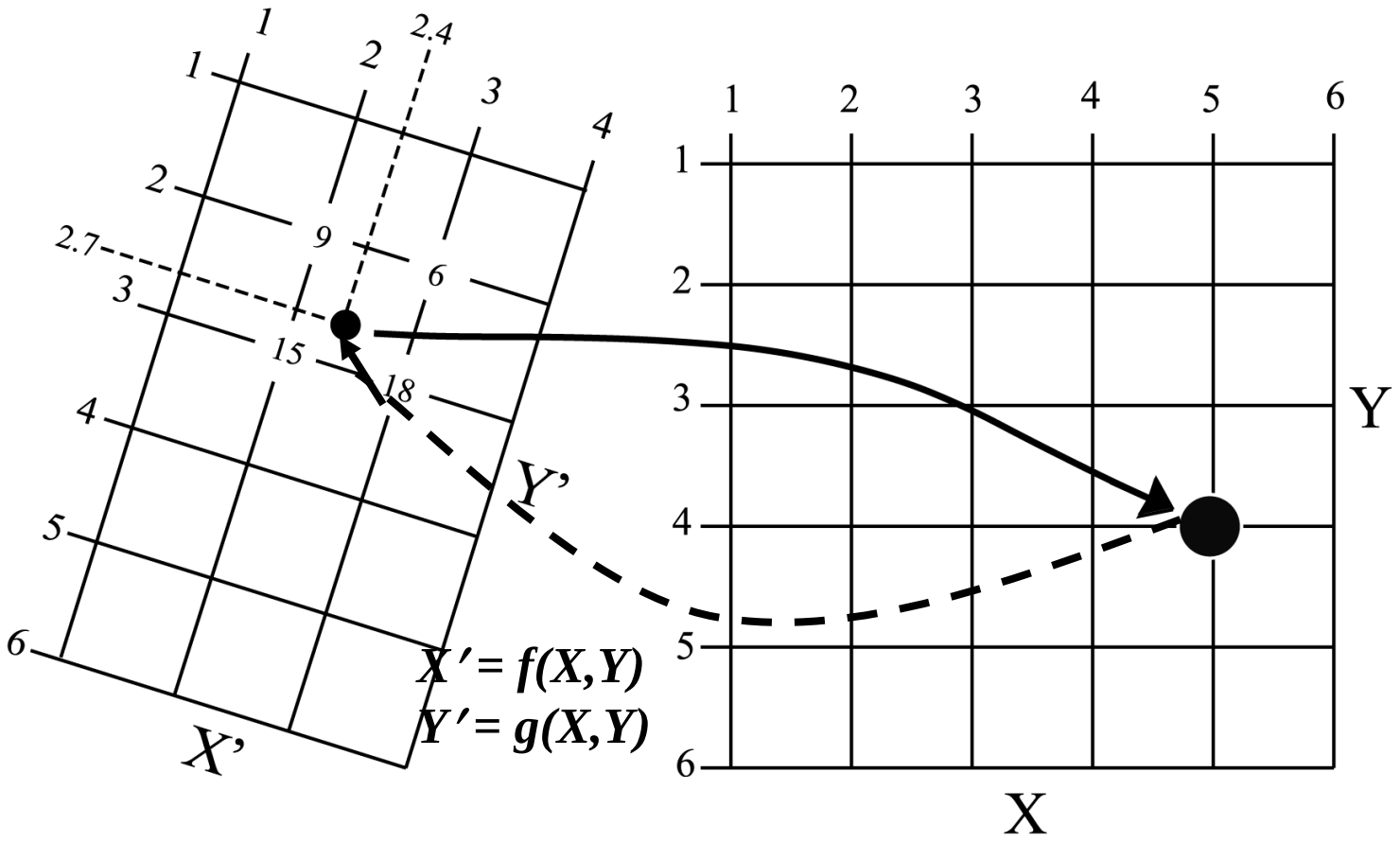

Original input image

(a)

Rectified output image

(b)

The goal is to fill a matrix that is in a rectified projection with the appropriate values from the acquired (distorted) image.

Among the most used technique, there is nearest neighbour

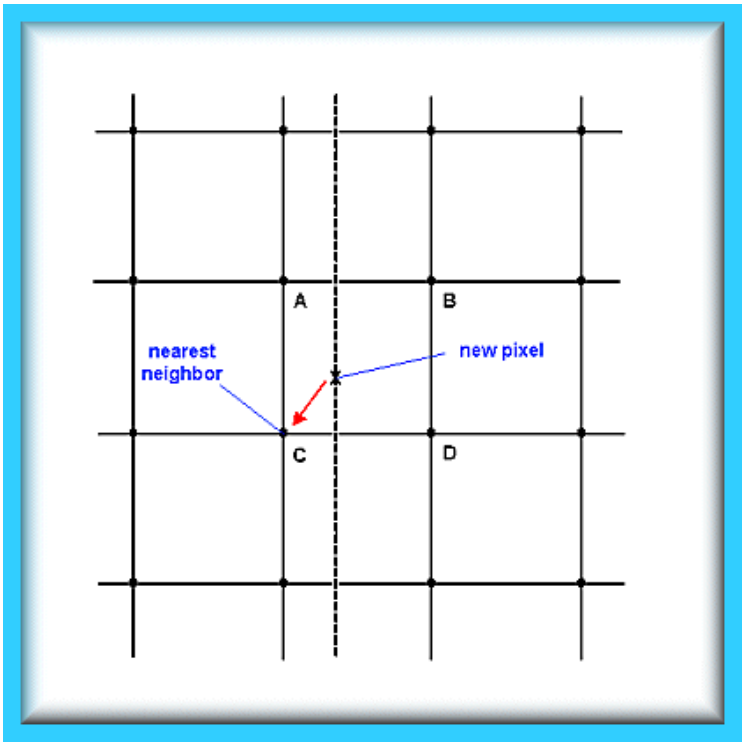

To each pixel in the corrected image, the **DN** from the nearest pixel is assigned

Resampling - Nearest neighbor

As the name implies, nearest neighbor simply grabs the closest image pixel to the desired resampled pixel

- Nearest neighbor has several good properties
  - Fast
  - Reversible
  - Saves the radiometric quality of the original data
- Problems are
  - Not very smooth
  - Image pixels can show up more than once and some will disappear
- Other resamplings, bilinear and cubic convolution do better at smoothing the data and including information about neighboring pixels
  - Irreversible
  - Destroys the radiometry
  - Bad pixels can propagate through the processing

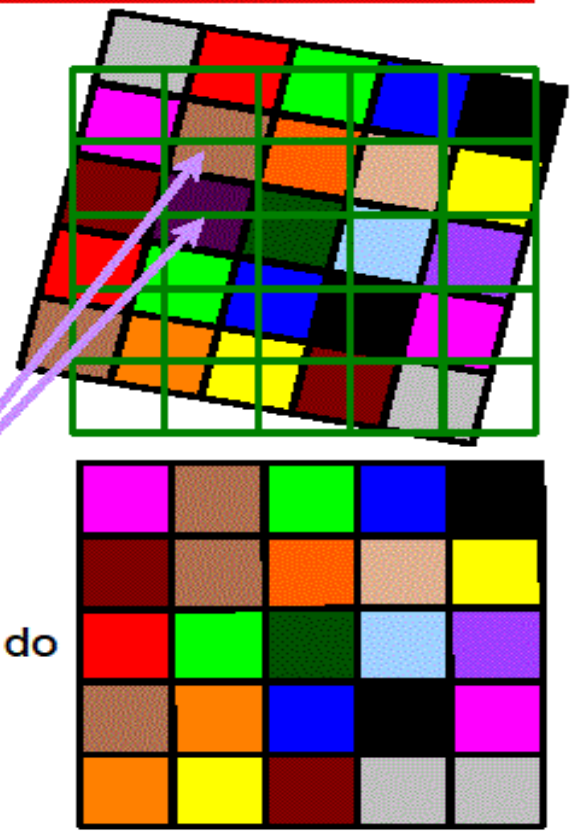

Original image

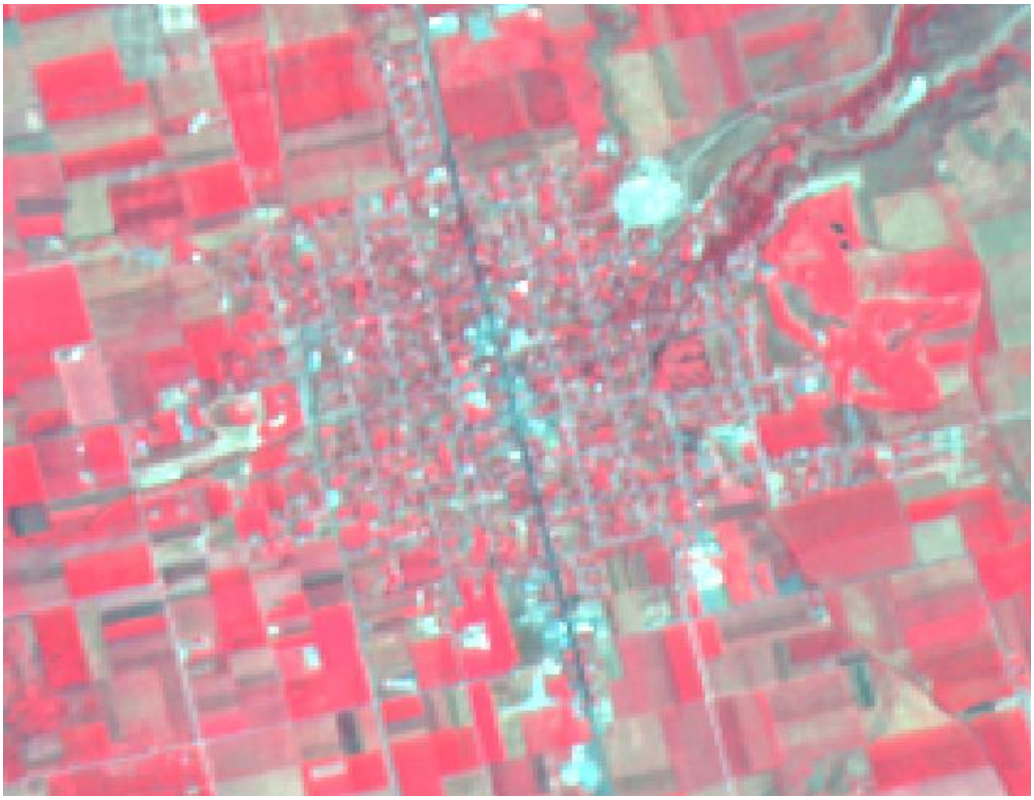

Image rectified with NN

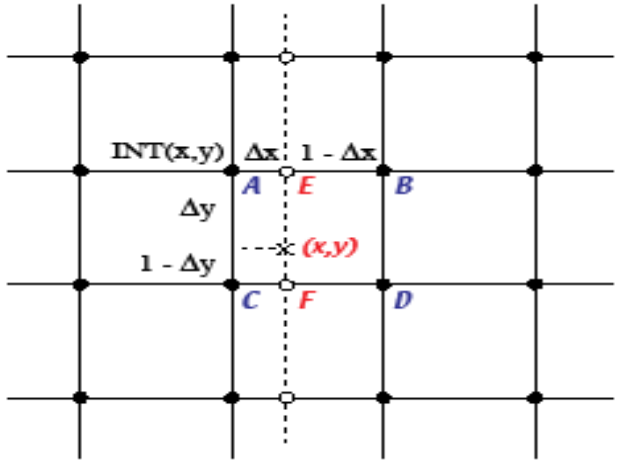

☞ *Fig. 7-39, p348: resampling distances*

- ***Pixels are resampled using a weighted average of the neighboring pixels***
- ***Three types of weighting functions:***
- ***nearest-neighbor: fast, but discontinuous***
- ***bilinear: slower, but continuous***

$$DN = [\Delta x DN_B + (1-\Delta x)DN_A](1-\Delta y) + [\Delta x DN_D + (1-\Delta x)DN_C]\Delta y \quad \text{(Eq. 7-28)}$$

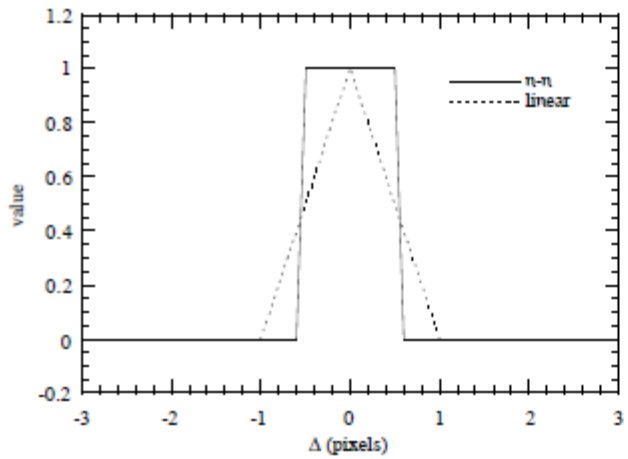

☞ *Fig. 7-40, p349: comparison of nearest-neighbor and bilinear weighting functions in 1-D*

- ***bicubic: slowest, but results in sharpest image***

special case of Parametric Cubic Convolution (PCC)

$$
\begin{aligned}
r(\Delta;\alpha) &= (\alpha+2)|\Delta|^3-(\alpha+3)|\Delta|^2+1 && |\Delta| \le 1 \\
&= \alpha(|\Delta|^3-5|\Delta|^2+8|\Delta|-4) && 1 \le |\Delta| \le 2 \\
&= 0 && |\Delta| \ge 2
\end{aligned}
\qquad \text{(Eq. 7-29)}
$$

"standard" bicubic is α = -1; superior bicubic is α = -0.5

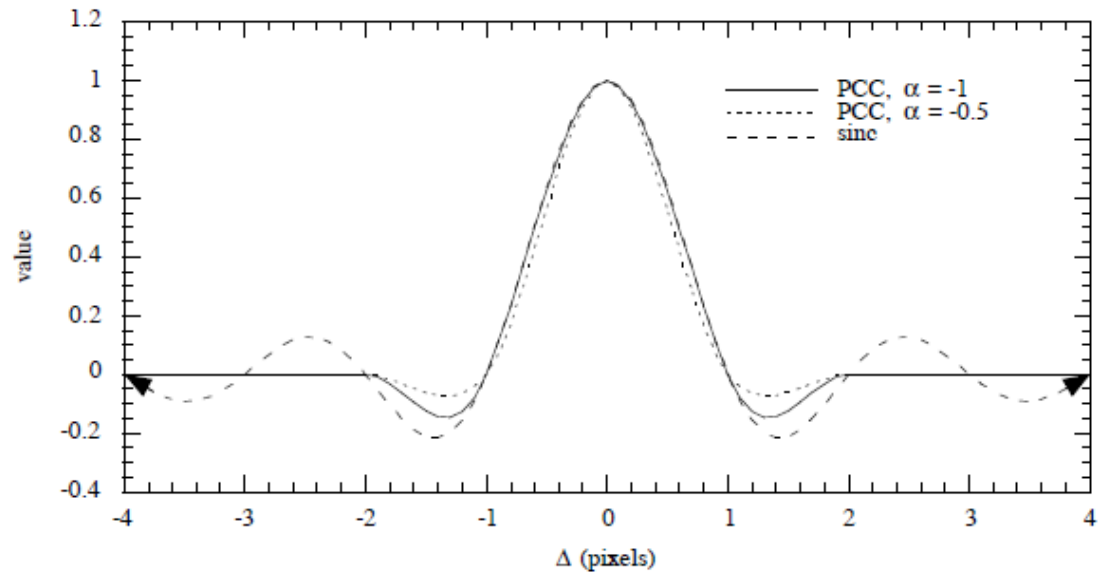

☞ ***Fig. 7-43, p353: bicubic weighting functions***

edge enhancement depends on side-lobe amplitude which is proportional to α

Nearest neighbour

Cubic Convolution

Nearest Neighbour is fast and does not modify DN's of an image (is reversible). May produce a "stair-stepped" effect in the rectified image; some pixels may be duplicated and others may be lost.

Bilinear or cubic interpolation reduce the "stair-stepped", but also the image contrast.
They require a higher calculation time.

The first method has a higher radiometric accuracy. The opposite is true for the other methods.

Radiometric calibration

consists in the transformation of **DN**'s into radiances.

In this way, it is possible to compare directly multispectral, multitemporal and multisensor data.

Later on, we will deal with radiometric correction that ensures that different measured spectral radiances correspond to spectral reflectance variations of the surface alone.

In order to perform radiometric calibration, it is necessary to know the calibration coefficients of the sensor. Usually, sensors are calibrated so as to respect a linear relationship between radiance and **DN**:

$$L = \frac{L_{\max} - L_{\min}}{2^M - 1} DN + L_{\min}$$

L is radiance expressed in [$W \cdot m^{-2} \cdot sr^{-1} \cdot \mu m^{-1}$]

L_{max}-L_{min} = dynamic interval of the sensor

M = radiometric resolution in bits

The calibrated radiances may be used as inputs to geophysical models.

From DN to Radiance to Reflectance

LANDSAT TM Spectral Band	Calibration Gain Coefficient (counts/(W/m^2/sr/μm))	Wavelength (μm)	Solar Irradiance (W/m^2/μm)
1	G=(-3.58E-05)*D+1.376	0.4863	1959.2
2	G=(-2.10E-05)*D+0.737	0.5706	1827.4
3	G=(-1.04E-05)*D+0.932	0.6607	1550.0
4	G=(-3.20E-06)*D+1.075	0.8382	1040.8
5	G=(-2.64E-05)*D+7.329	1.677	220.75
7	G=(-3.81E-04)*D+16.02	2.223	74.960

D = *days since launch*

Radiance = (DN - Offset)/Gain

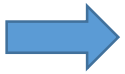

From calibrated radiances it is possible to obtain the reflectance of the observed surface.

When atmospheric effects are not corrected, you can get the so called "Top Of Atmosphere" Reflectance:

$$\rho_\lambda^{TOA} = \frac{\pi L_\lambda^S}{E_\lambda}$$

Where L_λ^S is the radiance measured by the sensor (at the Top Of Atmosphere).

$$E_\lambda = E_\lambda^0 \cos\vartheta$$

$$E_\lambda^0 = \pi B_\lambda(5900\,K) \cdot \frac{R_S^2}{R_{E-S}^2}$$

E_λ^0 = spectral solar irradiance at the mean Earth–Sun distance, incident at nadir.

$R_{E-S} = 149.6 \cdot 10^6\,Km$, $\boldsymbol{R_S}$ is the Sun radius.

$\boldsymbol{R_S/R_{E\text{-}S}}$=0.00465

Solar irradiance can be approximated as the one from a black body at **5900 K**.

$\boldsymbol{E_\lambda}$ is the fraction solar irradiance intercepted by Earth

ϑ=solar zenith angle

$\boldsymbol{B_\lambda}$=Spectral black body radiance

For the TM bands:

$$E_1^0 = 1957 Wm^{-2}\mu m^{-1}$$
$$E_2^0 = 1829 Wm^{-2}\mu m^{-1}$$
$$E_3^0 = 1557 Wm^{-2}\mu m^{-1}$$
$$E_4^0 = 1047 Wm^{-2}\mu m^{-1}$$
$$E_5^0 = 219.3 Wm^{-2}\mu m^{-1}$$

$$\rho_\lambda^{TOA} = \frac{\pi L_\lambda}{\delta^2 E_\lambda^0 \cos\vartheta}$$

$$\delta = 1/(1 - 0.0163\cos(0.9854(DoY - 4)))$$

δ is a corrective factor of the Sun-Earth distance: it takes account of the ecliptic eccentricity. Aphelion and perihelion differ from the mean $\boldsymbol{R_{E\text{-}S}}$ distance by some millions of km.

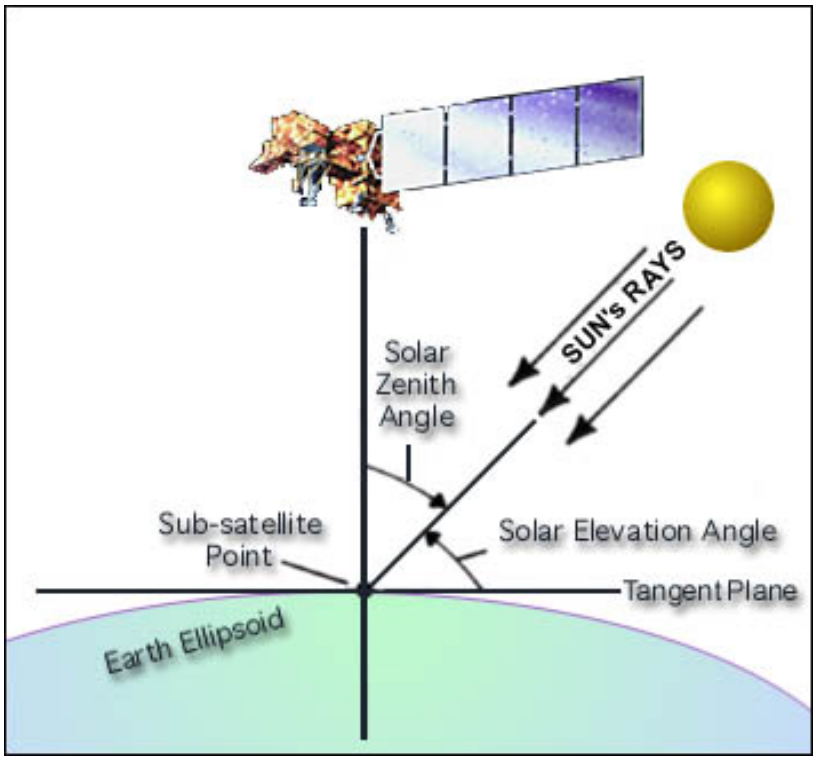
SUN's RAYS
Solar
Zenith
Angle
Sub-satellite
Point
Solar Elevation Angle
Tangent Plane
Earth Ellipsoid

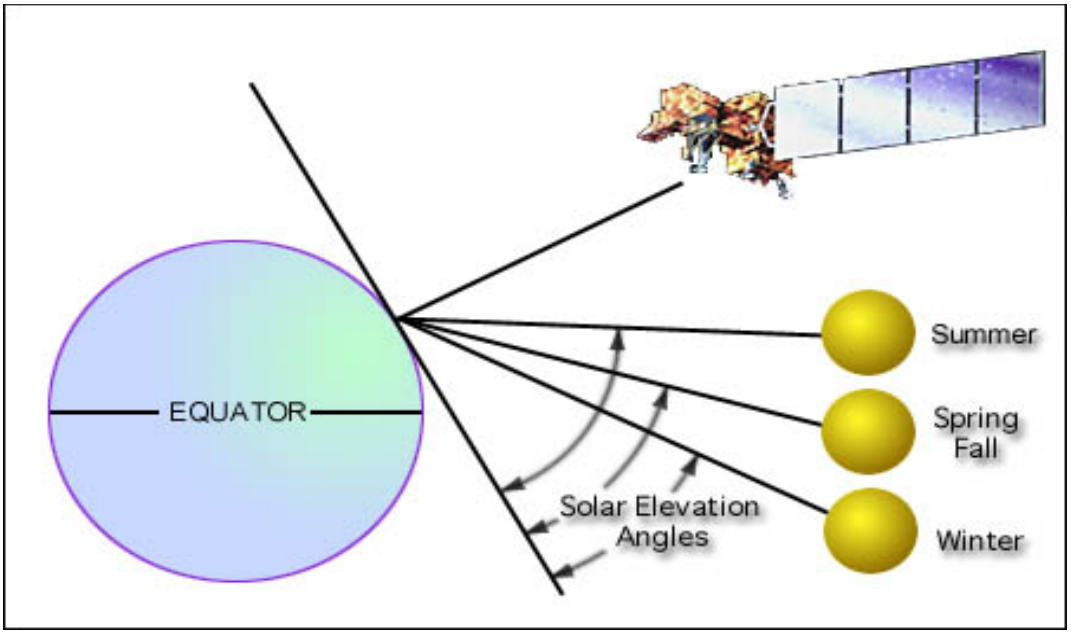
EQUATOR
Summer
Spring
Fall
Winter
Solar Elevation
Angles

☞ *Fig. 2-12, p51: effect of solar incidence angle and topography*

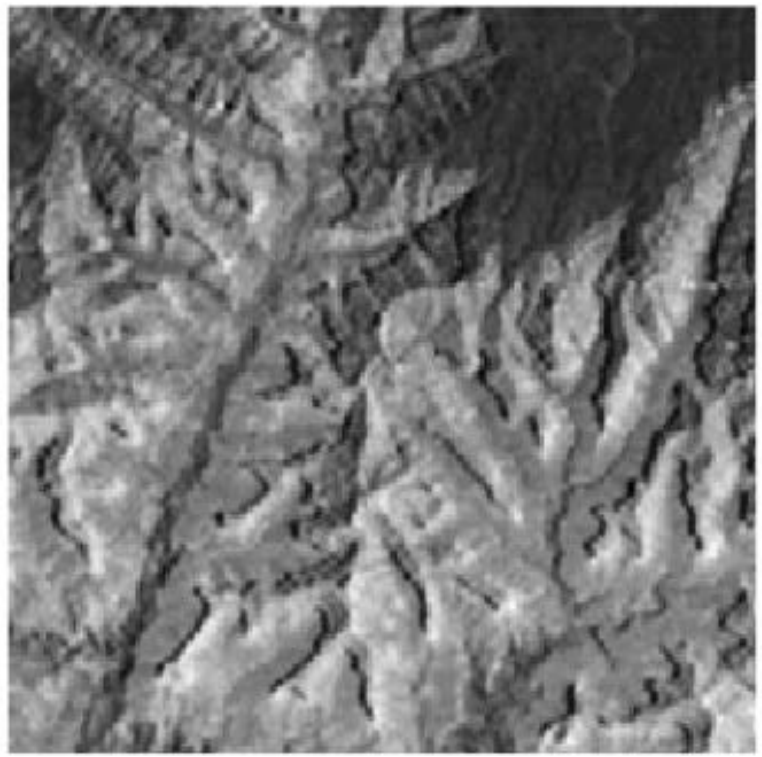

June 11, 1981

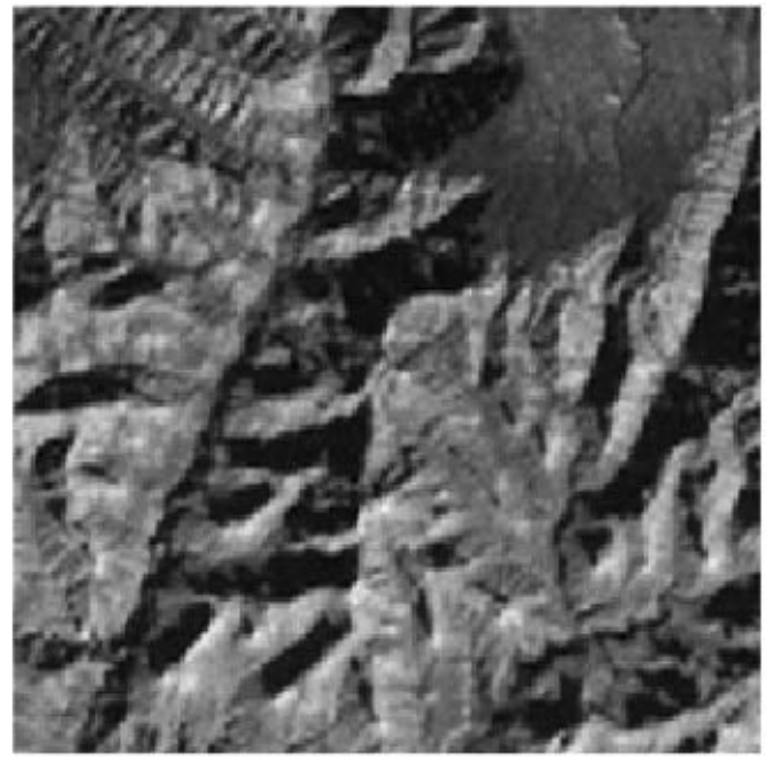

October 20, 1980

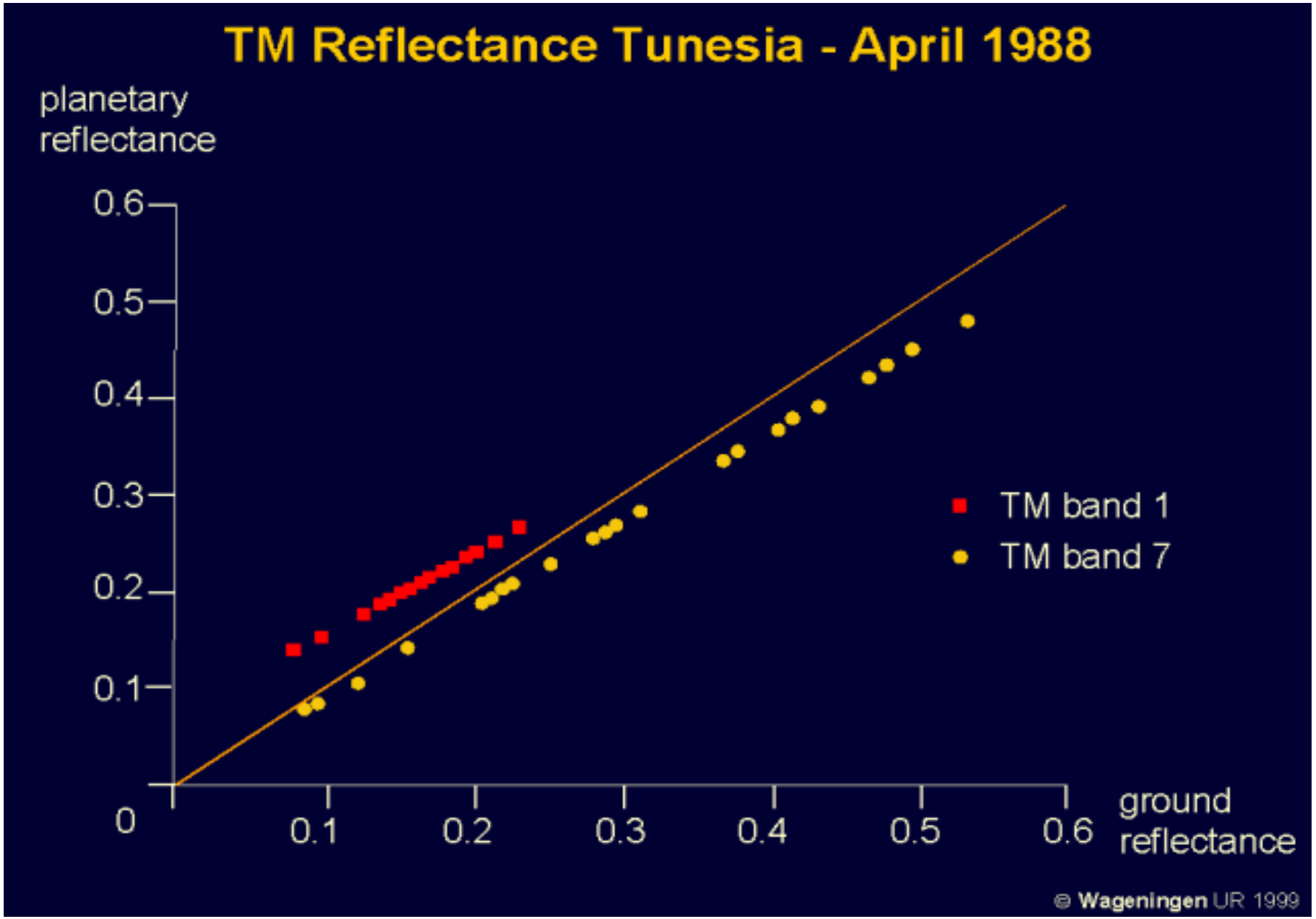
TM Reflectance Tunesia - April 1988
planetary reflectance
0.6
0.5
0.4
0.3
0.2
0.1
0
0.1
0.2
0.3
0.4
0.5
0.6
ground reflectance
TM band 1
TM band 7
© Wageningen UR 1999

In order to estimate the reflectance of the remote sensed surface,

atmospheric correction

must be applied on data.

Electromagnetic radiation passing through atmosphere experiences absorption and scattering

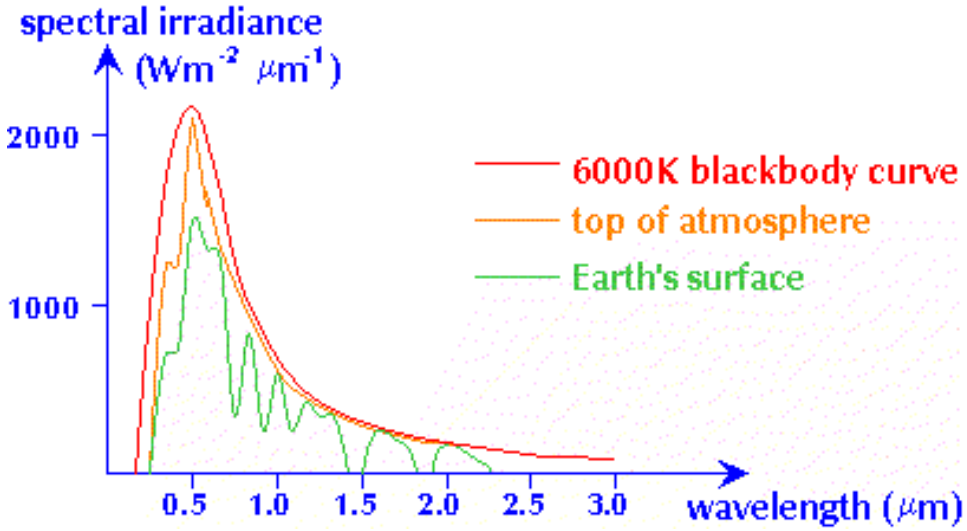

The absorption lines are determined by gases (ozone, water vapor, carbon dioxide).

Scattering is determined, in different ways, by particles present in the atmosphere under various forms.

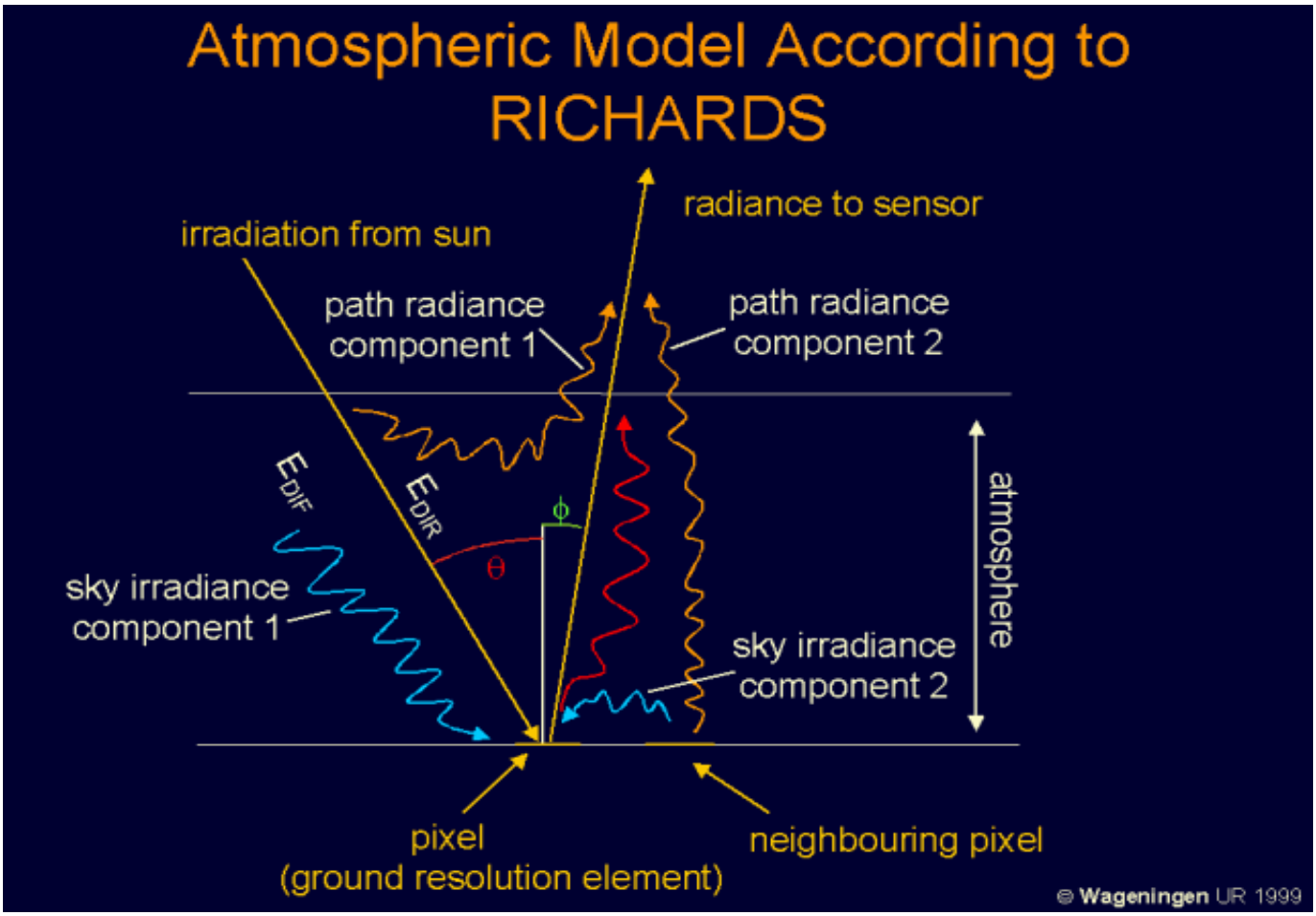

The remote sensed radiance contains not only the radiance from the resolution cell, but also radiance scattered by the atmosphere (originated by atmosphere itself or by surfaces close to the resolution cell).

- radiance from resolution cell attenuated by the atmosphere (going to and out the cell)
- radiance scattered by atmosphere toward the resolution cell (sky irradiance) and then reflected
- radiance scattered into sensor IFOV by atmosphere or by adjacent cells (path radiance)

- ***Summary for direct unscattered, surface-reflected component***

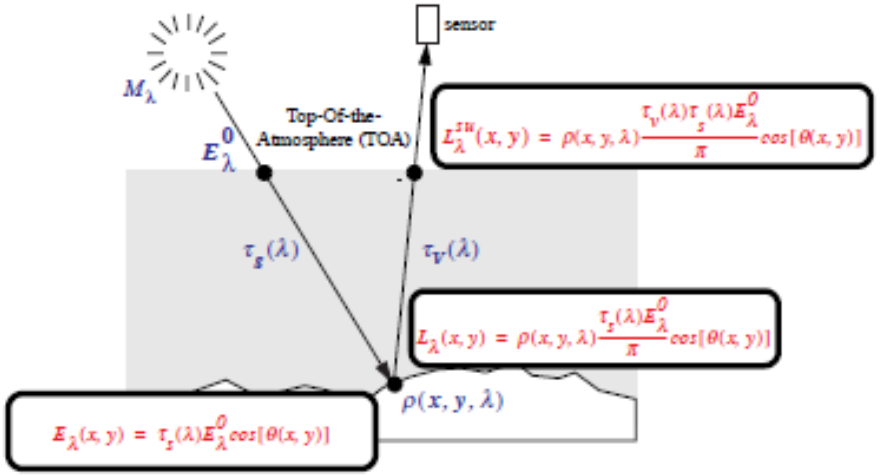

- ***incident irradiance transformed by reflection at Earth's surface to surface radiance***

$$L_\lambda(x,y) = \rho(x,y,\lambda)\frac{E_\lambda(x,y)}{\pi}$$

earth's surface:

$$= \rho(x,y,\lambda)\frac{\tau_s(\lambda)E^0_\lambda}{\pi}\cos[\theta(x,y)] \quad (\text{W-m}^{-2}\text{-sr}^{-1}\text{-}\mu\text{m}^{-1})\ (\text{Eq. 2-7})$$

- ***surface radiance modified by atmospheric transmittance along sensor view path to at-sensor radiance***

$$L^{su}_\lambda = \tau_v(\lambda)L_\lambda$$

at-sensor:

$$= \rho(x,y,\lambda)\frac{\tau_v(\lambda)\tau_s(\lambda)E^0_\lambda}{\pi}\cos[\theta(x,y)] \quad (\text{Eq. 2-8})$$

  - ***atmospheric transmittance varies with view angle (and solar angle)***

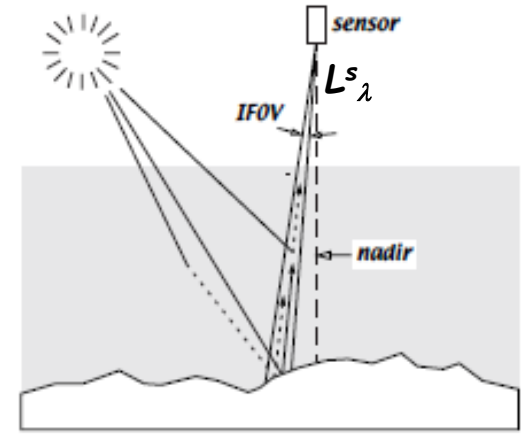

Down-scattered=sky irradiance

Path radiance contains no information about surface

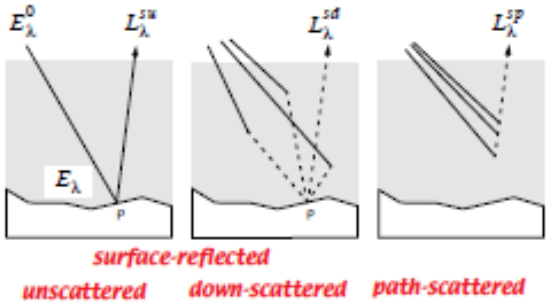

$$L^s_\lambda(x,y) = L^{su}_\lambda(x,y) + L^{sd}_\lambda(x,y) + L^{sp}_\lambda$$
$$= \rho(x,y,\lambda)\frac{\tau_v(\lambda)\tau_s(\lambda)E^0_\lambda}{\pi}\cos[\theta(x,y)] + F(x,y)\rho(x,y,\lambda)\frac{\tau_v(\lambda)E^d_\lambda}{\pi} + L^{sp}_\lambda$$
$$= \rho(x,y,\lambda)\frac{\tau_v(\lambda)}{\pi}\{\tau_s(\lambda)E^0_\lambda\cos[\theta(x,y)] + F(x,y)E^d_\lambda\} + L^{sp}_\lambda .$$

$\rho(x,y,\lambda)$:surface diffuse reflectance(unitless)

$\tau_v(\lambda)$:view path atmospheric transmittance(unitless)

$\tau_s(\lambda)$:solar path atmospheric transmittance(unitless)

E^0_λ :incident, exo-atmospheric spectral irradiance($W\text{-}m^{-2}\text{-}\mu m^{-1}$)

$\cos[\theta(x,y)]$:cosine of angle between solar vector and surface normal

$F(x,y)$:fraction of sky hemisphere visible from surface point

E^d_λ :downwelling atmospheric spectral irradiance($W\text{-}m^{-2}\text{-}\mu m^{-1}$)

L^{sp}_λ :upwelling atmospheric path spectral radiance($W\text{-}m^{-2}\text{-}sr^{-1}\text{-}\mu m^{-1}$)

☞ *Fig. 2-7, p44: atmospheric transmittance at nadir and 40°*

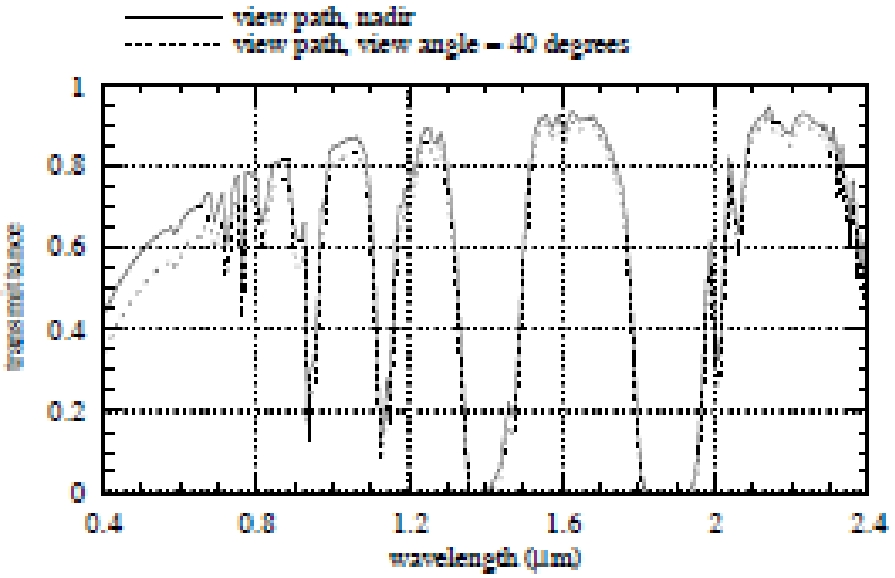

☞ *Fig.2-8, p47: compare path-scattered and ground-reflected components*

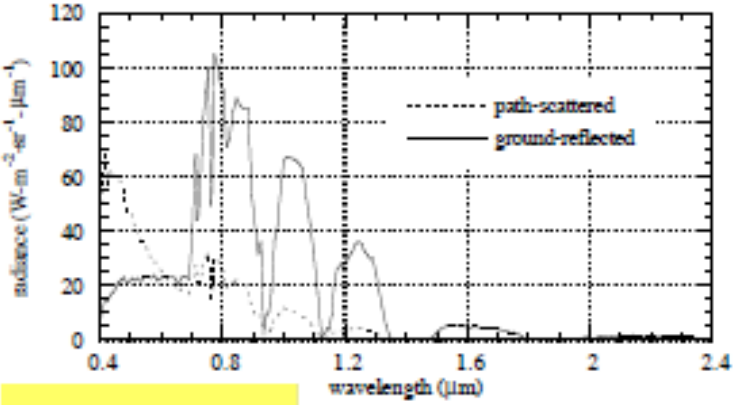

path-scattered component dominates below 600nm

In order to perform an
absolute atmospheric correction
it is necessary to know:

The solar zenith angle
- The spectral solar irradiance
- The sky (diffuse) irradiance and the path radiance
- The atmospheric transmittance (optical depth) at the wavelength of interest.

The last two factors depend on the humidity concentration in the atmosphere, on its temperature and on the kind of atmospheric particles.
Furthermore, they depend on the geographical site and on the season.

All of the above quantities may be provided by physical models that simulate the physical process of scattering and absorption at the level of individual particles and molecules.
The models are very complex and need many meteorological data as input, that may not always be available

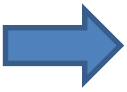

Atmospheric Correction Using ATCOR

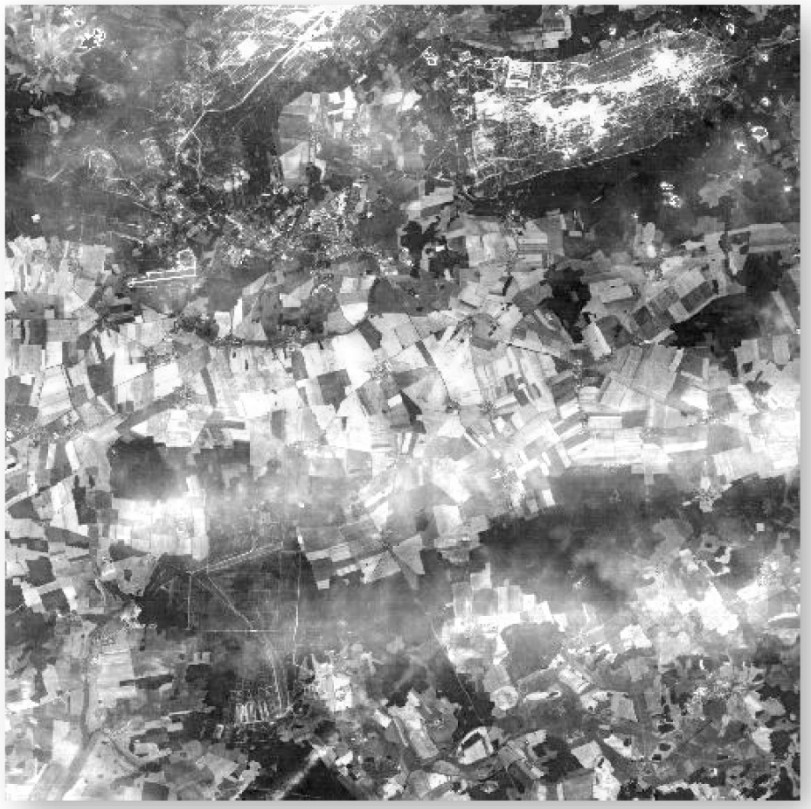

a. Before atmospheric correction.

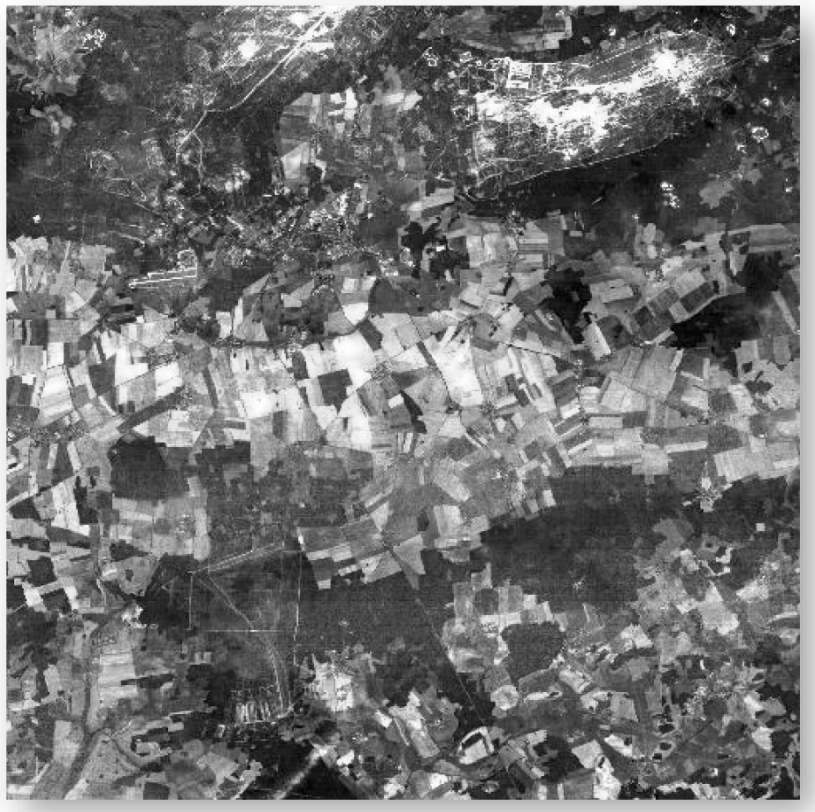

b. After atmospheric correction.

a) Image containing substantial haze prior to atmospheric correction.
b) Image after atmospheric correction using ATCOR (Courtesy Leica Geosystems and DLR, the German Aerospace Centre).

Dark object subtraction

DOS method assumes the radiance at the sensor is due to atmospheric scattering and this is subtracted from the scene

- Radiance at the sensor over a dark object is dominated by the path radiance term
- Thus, subtracting the output of the sensor over a dark object, such as water removes atmospheric scattering and leaves behind the reflected components
  - Problematic in bands with absorption
  - Does not fully account for surface-atmosphere interactions

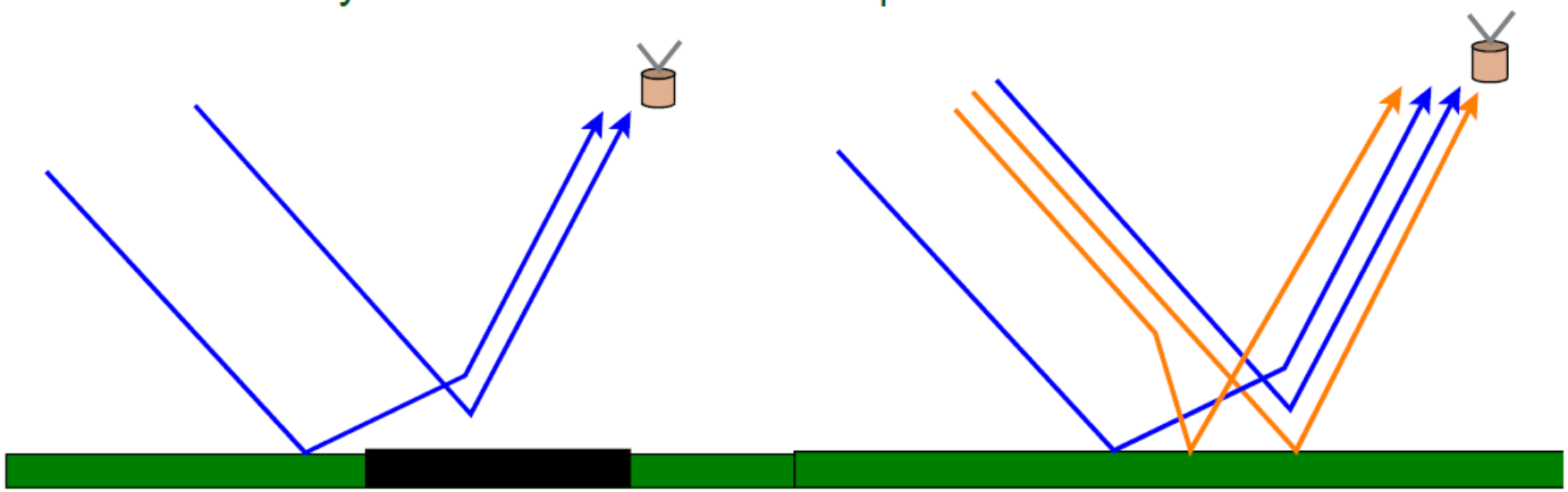

DOS example

Bands 1-3 from ETM+ showing original and corrected image without contrast enhancement

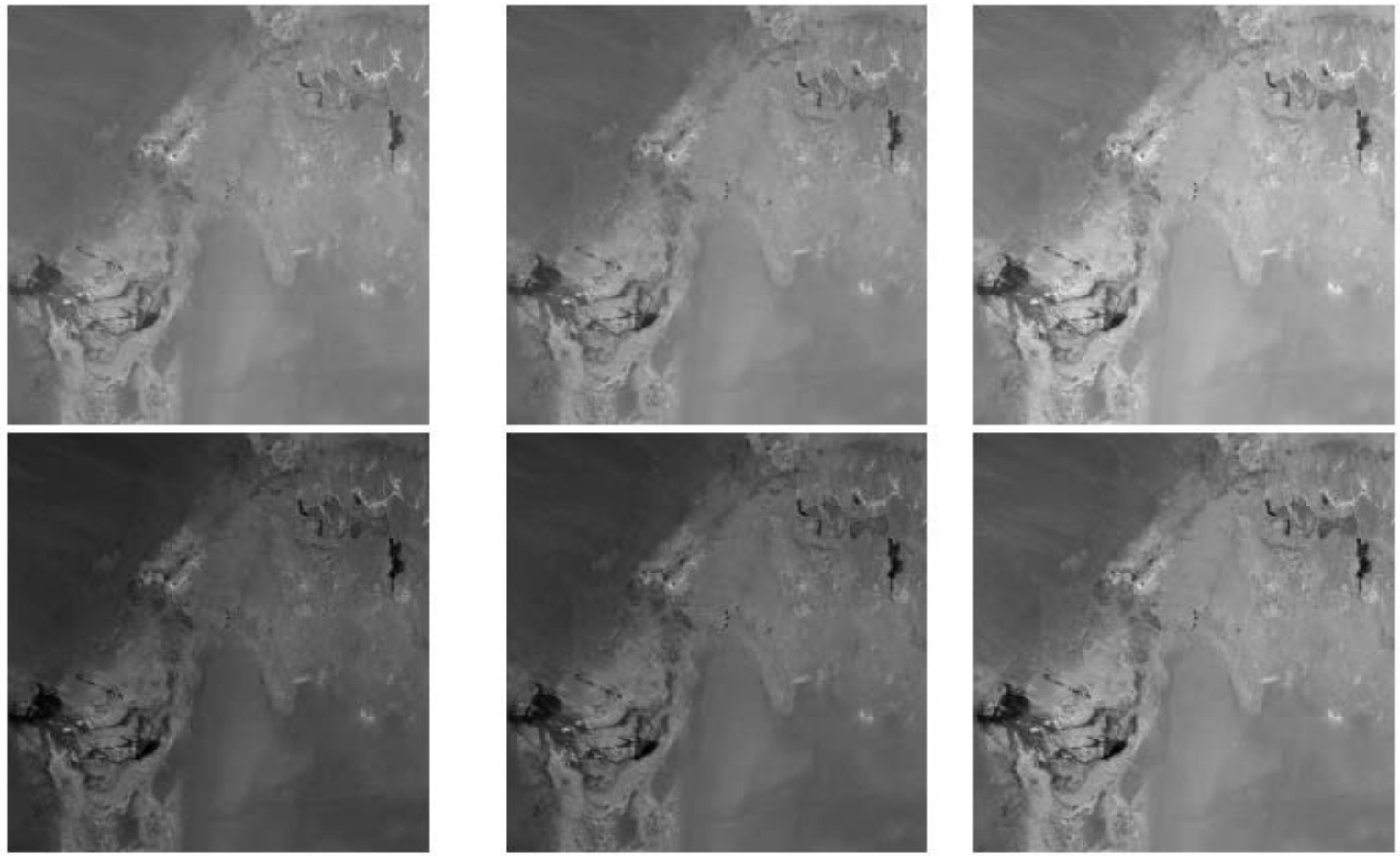

Empirical correction

Using known inputs, one can use a linear function to predict the at-sensor radiance for a given set of reflectances

- The at-sensor radiance of a known selected set of reflectances are used to determine the relationship between surface reflectance and at-sensor radiance
- This is very close to linear
- Using the linear assumption it is possible to interpolate/extrapolate from a given at-sensor radiance to a surface reflectance
- Method is most sensitive to the inputs that are assumed

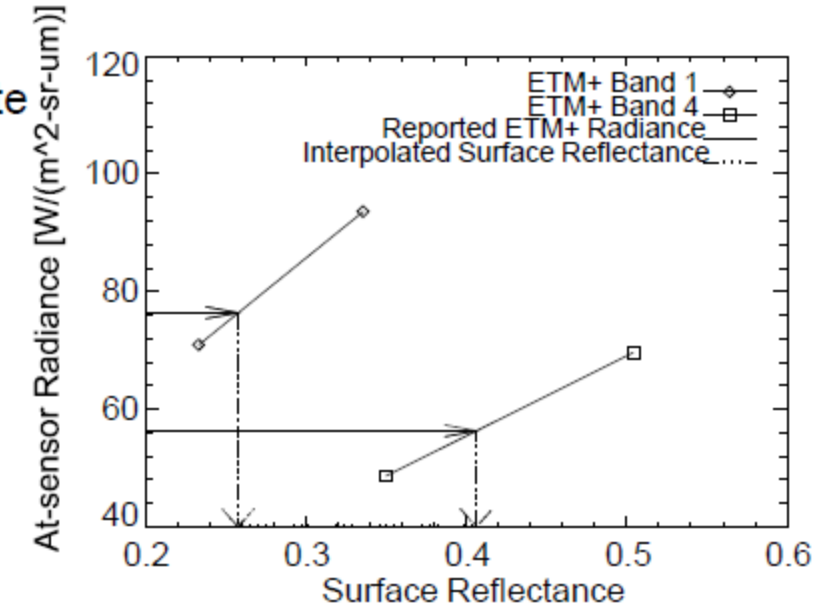

It is also possible to perform a

relative atmospheric correction

between two or more images, when lack of information does not allow absolute correction.

The relative correction aims at reproducing in the "slave" image the same atmospheric effects present in the "master" image.

This method consists in the development of a regression curve such that

$$DN_{ref} = f(DN)$$

that allows to predict what would have been the **DN** value in the slave image, if it had been acquired in the same atmospheric condition of the master image.

This can be achieved through

- Histogram Matching
- GCP

Histogram matching

Of course, it would be nice to actually include some of the physics of the atmosphere into the problem

- Simple contrast stretch improves the look of the imagery, but does not allow for true quantitative analysis
- A contrast stretch approach that includes quantitative correction forces the histograms from two separate dates to agree with each other
- Original histograms from the two dates in lower right quadrant shows one of the days having a larger atmospheric effect (white bars)
- The data represented by the white bars are stretched to give the same frequency distribution as the dark bars
- Assumes the surface reflectance did not change with time

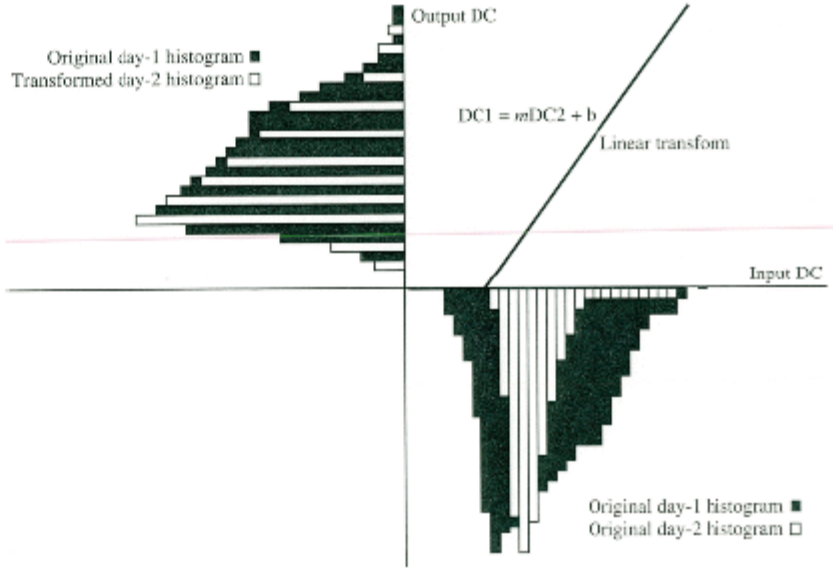

- Excellent for mosaicing and equalizing effects due to changing sun angle

Relative atmospheric correction using regression

GCP's must be pixels that presumably did not change their spectral features in the two images (time invariant).
In this way, one can suppose that any difference in **DN** of the **GCP**'s are solely due to different atmospheric conditions.

Applying a RMS minimization technique between DN_{MASTER} and DN_{SLAVE} on some **GCP**'s, it is possible to obtain a linear **f(DN)** function

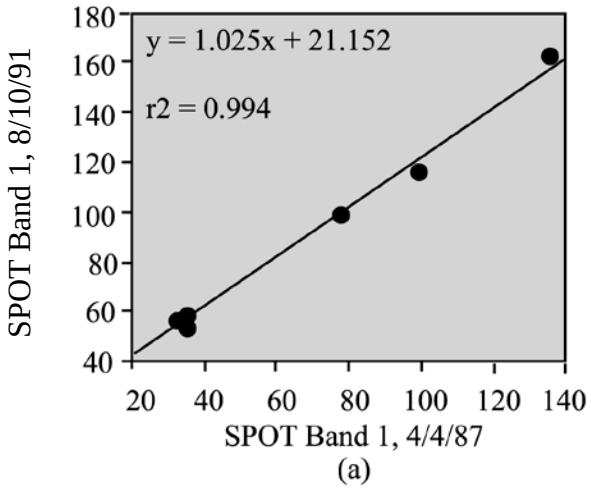

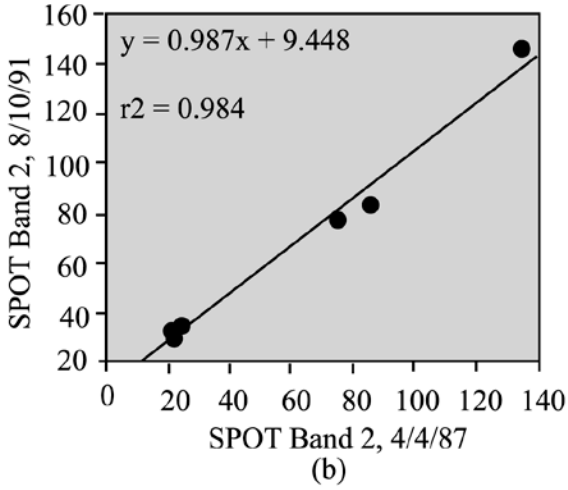

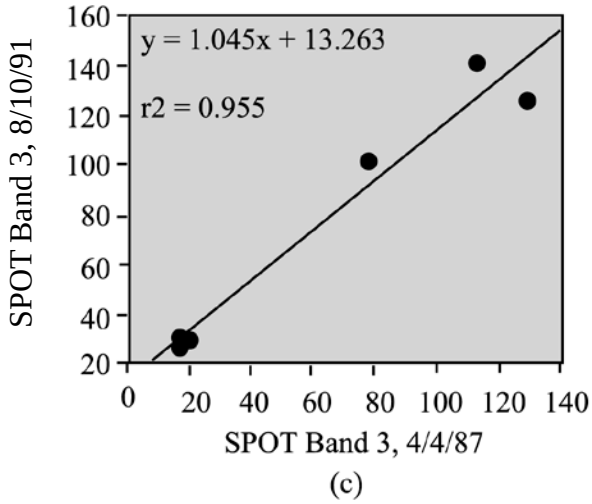

Example based on SPOT imagery obtained over Water Conservation 2A in South Florida